Fakultät für Medizin

Institut für vegetative Physiologie/ Walter Brendel Centre of Experimental Medicine

AMP-activated protein kinase as a novel regulator of vascular tone

Kai Michael Schubert

Vollständiger Abdruck der von der Fakultät für Medizin der Technischen Universität München zur Erlangung des akademischen Grades eines

Doctor of Philosophy (Ph.D.)

genehmigten Dissertation.

Vorsitzender: Prof. Dr. Agnes Görlach

Betreuer: Prof. Dr. Ulrich Pohl

Prüfer der Dissertation:

1. Prof. Dr. Dr. Stefan Engelhardt
2. Prof. Dr. Christian Kupatt

Die Dissertation wurde am 14.11.2016 bei der Fakultät für Medizin der Technischen Universität München eingereicht und durch die Fakultät für Medizin am 14.03.2017 angenommen.

Table of Contents

Summary:

Vascular smooth muscle cells (VSMC) are the central units integrating local and systemic signals to regulate vascular diameter. Therefore their physiology and pathophysiology has gained much interest in the progress of the metabolic syndrome, particular the development of essential hypertension. The AMP-activated protein kinase (AMPK) which is well known as a key enzyme in the regulation of the cell metabolism has been proposed to have a multitude of effects on vascular signaling pathways ultimately controlling blood flow and cellular oxygen supply. Thus the aim of this thesis was to determine the role of AMPK in the microcirculation with focus on the contractile state of the VSMC.

We found that AMPK stimulation induces an endothelium-independent dilation of rodent resistance arteries via a decrease of smooth muscle Ca^{2+}. This could be at first glance be explained by the finding in isolated cells that AMPK activated BKCa channels and causes membrane hyperpolarization which reduces Ca^{2+}-influx. Surprisingly, the inhibition of BKCa function with pharmacological compounds in intact vessels did not abolish the AMPK-induced relaxing effect and concomitant Ca^{2+}-decrease, a finding which was confirmed by studying vessels of global knock-out (KO) mice. We found that this effect could be attributed to AMPK-induced phosphorylation of the SERCA regulating protein phospholamban on Thr17 which was the main mechanism underlying the decrease of Ca^{2+} in the vascular smooth muscle cells. Interestingly AMPK is able to reduce vascular tone via an additional, calcium independent mechanism which develops more slowly. This Ca^{2+} desensitization was not due to the classical pathways i.e. reductions of myosin light chain kinase (MLCK) or myosin light chain phosphatase (MLCP) activities by inhibitory phosphorylation. Instead, in the microvessels observed, AMPK stimulation caused changes in the smooth muscle actin cytoskeleton with a significant increase of the globular over filamentous actin ratio (G/F-actin ratio) within 35 mins, which could be microscopically verified by rarefaction of cytosolic actin fiber network, thinning of actin filaments and reduction of actin branching. Mechanistically, we found that AMPK indirectly activated the actin-depolymerizing protein cofilin.

This work assigns a novel role to AMPK as a potent regulator of tone of small resistance arteries. As these are the main vessels controlling not only blood flow but also being involved in the development of hypertension, AMPK dysfunction may represent a novel key element in the vascular pathophysiology as part of the metabolic syndrome. Further studies have to clarify whether AMPK represents a therapeutic target for curing patients with vascular diseases.

List of Figures:

List of Tables:

List of Abbreviations:

Abl - abelson tyrosine-protein kinase

AKAP150 - A-kinase anchoring protein 150

AMATPase - actomyosin-atpase

AMPK - AMP-activated protein kinase

Arg - abelson tyrosine-protein kinase 2

Arp2/3 - actin related protein 2/3

AurB - aurora kinase B (also known as protein phosphatase 1, regulatory subunit 48)

BP – blood pressure

CACC - Ca2+ gated Cl2 channels

CamK2 - calcium/calmodulin dependent protein kinase II

CAS - Crk-associated substrate

Cdc42 - cell division cycle 42

CDK – cylin dependent kinase

CFTR - cystic fibrosis transmembrane conductance regulator

CK2A1 - casein kinase 2 alpha 1

CLIP - CAP-Gly domain containing linker protein (cytoplasmic linker protein)

CO – cardiac output

COX - cyclooxygenase

CPI-17 - Protein kinase C-potentiated inhibitor protein of 17 KDa

DAG - diacylglycerol

EC - endothelial cell

ECL - enhanced chemiluminescence ECL

EM - extracellular matrix

eNOS - endothelial Nitric Oxide Synthase

ERK - extracellular signal-regulated kinase (also named Mitogen-Activated Protein Kinase (MAPK)

FAK - focal adhesion kinase

Fer - FER tyrosine kinase (Feline Encephalitis Virus-Related Kinase FER)

FERM-proteins - F for 4.1 protein, E for ezrin, R for radixin and M for moesin

GAP - GTPase activating proteins

GDI - guanine dissociation inhibitors

GEF - guanine nucleotide exchange factors

GIT1 - G protein-coupled Receptor kinase interacting ArfGAP 1

GJA - gap junction protein alpha

GRK2 - G-protein coupled receptor kinase 2

HGK - hepatocyte progenitor kinase-like/germinal center kinase-like kinase (also named MAP4K4)

Hsp - heat shock protein

ILK - integrin linked kinase

IP3 - inositol 1,4,5-trisphosphate

IP3R - inositol 1,4,5-trisphosphate receptor

I-P-αP - ILK[integrin linked kinase]-PINCH[particularly interesting new Cys-His protein]-α-parvin-complex

ITGA - integrin subunit alpha

K_{ATP} - ATP-sensitive potassium channel

LIMK - LIM domain kinase

LTCC - L-type calcium channels

LYN - Lck/Yes-related novel protein tyrosine kinase

MEK - ERK activator kinase 1 (also named mitogen-activated protein kinase kinase)

MLCK - myosin light chain kinase

MLCP - myosin light chain phosphatase

MST4 - mammalian ste20-like protein kinase 4 (also called STK26)

MYPT1 - myosin phosphatase-targeting subunit 1

NOX - NADPH oxidase

Orai - CRAC calcium release activated calcium channel

p38MAPK - P38 mitogen activated protein kinase

PAK - P21 protein 8Cdc42/Rac)-activated kinase

Pax - paxillin

PKA - protein kinase A

PKB - protein kinase A (also named Akt)

PLC- phopholipase C

PLN - phospholamban

PMA - phorbol-12-myristat-13-acetat

PP1/PP2A - protein phosphatase 1 or protein phosphatase 2A

PTEN - phosphatase and tensin homolog

PTPN - protein tyrosine phosphatase, non-receptor type

PTPRA - protein tyrosine phosphatase, receptor type A

Pyk2 - protein tyrosine kinase 2 (Src family)

RIPK3 - receptor interacting serine/threonine kinase 3

ROK - Rho associated coiled-coil containing protein kinase 1

RyR - ryanodine receptor

SCX - sodium/calcium exchanger

SERCA - sarcoplasmic/endoplasmic reticulum calcium ATPase

SHP-2 - Src homology-2 phosphatase (also known as PTPN11 (protein tyrosine phosphatase, non-receptor type 11))

SK_{Ca}, IK_{Ca}, BK_{Ca} - small, intermediate, big conductance calcium-activated potassium channel

SOCE - store operate calcium entry

SR - sarcoplasmatic reticulum

STIM - stromal interaction molecule

SVR- systemic vascular resistance

TESK - testis-specific kinase

TrkB - tropomyosin-related kinase B

TRPV4 - transient receptor potential cation channels V4

VASP - vasodilator-stimulated phosphoprotein

VOCC - voltage operated calcium channels

VSM(C) - vascular smooth muscle (cell)

Yes - Yamaguchi sarcoma oncogene (Src family tyrosine kinase)

YWHA - tyrosine 3-monooxygenase/tryptophan 5-monooxygenase activation protein (14-3-3 gene name)

ZIPK - Zipper-interacting protein kinase

1. Introduction

1.1 Importance of Vascular Smooth Muscle Contraction on the Regulation of Microvascular Blood Flow in Physiology and Pathophysiology

Resistance arteries and especially the arterioles exert important functions since they control – via alterations of the flow resistance – the blood supply of the tissue and the arterial blood pressure. This function of the resistance vessels critically depends on the function of their vascular smooth muscle cells (VSM). Thus, the main functional role of VSM in most small arteries (especially resistance arteries) is to maintain tone and controlling size of blood vessel lumen (Brozovich et al., 2016; Raghow, Seyer, & Kang, 2006; Sarelius & Pohl, 2010). To this end, they are regulated by a plethora of mechanisms which are activated or inhibited by nerval, as well as tissue derived signals and, in addition by signals generated in the endothelium as well as in the smooth muscle cells themselves.

Not only the physiologic control of blood flow and blood pressure is critically dependent on the function of microvascular smooth muscle but it also has pathophysiologic implications: More than 90% of patients with hypertension are diagnosed with essential hypertension or hypertension of unknown etiology. Most of the current pharmacological treatments options rather act indirect than direct on the VSM (Schiffrin, 2012). Several mouse models targeting directly the VSM in the recent years highlighted that indeed the VSM and VSM contraction is vitally important in health and disease of blood flow regulation and the development of hypertension (Aldrich et al., 2000; Chutkow et al., 2002; Huang et al., 1995; Michael et al., 2008; Qiao et al., 2014; M. Tang et al., 2003; Y. Zhu et al., 2002). The most convincing experiment from Crowley et. al showed that targeted KO from AT_{1A}-receptor in kidney and/or VSM contributes equally to blood pressure regulation and underlined the underestimated role of VSM in the development of hypertension (Crowley et al., 2005). Fig. 1.1 summarizes major regulation mechanisms controlling blood pressure and its interplay to adapt blood supply to the needs of the respective tissues.
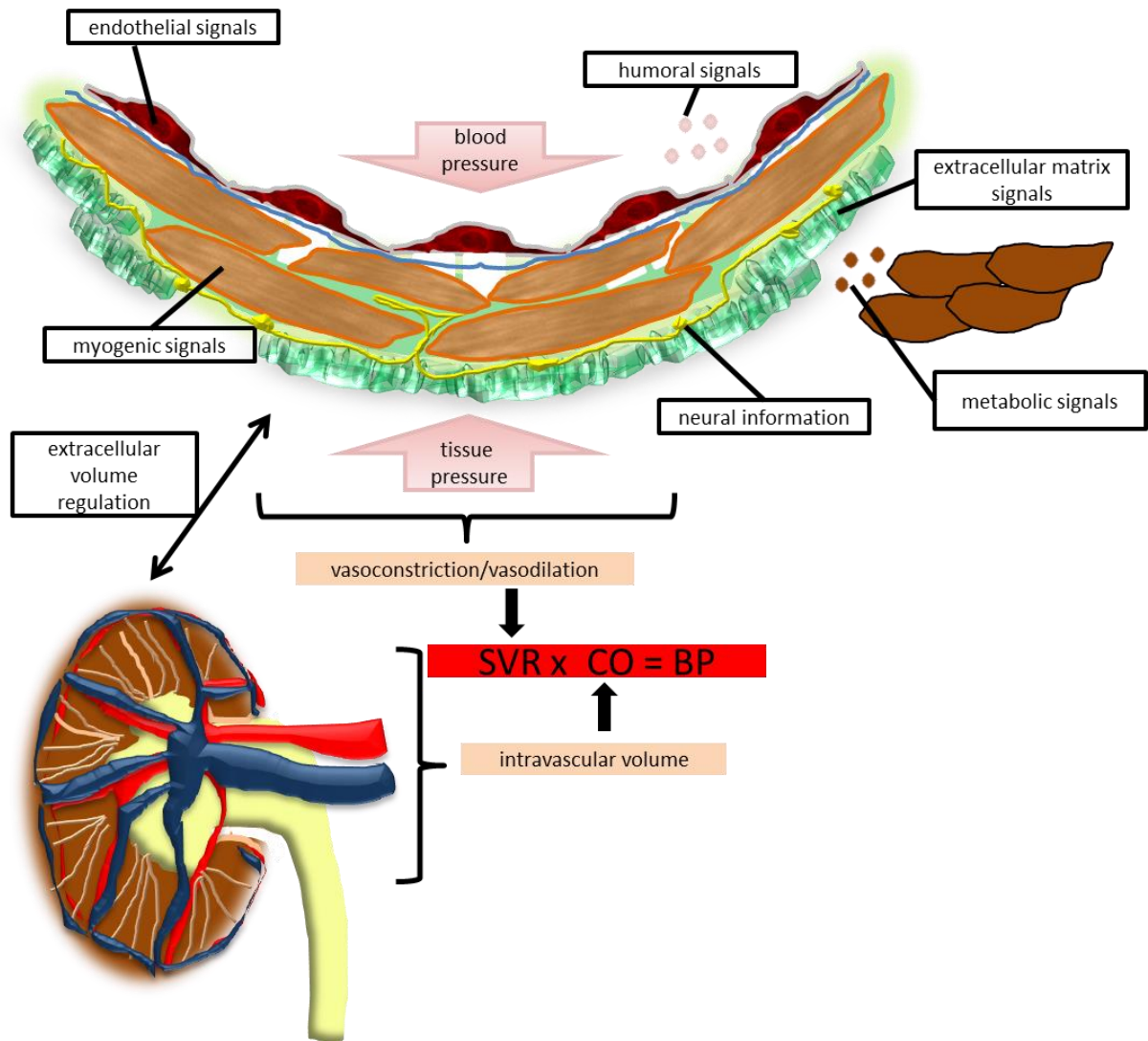
Fig. 1.1: Major regulation mechanisms of blood pressure: VSMC are integrating signals from endothelial cells, surrounding extracellular matrix, metabolic signals from parenchymal cells, nerval input from the sympathetic system and hemodynamic signals (blood flow and pressure). Intravascular volume is controlled by the kidneys and fluid intake. As blood pressure is the product of systemic vascular resistance and cardiac output (BP = SVR x CO) both parameters are closely adapted and can partly compensate for each other. Thus, hypertension can be due to a failure in any one of the components depicted in this image and results in compensatory changes of the other systems. Blood pressure (BP), systemic vascular resistance (SVR), cardiac output (CO).

1.2 Vascular Smooth Muscle Signal Transduction

There is plenty of evidence that microvascular constriction or dilation is caused by changes in cytosolic calcium ($[Ca^{2+}]_i$) levels in VSM. Microvascular smooth muscle

$[Ca^{2+}]_i$ is meticulously controlled by voltage-dependent calcium channels (Ca_V), sodium/calcium exchanger (SCX) (Blaustein & Lederer, 1999) and the sarcoendoplasmic Ca^{2+}-ATPase (SERCA) (Brini & Carafoli, 2009). While the roles of Ca_V and SERCA are mainly to increase or decrease $[Ca^{2+}]_i$, respectively, is the role of the SCX in VSMC less well understood. In particular, recent papers favor mechanism in which the SCX predominantly imports Ca^{2+} as evidenced by KO models or overexpression systems (Iwamoto et al., 2004; Youhua Wang et al., 2015). An increase of $[Ca^{2+}]_i$ by any of these processes controls via the formation of a calcium-calmodulin complex (($Ca^{2+})_4$ CaM) the activity of the myosin light chain kinase (MLCK) increasing the phosphorylation of myosin light chain (MLC_{20}). An equally important mechanism which occurs however, independently of dynamic changes of $[Ca^{2+}]_i$, is the regulation of the activity of MLC_{20} phosphatase (MLCP) since by this mechanism, MLC_{20} phosphorylation can be altered independently of MLCK activity (Somlyo & Somlyo, 2009). Most therapeutic approaches to affect peripheral resistance in hypertension or inadequate blood supply focus on one of these mechanisms.

However, there is also substantial information that additional mechanisms may be involved in the control of smooth muscle tone (Gallant et al., 2011; Lehman & Morgan, 2012), especially when longer lasting changes of vascular diameter and tone come into focus. Some of these mechanisms are subsumed as vascular plasticity or short term remodeling and are considered to be mediated, amongst other mechanisms, by functional alterations of vascular smooth muscle structure. Such are thought to be achieved by alterations of the smooth muscle cell cytoskeleton, the anchoring of the contractile apparatus with the matrix as well as a dynamic rearrangement of the smooth muscle cell length and smooth muscle intercellular adhesions (Van Den Akker, Schoorl, Bakker, & Vanbavel, 2010). In fact, a complex set of cytoskeletal events can be triggered by classical vasoactive compounds and hormones that appear to play a fundamental role in the mechanical response of the muscle tissue (Gunst & Zhang, 2008; D D Tang & Anfinogenova, 2008; Yamin & Morgan, 2012). Thus, actin dynamic cytoskeletal processes may contribute to the unique adaptive properties of smooth muscle that enable them to modulate their contractile and mechanical properties to adapt to changes in mechanical load and to maintain long term alterations of vascular tone. Increasing data suggests that the cytoskeletal processes that appear during contractile activation of VSMC may have

much in common with the cytoskeletal mechanisms that direct cell motility and migration (Gunst & Zhang, 2008).
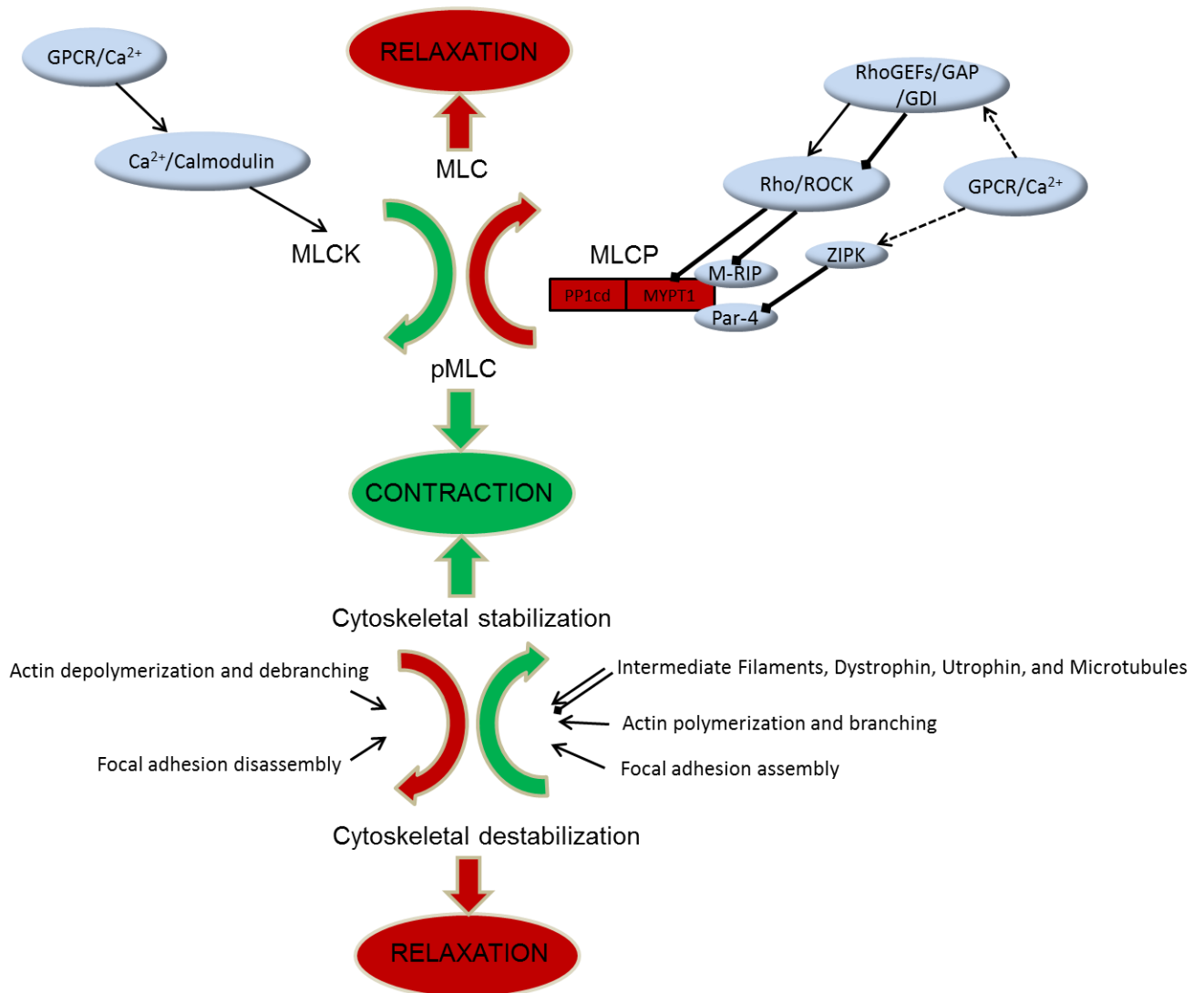
Fig. 1.2: Central pathways regulating vascular tone: Smooth muscle contraction is controlled by reversible phosphorylation and dephosphorylation of the MLC_{20} on the myosin heads of the the thick filament and cytoskeletal stabilization and destabilization of the thin (actin) filament.

1.3 AMPK

The 5'-adenosine monophosphate-activated protein kinase (AMPK) is a heterotrimeric enzyme which is expressed ubiquitously in mammalian cells and in essence in all other eukaryotes (Hardie & Ashford, 2014; Hardie, 2014; Steinberg &

Kemp, 2009). Its function in liver and skeletal muscle has gained tremendous interest since it is considered to work as a cellular fuel sensor acting on glucose uptake and inhibiting anabolic pathways of cell metabolism under conditions of reduced energy supply. These pleiotropic effects render AMPK activators potential anti-diabetic drugs (Gruzman, Babai, & Sasson, 2009; Hardie, 2013) which could be employed in diseases such as the metabolic syndrome. Since in patients suffering from the metabolic syndrome alterations of microvascular vasomotor function and arteriolar rarefaction are reported (Serné, de Jongh, Eringa, IJzerman, & Stehouwer, 2007), it is important to understand not only the metabolic but also the vascular effects of AMPK and AMPK-stimulating drugs, especially in resistance vessels. While AMPK has already been shown to have significant effects not only on endothelial cells but also on blood cells, i.e. leukocytes, platelets and macrophages (Alba et al. 2004; Randriamboavonjy et al. 2010; Sag et al. 2008; Fisslthaler and Fleming 2009), very little is known about its effect in vascular smooth muscle. Moreover most of the studies conducted on blood vessels were performed in large vessels. These findings cannot simply be extended to microvessels (Blodow et al., 2014; Boels, Troschka, Rüegg, & Pfitzer, 1991).

1.4 Aim of the Study

There is still lacking information how AMPK is controlling microvascular tone and by which of the aforementioned mechanism AMPK is doing so. Thus, the main aim of this thesis was to determine whether AMPK exerts vasomotor effects in microvessels and which cellular mechanisms might be involved. Therefore, we aimed to address the following questions:

1. Does AMPK activation lead to a change of tone of small resistance arteries?
2. Is an intact endothelium required for the vasomotor actions caused by AMPK?
3. Does (and to which degree) AMPK influence major Ca^{2+}-dependent and – independent pathways involved in the regulation of vascular tone?
4. Can molecular targets of AMPK in the microcirculation be identified which influence $[Ca^{2+}]_i$ and/ or calcium-sensitivity?

We therefore studied the effects of AMPK activation on vascular tone and smooth muscle intracellular free calcium in small resistance arteries freshly isolated from skeletal muscle or the mesentery. We performed these experiments initially in hamster vessels, since many intravital and *ex vivo* microscopic investigations have characterized these vessels in the microcirculation very well (Bolz et al., 2003; de Wit, Schäfer, von Bismarck, Bolz, & Pohl, 1997). In particular, we studied whether stimulation with two structurally distinct AMPK activators induced changes of vascular tone predominantly *via* endothelial or smooth muscle mechanisms.

We also studied whether AMPK stimulation elicited changes of $[Ca^{2+}]_i$ in these vessels, and which of the several processes potentially involved in the control of $[Ca^{2+}]_i$ was affected by AMPK stimulation. Later Ca^{2+}-independent dilation experiments were conducted in murine vessels to use more diverse genetical tools, antibodies and KO-models. It is known that AMPK can interfere with the upstream regulators of the MLC_{20} MLCK and MLCP in large artery models and thereby cause Ca^{2+}-independent vasodilation. We wanted to test if these mechanisms are also important in resistance arteries. As AMPK is thought to have a major role in the regulation of actin cytoskeletal dynamics and reorganization at the plasma membrane in the control of cell motility, (Bae et al., 2011; Kondratowicz, Hunt, Davey, Cherry, & Maury, 2013; Miranda et al., 2010; Moon et al., 2014; E. Ross et al., 2015; Stone et al., 2013), it may be hypothesized that AMPK is also regulating vascular tone by influencing actin polymerization, turnover and reorganization. This would establish a pathway by which the energy sensing enzyme AMPK could induce long term adaptations of cytoskeletal stability, cell morphology and motility, features which are important for a remodeling process which can occur independently of a permanent decrease of $[Ca^{2+}]_i$ in vascular smooth muscle cells.

2. Methods

2.1 Animals

All animal care and experimental protocols were conducted in accordance with German federal animal protection laws. Golden Syrian Hamsters (Janvier, Le Genest-Saint-Isle, France; 90-120g, 12-24 weeks) were euthanized by a lethal intraperitoneal injection of pentobarbital sodium (50 mg/kg) as described before (Bolz, Pieperhoff, de Wit, & Pohl, 2000). Male C57BL6/N mice (20-30g, 12-24 weeks) were purchased from Charles River Laboratories (Sulzfeld, Germany). The mice were killed by cervical dislocation. LifeAct mice were kindly provided by Reinhard Fässler (Max Planck Institute of Biochemistry, Martinsried, Germany) and Eloi Montanez (Biomedical Center, Martinsried, Germany). Immediately thereafter the respective vessels were dissected as described in detail below.

2.2 Drugs and buffer solutions.

The MOPS (3-morpholinopropanesulfone acid) -buffered salt solution used in the experiments contained (in mM): $CaCl_2*2H_2O$ 3.0, EDTA (ethylenediaminetetraacetic acid) 0.02, glucose 5.0, K^+ 4.7, $MgSO_4*7H_2O$ 1.17, MOPS 3.0, NaCl 145, $NaH_2PO_4*1H_2O$ 1.2, pyruvate 2.0. In MOPS buffers containing 125 mM KCl and varying concentrations of $CaCl_2$, concentrations of NaCl were adjusted accordingly so guarantee unchanged overall osmolality. PBS+ (phosphate-buffered saline with divalent cations) contained (in mM): $CaCl_2*2H_2O$ 0.9, glucose 5.6, KCl 5.4, $MgSO_4*7H_2O$ 0.3, $MgCl_2*6H_2O$ 0.3, NaCl 136.9, $NaH_2PO_4*1H_2O$ 0.8, KH_2PO_4 0.4, $NaHCO_3$ 3.6. Manganese (II) chloride tetrahydrate was purchased from Sigma Aldrich (Deisenhofen, Germany). Relaxing solution for α-toxin permeabilized arteries contained (in mM) 20 imidazole, 7.5 Na_2ATP, 10 EGTA, 10 Mg-acetate, 10 creatine phosphate, 31.25 potassium-methanesulfonate, 5 NaN_3, 0.01 GTP, 0.001 leupeptin, 2 DTT, pH 7.00 at 22°C; submaximal contraction solution contained in addition 2 mM and 6.5 mM $CaCl_2$ yielding a pCa (=$-log[Ca^{2+}]$) of respectively 6.99 (mesenteric) and 6.1 (tail arteries).   Norepinephrine was purchased from Aventis, indomethacin from

Fluka, nifedipine and Nω-Nitro-L-arginine methyl ester (L-NAME) and manganese (II) chloride tetrahydrate from Sigma Aldrich (Seelze, Germany), thapsigargin, PT1, iberiotoxin, Calyculin A, latrunculin A, jasplakinolide, LIMKi3, compound C, A769662 (A76), ML7 and paxilline from Tocris (Bristol, UK). A769662 (A76) was a generous gift from D. Grahame Hardie (University of Dundee, Scotland, UK) and later on purchased from Tocris or Adooq Bioscience (Irvine, USA).

2.3 Probes and Antibodies

Anti-AMPK α_1 and α_2 antibodies were kindly provided by Beate Fißlthaler (Goethe University, Frankfurt a. M., Germany), anti-SERCA 2 (atp2a2), anti-AMPK β_1 and β_2 antibodies were purchased from New England Biolabs (Frankfurt a. M., Germany), anti-GAPDH antibody from Merck Millipore (Billerica, MA, USA) and anti-phospholamban and phospho-phospholamban (pT17) antibodies from Badrilla (Leeds, UK). DNAse I-Alexa 488 and Phalloidin-Alexa546 were purchased from Thermo Fisher Scientific (Waltham, MA, USA), anti-pMYPT-Thr696 and anti-pMYPT-Thr853 antibody from Millipore (Darmstadt, Germany), anti-MYPT-Total from BD Transduction Laboratories (San Jose, USA), Anti-pMLC20-Ser19 from Rockland (Limerick, USA), anti-phospho-cofilin from CellSignaling (Danvers, MA, USA), anti-alpha-actin from Sigma Aldrich (Deisenhofen, Germany), DRAQ5 from Biostatus (Shepshed, UK), anti-pan-14-3-3 from Santa Cruz (Heidelberg, Germany).

2.4 Isolation and cannulation of resistance-type arteries.

Segments of small resistance arteries were excised under sterile conditions from the hamster gracilis muscle, cannulated with glass micropipettes, and transferred to an organ bath according to a protocol from Bolz et. al (Bolz, Pieperhoff, et al., 2000). The cannulated segments were stretched to their in situ length and a constant transmural hydrostatic pressure was maintained throughout the experiment.

Likewise, arteries from mouse mesentery were removed and pinned onto a silicon-coated petri dish for subsequent vessel dissection. Fine dissection of mesenteric arteries was performed in ice-cold MOPS buffer. Isolated arteries were then cannulated as described before (S. Bolz, de Wit, and Pohl 1999).
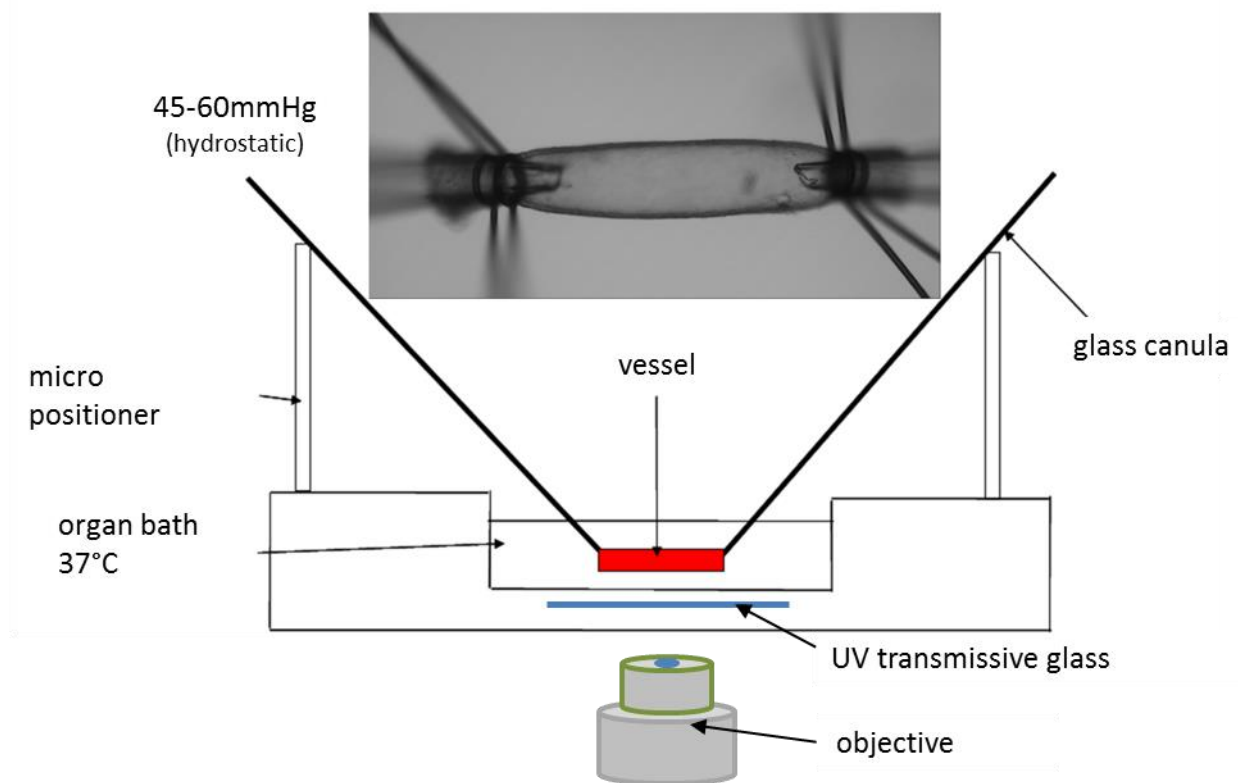
Fig. 2.1: Setup for pressurized arteries: arteries were dissected from mouse mesentery or hamster gracilis muscle, cannulated and fixated with ethilon 11-0 suture. Experiments were conducted in thermoregulated organ baths (37°C) and equilibrated for respective experiments.

2.5 Calcium- and diameter-registration.

The isolated arteries were treated as published before (Bolz et al., 1999; Bolz, Pieperhoff, et al., 2000). Briefly, the setup was transferred to the stage of a modified inverted microscope (Diaphot 300, Nikon, Düsseldorf, Germany) equipped with a 20x lens (D-APO 20 UV / 340, Olympus) and a video camera (Watec, WAT-902B). Organ bath temperature was raised to 37 °C and kept constant for the whole experiment. The transmural pressure was hydrostatically set to 45 mmHg for hamster vessels and 60mmmHg for arteries of mice. The smooth muscle layer was selectively loaded from the abluminal side with the calcium indicator Fura-2-AM (2 µM, LifeTechnologies, Carlsbad, CA, USA) over an incubation period of 2 h for hamster vessels and 90minutes for mouse vessels, respectively (Bolz et al., 1999). At the end of each experiment the measured Fura-2-AM signals were corrected for background

fluorescence with 8 mM $MnCl_2$. Fura ratio was preferred over measurement of absolute calcium concentrations as several research groups have shown that in heterogenic biological systems the dissociation constant is difficult to obtain and varies over different preparations (Almers & Neher, 1985; Meininger, Zawieja, Falcone, Hill, & Davey, 1991). Vascular diameters videomicroscopy (Hasotec, Rostock, Germany) were recorded in conjunction with the $[Ca^{2+}]_i$.

As shown by us before, the aforementioned vessels develop little myogenic tone (about 10% of resting diameters) at 45 mmHg/60mmHg (hamster/mouse) transmural pressure (Bolz et al., 1999). Nifedipine or Ca^{2+}-free MOPS buffer was used to achieve a minimal calcium level and maximal diameter in pre-constricted vessels at the end of each experiment. Normalization was done by building the difference between maximum values and minimum values for outer diameter and the (background corrected) Fura ratio (diameter: maximum with nifedipine or Ca^{2+}-free MOPS buffer (d_{max}) and minimal diameter after stimulation with norepinephrine or Ca^{2+}-containing [0.5mM] buffer (d_v); calcium: maximum with norepinephrine or Ca^{2+}-containing [0.5mM] buffer (R_v) and minimum with nifedipine or Ca^{2+}-free MOPS buffer (R_{min})). Nifedipine or Ca^{2+}-free MOPS in the concentrations used at 5 μM/0mM always induced a full dilation and minimal calcium unless this was already reached with the highest concentration of PT1/A76. Maximal diameters were close to the initial resting diameters. Maximal diameter and minimal calcium levels were not different between (A76/PT1) treated and control vessels.
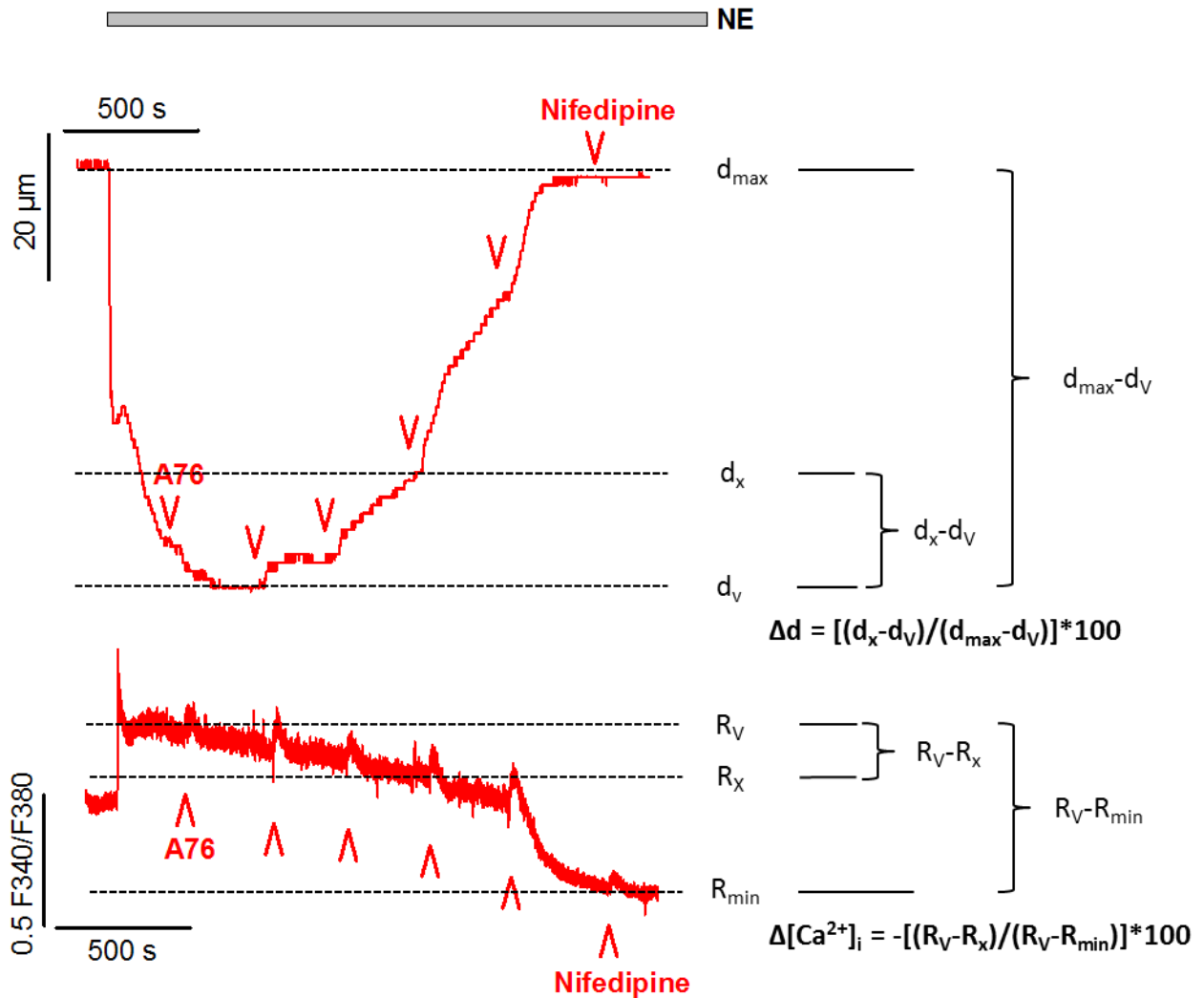
Fig. 2.2: Representative experimental trace illustrating how normalization for diameter and calcium measurements were performed

While 0.3 µM norepinephrine were sufficient to induce more than 30% of pre-constriction in hamster vessels, slightly higher concentrations, up to of 1 µM norepinephrine were necessary to constrict mouse arteries to the same extent. Norepinephrine induced a stable constriction and calcium signal in time control experiments and was therefore chosen as preconstrictor.

Addition of any substances or of solvent as control to the organ bath usually elicited small, transient elevations of $[Ca^{2+}]_i$. Since these were considered unspecific and to be due to mechanical irritation and did not lead to a change in vascular tone they were not studied and evaluated further.

In order to destroy the endothelium and thus, deendothelialize vessels in some experiments, an air bubble of 1 ml volume was passed through the lumen with a syringe. Absence of functional endothelium was verified by the absence of a dilator response to acetylcholine (3 µM) in preconstricted arteries (300 nM norepinephrine) which had dilated prior to deendothelialization by at least 90 % in response to the same dose of acetylcholine.

Ca^{2+} sensitivity curves were performed as described elsewhere (Bolz, Galle, Derwand, de Wit, & Pohl, 2000): Arteries pressurized at 60mmHg were first placed in Ca^{2+}-free MOPS buffer ($[Ca^{2+}]_o = 0$) with normal extracellular potassium concentration (4.7 mM). $[Ca^{2+}]_o$ was elevated stepwise from zero to 0.5, 1, 2 and 3 mM after the potassium concentration was increased to 125 mM to permanently open voltage operated calcium channels (VOCC). Resulting changes in intracellular calcium and diameter were recorded at a frequency of 5 Hz. The whole procedure was repeated again in the presence of AMPK activators (A769662 [A76], 100 µM and PT1, 30 µM) and after wash out of the activators for 30 minutes.

Another set of experiments was conducted to investigate the kinetics of the vasodilation caused by PT1 and A76. The protocol started with incubation of the mouse arteries in standard MOPS, followed by a normal potassium (4.7 mM) zero $[Ca^{2+}]_o$ MOPS and a high potassium (125 mM) zero $[Ca^{2+}]_o$ MOPS (each for five minutes). Finally the arteries were constricted with MOPS containing 125 mM potassium and 0.5 mM $[Ca^{2+}]_o$ to continuously open VOCC. The respective AMPK activators or DMSO as vehicle were applied after additional five minutes. Again the calcium signal and corresponding diameter values were recorded.

2.6 Western blot and Co-immunoprecipitation.

Western blots were performed using different approaches. Samples were either single arteries, pooled arteries, mesenteries or cultured cells. Arteries and mesenteries were isolated, cannulated and fixed on one side and cleared from intraluminal blood. After excerting the respective treatment protocols, the tissue samples were either shock frozen with liquid nitrogen, flash-frozen in 15 % trichloroacetic acid (TCA) in acetone (w/v) or directly lysed in radioimmunoprecipitatiion assay buffer (RIPA) with the following ingredients: NaCl

150 mM, Tris·HCl 50 mM at pH = 8, Triton X-100 0.1 %, Na$^+$ deoxycholate 0.5 %, SDS 0.1 %, EDTA 5 mM with protease inhibitor cocktail containing: AEBSF 500 μM, antipain 14.7 μM, aprotinin 0.77 μM, leupeptin 10 μM, NaF 500 μM and Na$_3$VO$_4$ 500 μM. Unless not otherwise indicated samples were processed as described by Lubomirov et al. (Lubomirov et al., 2006). Briefly, the arteries were thoroughly minced in SDS sample buffer (4% glycerol, 4% SDS, 2.5% bromophenol blue, 0.125 M Tris-HCl and water to desired volume; DTT plus protease and phosphatase inhibitors as in RIPA buffer) with a glass pestle (Kimble Chase LLC, Tissue Grinder Micro PKG/6, art. No. 885470-0000) and repeatedly centrifuged. Than they were pipetted until only foam was seen in the glass mortar. The foam was then transferred into a new Eppendorf tube and protein concentration measured. Table 2.1 gives an overview of the modifications used for different targets or tissues.

target	sample	stimulation	freezing	lysis buffer	notes
phospho-lamban (PLB)	half mesentery or both femoral arteries of mice	1 μM norepinephrine for 5 minutes followed by 5 minutes of norepinephrine plus 0.03 % DMSO or norepinephrine plus 30 μM A76.	TCA	SDS sample buffer	sonication with three pulses for ten seconds after lysis
AMPK subunit expression	hamster femoral arteries	-	liquid nitro-gen	lysis buffer: EDTA (pH 8.0) 1mM, KH$_2$PO$_4$ 18mM, Leupeptin 1μg/ml, NaF 50mM, NA$_4$P$_2$O$_7$ (10H$_2$O) 40mM, Na$_3$VO$_4$ (pH 7.5) 1mM, pepstatin 1 μg/ml	Repeatedly deep frozen and scraped with a metallic needle
G-actin	cannulated single	15 min MOPS with PT1/DMSO	liquid nitro-	actin-stabilizing	2mm unstretched

	mouse mesenteric arteries	followed by 20min potassium rich MOPS (125mM K$^+$, 0.5mM Ca^{2+}) with PT1/DMSO	gen	buffer from a commercially available kit (G-actin / F-actin In Vivo Assay Kit Cat. # BK037, Cytoskeleton, Denver, CO, USA).	length; centrifugation for 1h with 155.000g at 22°C (Moreno-Domínguez et al., 2014)
pMLC$_{20}$, pMYPT1 (T696), pMYPT1 (T853) and β-actin	cannulated single mesenteric arteries or isometric arteries	5 min MOPS, 5 min calcium-free MOPS, 5 min calcium-free high potassium (125mM) MOPS, 20min potassium rich MOPS (125mM K$^+$, 0.5mM Ca^{2+}) all solutions with PT1 or DMSO	TCA	SDS sample buffer	2mm unstretched length; isometric arteries were permeabilized with α-toxin (5 U/µl) in a EGTA (free [Ca^{2+}] pCa = -log [Ca^{2+}] >8) and ATP-containing buffer (relaxing solution) as described earlier (Lubomirov et al., 2006).
cofilin Ser3	half murine mesentery, single cannulated mesenteric arteries, PCASMC	15 min MOPS with PT1/DMSO followed by 20min potassium rich MOPS (125mM K$^+$, 0.5mM Ca^{2+}) with PT1/DMSO (120min for A76)	Liquid nitro-gen (ar-teries)	SDS sample buffer (arteries), RIPA (cells)	Enhanced chemilumines-cence (ECL) or near infrared Western blot
14-3-3	PCASMC	15 min MOPS with PT1/DMSO followed by 20min potassium rich MOPS (125mM K$^+$, 0.5mM Ca^{2+}) with PT1/DMSO	-	150 mM NaCl 150, 50 mM TrisHCl (pH = 8.0), 1% Triton X-100 in water plus protease and phosphatase inhibitors	Co-immunopre-cipitation

Table 2.1: Western blot techniques

Protein band visualization was achieved by one of the following techniques:

Enhanced chemiluminescence (ECL) Western blot: The isolated proteins were separated via sodium dodecyl sulfate polyacrylamide gel electrophoresis (SDS-PAGE), transferred onto a nitrocellulose membrane (AMPK detection) or 0.2 µm PVDF membrane (pMLC$_{20}$, pMYPT1 (T696), pMYPT1 (T853) and β-actin, G-actin, Cofilin, phospholamban detection, 14-3-3, GAPDH), fixed by incubation with 0.5 % PonceauS and incubated with the primary antibody overnight in a shaker at 4 °C. After that step, the membrane was washed with Tris-buffered saline and tween (TBST) buffer and incubated with the horseradish peroxidase (HRP)-conjugated secondary antibody. Finally, bound secondary antibody was visualized by HRP-mediated luminol oxidation (AppliChem, Darmstadt, Germany) which was detected with a CCD camera.

Near-infrared Western blot: Lysates from single arteries and PCASMCs were separated via PAGE and transferred to a PVDF membrane. The membrane was blocked with 5 % BSA in TBST. Afterwards, it was incubated with a mixture of anti-phospho-cofilin and anti-total-cofilin antibody at 4°C. The membrane was washed subsequently and incubated with a mixture of a goat anti-mouse (IgG IRDye 680RD goat anti mouse) and a goat anti-rabbit secondary antibody (IgG IRDye 800CW goat anti rabbit, both LI-COR Biosciences, Bad Homburg, Germany). After washing the membrane was dried and scanned with a LiCor Odyssey CLx system (LI-COR Biosciences, Bad Homburg, Germany). The secondary antibodies were detected by excitation at 700 and 800 nm, respectively. Quantification was performed using Image Studio Lite version (LI-COR Biosciences, Bad Homburg, Germany).

Co- immunoprecipitation: Cells were grown in 10 cm culture dishes until 80 % confluence. Medium was removed and the cells were kept in MOPS buffer for 1 h to equilibrate. Then they were stimulated according to the Ca^{2+}-sensitivity protocol (see section 2.5 calcium an diameter registration) for 15 min with MOPS + 0.03 %DMSO or 30 µM PT1 followed by 125 mM K$^+$ plus DMSO/PT1 for 20 min. Cells were then lysed in a buffer of the following composition: 150 mM NaCl 150, 50 mM TrisHCl (pH = 8.0), 1% Triton X-100 in water(?) plus protease and phosphatase inhibitors (AEBSF

500 µM, antipain 14.7 µM, aprotinin 0.77 µM, leupeptin 10 µM, NaF 500 µM, Na_3VO_4 500 µM). Lysates were incubated over night at 4°C with a polyclonal pan-14-3-3 antibody and with µMACS Protein A MicroBeads (Miltenyi Biotec, Bergisch Gladbach, Germany). The mixture was then loaded onto MACS separation columns (Miltenyi Biotec, Bergisch Gladbach, Germany) and processed according to the manufacturer's instructions. Lysates, precipitates and flow-through samples were subsequently quantified by Western blot.

2.7 Cell culture.

Human Umbilical Artery Smooth Muscle Cells (HUASMCs, Lonza, Verviers, Belgium) or Porcine Coronary Artery Smooth Muscle Cells (PCASMCs, Sigma Aldrich, Deisenhofen, Germany) were cultured according to the provider's instructions in a humidified chamber with ambient conditions of 95 % O_2 and 5 % CO_2.

2.8 Isolation of vascular smooth muscle cells and patch clamp measurements.

Gracilis muscle arteries of mouse and hamster were dissected and carefully freed of surrounding muscle, fatty and connective tissue. The vessel segments were then isolated and the cells thereof enzymatically digested as described elsewhere (Dietrich et al., 2005). Different time periods of the digestion protocol were tested and for the specific samples (hamster/mouse arteries) optimized. Isolated vascular smooth muscle cells (VSMC) were plated on a cell culture dish coated with polylysin and allowed to adhere. Then the cells were analysed with the perforated patch technique (this technique was used to retain the integrity of cytoplasmic components like soluble second messengers): After adhesion, VSMCs were superfused with an extracellular solution: NaCl 135 mM, KCl 5 mM, $CaCl_2$ 1 mM, $MgCl_2$ 1 mM, glucose 10 mM, HEPES 10 mM, adjusted to pH 7.4 with NaOH. Glass cannulas with resistances of 2.5 to 4.0 MΩ were choosen as patch pipettes and caused series resistances of 6 to 11 MΩ. The tip of a patch electrode was first filled with an amphotericin B-free solution (KCl 30 mM, K-aspartat 110 mM; $MgCl_2$ 1 mM, EGTA 0.1 mM and HEPES 10 mM, titrated to pH 7.2 with NaOH) and carefully controlled

that no air bubbles got into the system. The osmolarity of all solutions was controlled with vapor osmometer Vapro 5520 (Wescor, Logan, USA). The liquid junction potential was +13.8 mV and offset corrections were made by the Patch Master software (v2.52, HEKA, Lambrecht, Germany). The perforation induced by amphotericin started shortly after seal formation and reached a steady-state level within a few minutes. Cells with high leakage current were excluded from analysis. Patch Master software was used to automatically approximate and adapt the values of pipette and cell membrane capacitance and limiting voltage errors. Data acquisition was done with a frequency of 10 kHz after using a low bandpass filter (1.67 kHz) with an EPC10 patch clamp amplifier (HEKA, Lambrecht, Germany) integrated in the Patch Master software. The cells were depolarized in a stepwise manner from -70 to +40 mV (with increments of 10 mV) and certain substances applied. Concomitant currents (membrane potentials) were measured in the perforate patched mode.

2.9 Determination of mRNA levels in isolated arteries.

cDNA isolation was carried out from murine mesenteric arteries as previously described (Blodow et al., 2014). Total RNA from hamster and mouse vessels was isolated using Tri Reagent (Sigma, Munich, Germany). First strand synthesis was performed with random hexamers as primers, using RevertAid reverse transcriptase (Thermo Fisher Scientific, Waltham, MA, USA). The Quantitative PCR was performed on a StepOne machine (LifeTechnologies, Carlsbad, CA, USA) using the SYBR-Green reagent (Power SYBR Green, LifeTechnologies, Carlsbad, CA, USA) with normalization of the target genes to the geometric mean of hprt1 (hypoxanthine phosphoribosyltransferase 1), ywhaz (tyrosine 3-monooxygenase/tryptophan 5-monooxygenase activation protein, zeta polypeptide) and sdha (succinate dehydrogenase complex, subunit A) (Vandesompele et al., 2002). PCR primer sequences were:

Phospholamban:	(plb_for):	tgagctttcctgcgtaacag
	(plb_rev):	tggtcaagagaaagataaaaagttga

SERCA2:	(atp2a2_for):	tcgaccagtcaattcttacagg
	(atp2a2_rev):	cagggacagggtcagtatgc
AMPKα1:	(prkaa1_for):	ccttcgggaaagtgaaggt
	(prkaa1_rev):	gaatcttctgccggttgagt
Hprt1:	(hprt1_for):	tcctcctcagaccgctttt
	(hprt1_rev):	cctggttcatcatcgctaatc
Ywhaz:	(ywhaz_for):	taaaaggtctaaggccgcttc
	(ywhaz_rev):	caccacacgcacgatgac
Sdha:	(sdha_for):	ccctgagcattgcagaatc
Sdha:	(sdha_rev):	tcttctccagcatttgcctta.

1 µM of each primer pair and 1 µl of synthesized cDNA were added to the reaction mixture (5µl SYBR Green and 3µl aqua dest), and PCR was carried out using the following conditions: 10 min initial activation and 45 cycles of 15 s at 95 °C and 60 s at 60 °C each. All primers were tested by using diluted complementary DNA (cDNA) of reference tissues from skeletal muscle, heart, kidney and liver to confirm linearity of the reaction and to determine particular efficiencies. Gene of interest expression levels were calculated by normalizing to the geometric mean expression of the three reference genes. Melting curves were performed to assess whether their intercalating dye PCR/qPCR assays have produced single, specific products with continuous fluorescence registration from 60 °C to 95 °C. Crossing points were determined by the software program. For each qPCR experiment, the arteries of a whole mesentery were pooled and mRNA levels were measured in triplets. At least three independent qPCRs experiments were performed.
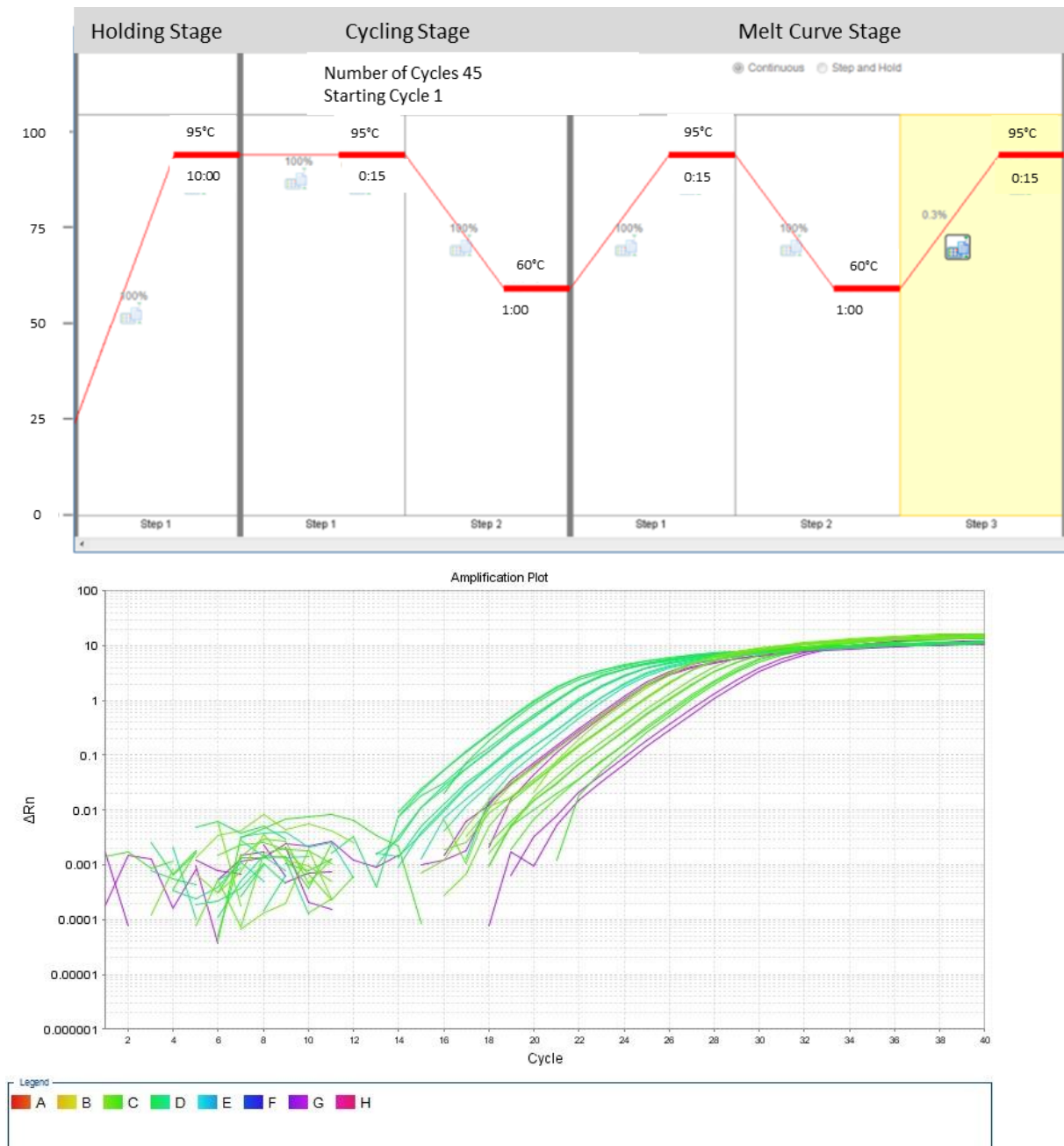
Fig. 2.3: PCR of isolated arteries: PCR protocol and amplification plot: A, after an initial activation step, 45 cycles were performed to amplify the PCR products. Finally a melting curved was conducted. B, amplification plot with different dilutions of cDNA ranging from 1:40 to 1:640. The y-axis is depicting the fluorescence signal and thus the products generated by the PCR cycles.

2.10 Measurement of membrane potential of VSMC in intact arteries.

Membrane potential was recorded in intact pressurized arteries using conventional intracellular glass microelectrodes filled with 3% agarose in 3M KCl solution. An AgCl

counter electrode was connected to this setup. Glass cannulas with a tip size <1 μm and resistance of 60-100 MΩ were shaped with an laser based micropipette puller system (P-2000, Sutter, Novado, CA, USA) and mounted on a micromanipulator unit (Scientifica, Uckfield, UK). The arteries were impaled and membrane potential continuously recorded. Therefore a pre-amplifier (BA-01X, Npi Electronic GmbH, Tamm, Germany) was connected to a data-acquisition system (LabChart, ADInstruments, Bella Vista, Australia). Two different protocols were conducted: In a first series of experiments arteries were constricted with 1 μM norepinephrine and subsequently relaxed by application of 30 μM A769662 followed by application of 100 nM iberiotoxin. In a second set of experiments 1 μM thapsigargin was applied after pre-constriction with 1 μM norepinephrine, followed by 30 μM A76. Criteria for acceptance of recordings were: (1) a sharp negative deflection in potential on impalement of the cell; (2) stable membrane potential for at least 2 min before experimental manipulations; (3) sharp positive deflection upon retraction of the microelectrode with no change in tip potential compared to the initial values.
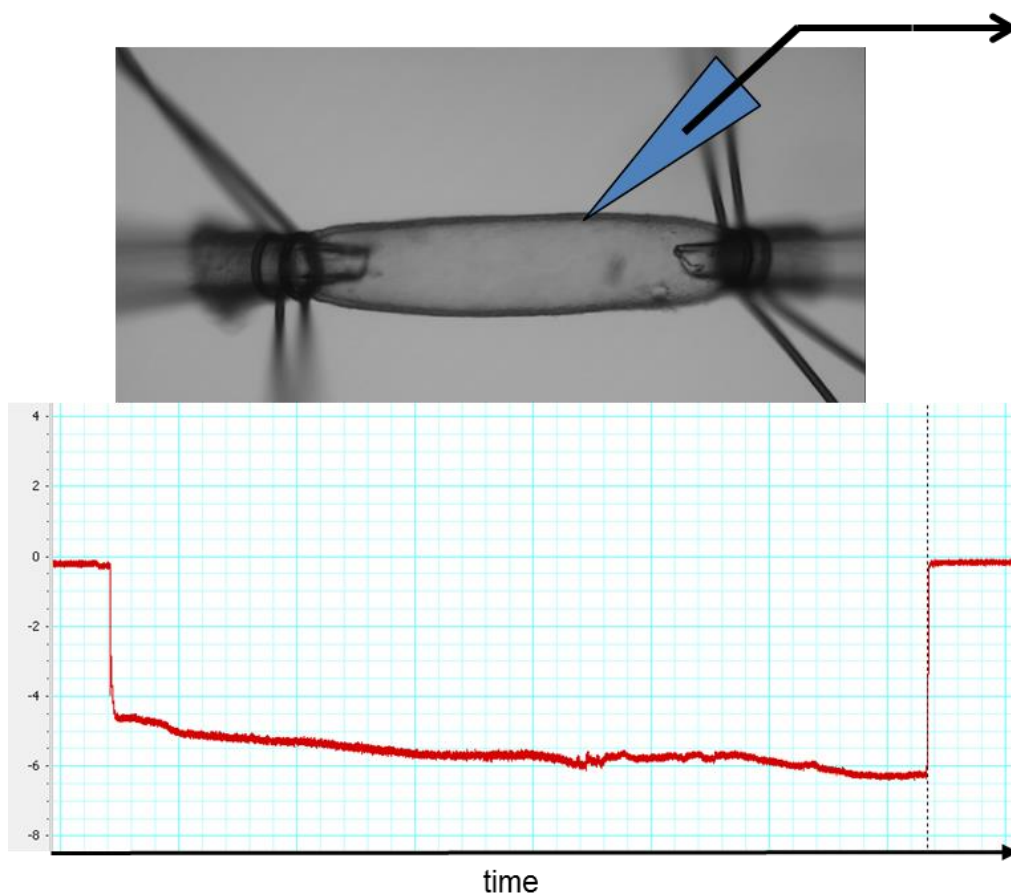
Fig. 2.4: Membrane potential measurement of intact arteries

2.11 Image analysis and calculation of anisotropy.

An anisotropy index was calculated from time lapse Life-Act images or arteries which were fixed in a pressurized state and thereafter stained for G- and F-Actin. Individual VSMC were identified and encircled thereby defining them as a region of interest. For Life-Act time-lapse images, changes in anisotropy were followed over time after sequential application of the following substances for indicated time periods: high potassium (125mM) MOPS buffer for 20minutes, PT1 for 60 minutes and Compound C/PT1 for additional 30 minutes. Pressurized arteries were also treated alternatively with several substances (PT1, Compound C, LIMKi3 (a LIM kinase inhibitor), Latrunculin, Jasplakinolide), fixed and stained (details in chapter 2.x Immunfluorescence). Again, borders of individual VSMC were detected and circled and anisotropy measured. To do so, computation of anisotropy was performed with the Fiji ImageJ plugin FibrilTool (Boudaoud et al., 2014). Briefly, this technique is based on building unit vector tangents to fibrils depending on the gradient of intensity levels in a region of interest in an image. These unit vectors build a tensor and the circular variance of their direction expresses a score how well fibrils are ordered (0 for no order (isotropic) and 1 for perfectly parallel ordered fibrils (anisotropic)).
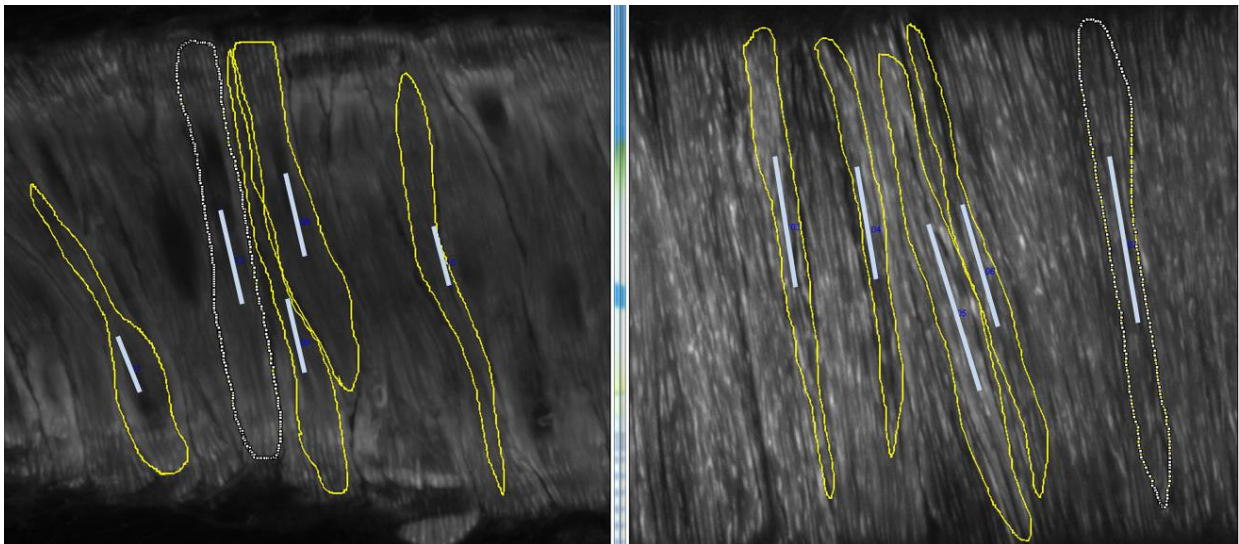
Fig. 2.5: Measurement of anisotropy in pressurized arteries: VSMC were encircled and the Fiji ImageJ Plugin FibrilTool used to calculate the anisotropy after different treatments. DMSO control on the left and PT1 on the right. The light blue line is an index of the anisotropy. The higher the anisotropy the more parallel and directed are the actin filaments.

2.12 Immunofluorescence.

Cannulated and pressurized or isometrically mounted arteries were fixed for one hour with 3.7% formaldehyde. Thereafter, the vessels were permeabilized for 30 minutes with 0.5% Triton X-100, blocked with 1% BSA in phosphate-buffered saline with divalent cations (PBS+) followed by incubation with the respective dyes for 2h or the indicated antibodies overnight. After thorough washing with PBS+, transmural image stacks (thickness 3μm) of three adjacent areas were obtained in each vessel using Leica TCS SP5 confocal microscope (Leica Microsystems). Images were analyzed in a blinded manner using Fiji ImageJ Software as follows. For F/G-ratio analysis the mean grey values of 5 random cytosolic areas of 3 μm z-stacks (0.3 μm slice distance, maximum intensity projection) of the phalloidin as well as the corresponding DNAseI images were calculated.

Profiles of Life-Act intensity through individual VSMCs in isometrically mounted arteries were analyzed according to Flavahan et al. (Flavahan, Bailey, Flavahan, Mitra, & Flavahan, 2005). Therefore, time lapse images of the same vessel area (61.51 μm x 61.51 μm) were recorded after sequential application of high potassium (125 mM, 10 minutes incubation time), PT1 (30 μM, 60 minutes incubation time) and compound C (15 μM, 30 minutes incubation time), respectively. A line perpendicular (y-axis) to the long axis of the VSMC (x-axis) was drawn through individual VSMCs. The edges of the cell were defined as the first and final peaks in relative Life-Act intensity with normalization to the maximum value of each cell. The width of the VSMC was normalized and calculated as the distance between the two peaks with the first peak being defined as site 0 and the final peak as site 1. Curves were plotted with an additional 0.2 margin of normalized Life-Act intensity distance on either side. Area under the profile curve (AUC) was determined with a Sigma Plot-Plugin for each individual cell and used for statistical evaluation via One Way Repeated Measures ANOVA followed by Holm-Sidak method (representative image in Fig. 3.15).

To investigate morphological changes in cytoskeletal architecture caused by AMPK HUAMSC were cultured and seeded on 8 well μ-slides (Ibidi, Martinsried, Germany) coated with poly-L-lysine (6 μg/cm^2) (Biochrom, Berlin, Germany) for 24 hours. Adherent HUASMC were incubated either with DMSO or PT1 in 125 mM K$^+$. Afterwards, HUASMC were fixed for 15 minutes in 3.7% formaldehyde, thoroughly

washed, permeabilized for 30 minutes in 0.5% Triton X-100, blocked with 1% bovine serum albumin (BSA) in phosphate buffered saline plus divalent cations (PBS+), carefully washed again, incubated with alpha-actin-antibody overnight and stained with a secondary anti-actin antibody and phalloidin on the next day. Cells were then embedded in confocal matrix (Micro Tech Lab, Graz, Austria). Leica TCS SP5 confocal microscope was used to record 3 random 120.6 µm x 120.6 µm images from each well (Leica Microsystems). These images were automatically pre-processed with Fiji ImageJ Software with following algorithm to achieve comparability between different samples as further explained after each command:

Firstly, z-stacks (0.3 µm slice distance, maximum intensity projection) of 3µm thickness were calculated to correct for filaments running slightly oblique in z-direction:

run("Z Project...", "projection=[Max Intensity]");

run("Grays");

run("Unsharp Mask...", "radius=4 mask=0.90");

A high-pass filter was applied to the picture to account for uneven illumination at the outskirts of the image

run("Bandpass Filter...", "filter_large=40 filter_small=3 suppress=None tolerance=5 autoscale saturate");

run("Enhance Contrast...", "saturated=5");

getRawStatistics(nPixels, mean, min, max);

t2 = max;

t1 = 1.2*mean;

setThreshold(t1, t2);

setOption("BlackBackground", false);

run("Convert to Mask");

run("Invert");

For the indirect analysis of intersection density by measurement of the mean actin filament length between intersections a Fiji ImageJ Plugin DiameterJ was used (Hotaling, Bharti, Kriel, & Simon, 2015). Filament thickness was calculated by building the mean of the minors (minimal diameter of the shorter axis of a region of interest (ROI)) of all particles of the pre-processed images with following characteristics:

size (in microns): 2-infinity (to subtract for background fluorescence)

circularity: 0.0-0.4 (to analyze only particles/filaments and not round antibody aggregates)

2.13 Statistics

For data presentation and computation of statistical tests SigmaPlot (Systat, Erkrath, Germany) was used. An initial pre-test for normality distribution (Shapiro-Wilk test) was run to decide if a subsequent parametric or non-parametric test was appropriate. Parametric tests comprised Two Way ANOVA followed by post hoc Tukey's test or Holm-Sidak method, One Way ANOVA was followed by post hoc Holm-Sidak method, One Way Repeated Measures ANOVA was followed by post hoc Shapiro-Wilk test. I addition paired t-test, and t-test for unpaired data were performed when appropriate. When the data not normally distributed, non-parametric tests, i.e. signed Rank test, Friedman Repeated Measures ANOVA on Ranks followed by Tukey's test were used. The exact method used in a particular set of experiments is indicated in the figure legends or in the description of specific results, respectively. For descriptive reasons, all values are presented as means ± standard error of the mean (SEM) plus n designating sample size. Differences were considered statistically significant when the error probability was < 0.05.

3. Results

3.1 Expression of AMPK subunits targeted by the AMPK stimulators.

First we tested if the AMPK subunits through which our AMPK activators act are expressed in VSMC of small arteries. While PT1 has been reported to activate AMPK by binding between the kinase and auto-inhibitory domains of the α_1 or α_2 subunits (Pang et al., 2008), A769662 (A76) has been shown to stimulate AMPK on a carbohydrate-binding module of the β_1 subunit and the N-lobe of the kinase domain (Scott et al., 2008). Western blots from hamster arteries were performed and yielded signals consistent with the expression of α_1, α_2, β_1 and β_2 subunits of AMPK (Fig. 3.1).
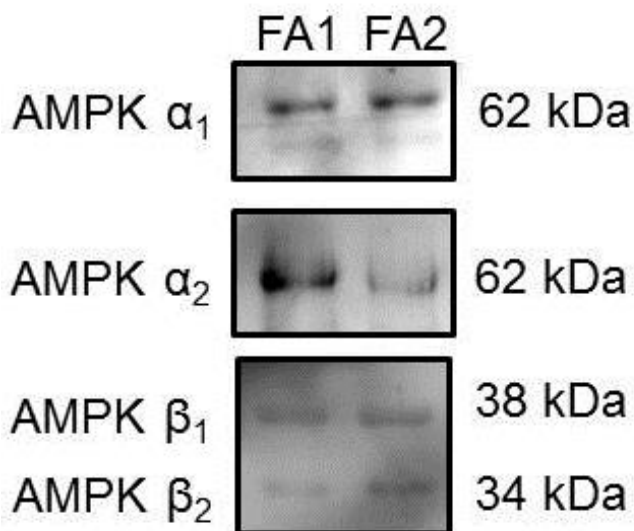
Fig. 3.1: Western blots demonstrating the expression of all AMPK α (upper and middle lane) and β subunits (lower lane) in two hamster femoral arteries (FA1, 2). Taken from Schneider&Schubert et al.(Schneider et al., 2015).

3.2 AMPK-mediated, endothelium-independent vasodilation paralleled by a decrease in $[Ca^{2+}]_i$.

Stimulation of AMPK by A76 in pressurized arteries which had been pre-constricted with norepinephrine induced a concentration-dependent decrease in cytosolic calcium along with vasodilation (Figs. 3.2A, 3.2B are depicting a representative single experiment). A second AMPK activator was used to exclude non-specific pharmacological actions of A76. PT1 was chosen because this compound activates AMPK at a subunit different from the A76 binding one (Pang et al., 2008). PT1 caused comparable vasodilation (Fig. 3.2E), and calcium decrease (see below). Unfortunately, PT1 interfered with the fluorescence signal at one of the wavelengths required to obtain the Fura-2 ratio. Thus, a quantitative analysis of the Fura-2 ratio, reflecting intracellular calcium levels was not possible in the presence of PT1.

Both compounds induced a maximal dilation of the vessels at their highest concentrations (A76 100µM, PT1 30µM; see Fig. 3.2C and Fig. 3.2E). To test if the effects of the AMPK stimulators were mediated by the endothelium, the endothelium was removed by perfusion with an air bubble. Neither vasodilation nor calcium decrease were reduced by removal of the endothelium. The responses to A76 and PT1 were rather slightly pronounced (Fig. 3.2C, 3.2D, 3.2E). In arteries with intact endothelium incubation with L-NAME (30 µM) and indomethacin (30 µM) to inhibit the function of NO-synthase (NOS) and cyclooxygenase (COX), respectively, showed no effect on the AMPK-induced dilation and calcium decrease. Nonetheless, all further experiments on pressurized arteries were conducted in the presence of L-NAME and indomethacin as part of the standard procedures established in our laboratory.
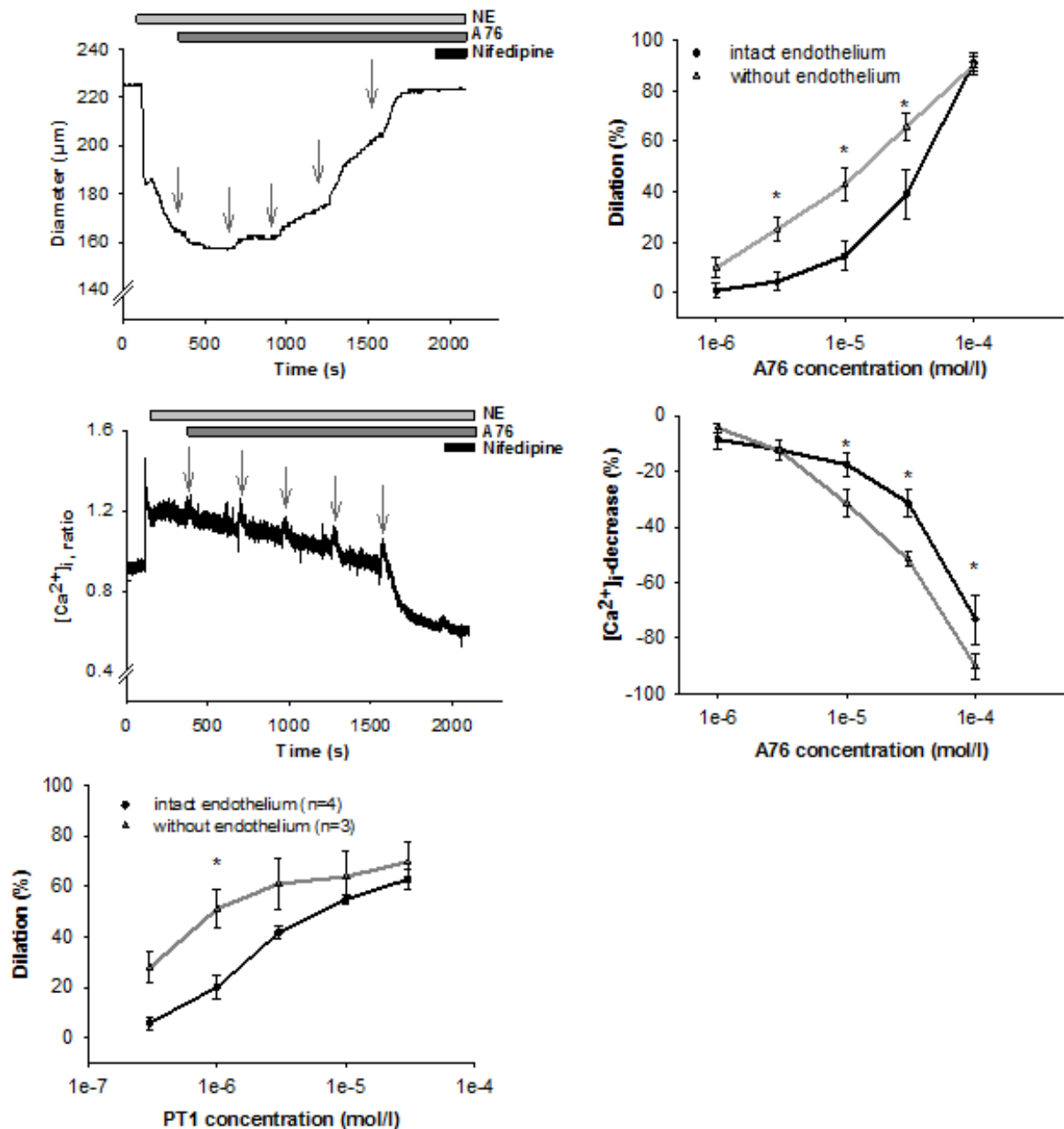
Fig. 3.2: Representative example of an original recording of the effects of A76 (1 - 0.1 mM) on diameter (**A**) and intracellular calcium (**B**). Arrows indicate application of A76 at increasing concentrations. The small resistance artery pre-constricted with 0.3 µM norepinephrine showed potent vasodilatation associated with a decrease of $[Ca^{2+}]_i$ especially at the higher concentrations. The application of the Ca_V-channel blocker nifedipine (5 µM) elicited no further dilation and only minor additional calcium decrease. Microvessels showed dose-dependent and endothelium-independent vasodilation (**C**) associated with a decrease of $[Ca^{2+}]_i$ (**D**) when exposed to A76 in concentrations reaching from 10^{-6} to $3*10^{-4}$ M (n=4-5). **E**: The application of the alternative AMPK stimulator PT1 ($3*10^{-7}$ to $3*10^{-5}$ M) also caused dose-dependent and endothelium-independent vasodilation (n=3-4 per group). The dilatations were normalized to the maximal possible dilator responses of the pre-constricted vessels as obtained in the presence of nifedipine (*=P<0.05, intact endothelium vs. without endothelium). Taken from Schneider&Schubert et al.(Schneider et al., 2015).

Table 2.1 summarizes the absolute diameters of hamster vessels under various conditions (basal, 0.3 µM norepinephrine, 0.3 µM norepinephrine + 100 µM A76, 5 µM nifedipine) to allow evaluation of relative changes.

Treatment	Mean diameter ± SEM, n (steady state)
Basal	233.1 ± 8.5 µm, n=55
0.3 µM norepinephrine (NE)	125.9 ± 9.4 µm, n=15
0.3 µM + 100 µM A769662	206.1 ± 14.3 µm, n=10
5 µM nifedipine	228.5 ± 6.9 µm, n=55

Table 3.1: Mean diameters of hamster vessels in response to various stimuli. Taken from Schneider&Schubert et al.(Schneider et al., 2015)

3.3 AMPK effects in VSMC involve activation of BK_{Ca} channels and associated hyperpolarization.

To investigate the potential role of potassium channels which may cause membrane hyperpolarization and dilation, VSMC were freshly isolated from hamster or mouse resistance arteries to perform perforated patch clamp analysis in single cells. AMPK activation by A76 or PT1 (again two independent activators of AMPK were chosen to exclude unspecific pharmacologic effects) showed a concentration-dependent increase in outward current that was sensitive to inhibition by paxilline and iberiotoxin (Ibtx), suggesting the involvement of BK_{Ca} potassium channels. This BK_{Ca}-dependent outward current was abolished upon stimulation with A76/PT1 in BK_{Ca} -/- mice. Furthermore, the AMPK inhibitor compound C (dorsomorphin), while not a completely specific inhibitor of AMPK (Bain et al., 2007), also abolished the outward current induced by A76 (Fig. 3.3H).
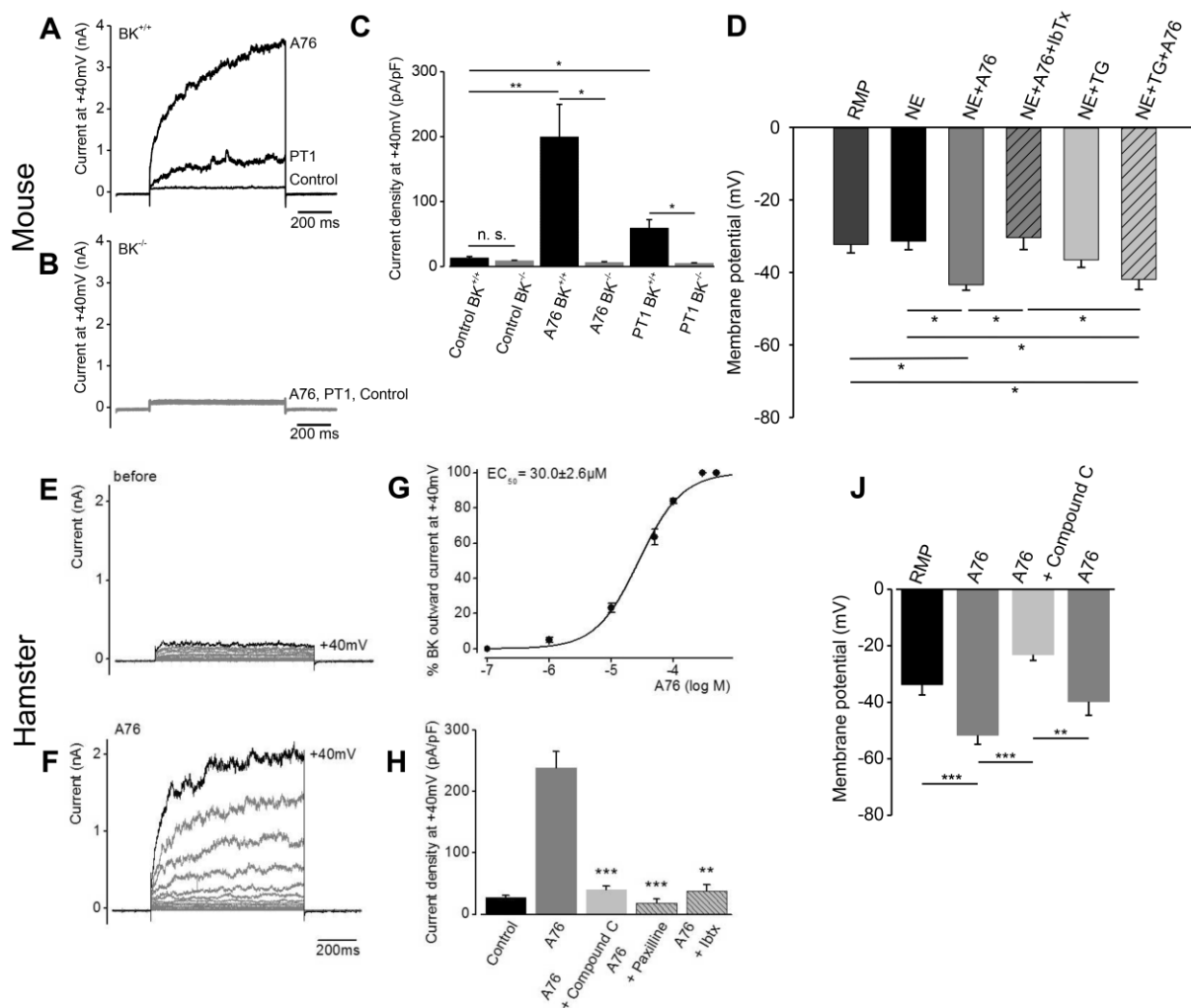
Fig. 3.3: AMPK effects in VSMC involve activation of BK$_{Ca}$ channels and associated hyperpolarization. Top row, **A**: Patch clamp studies in freshly isolated smooth muscle cells derived from small mouse mesenteric arteries demonstrating BK$_{Ca}$-dependent outward currents upon stimulation with A76 in WT but not in BK$_{Ca}$ -/- mice (**B**) and increased current densities upon the two independent AMPK stimulators A76 and PT1 in WT but not -/- cells (**C**; n=3-4, *=P<0.05, t-test). **D**: Membrane potential recordings obtained in smooth muscle cells of mouse mesenteric arteries in situ under non stimulated conditions (resting membrane potential, RMP), upon stimulation by norepinephrine (NE) alone, together with A76 in the presence or absence of iberiotoxin (IbTx) and thapsigargin (TG; n= 13-25 measurements from 5-13 vessels, *=P<0.05, One Way ANOVA, Holm-Sidak).
Bottom row: Results in isolated smooth muscle cells freshly obtained from hamster vessels. **E**: BK$_{Ca}$-dependent outward currents in the absence and presence (**F**) of A76 at increasing holding potentials. **G**: Dose dependency of A76 induced outward currents and effects of compound C and BK$_{Ca}$ channel blockers (**H**). **J**: Membrane potentials of isolated cells, showing hyperpolarization induced by A76, and reversible inhibition by the AMPK inhibitor compound C (n=5-27, **=P<0.01, ***=P<0.001, paired t-test). Taken from Schneider&Schubert et al.(Schneider et al., 2015).

3.4 PT1 mimics the effect caused by A76

PT1 also produced a BK$_{Ca}$-dependent outward current (Fig. 3.4B) similar as observed with A76 at a concentration that induced 15% dilation (Fig 3.2C and 3.3G) Again, the inhibitor of AMPK, compound C, virtually eliminated the outward current elicited by PT1 (Fig. 3.4B).
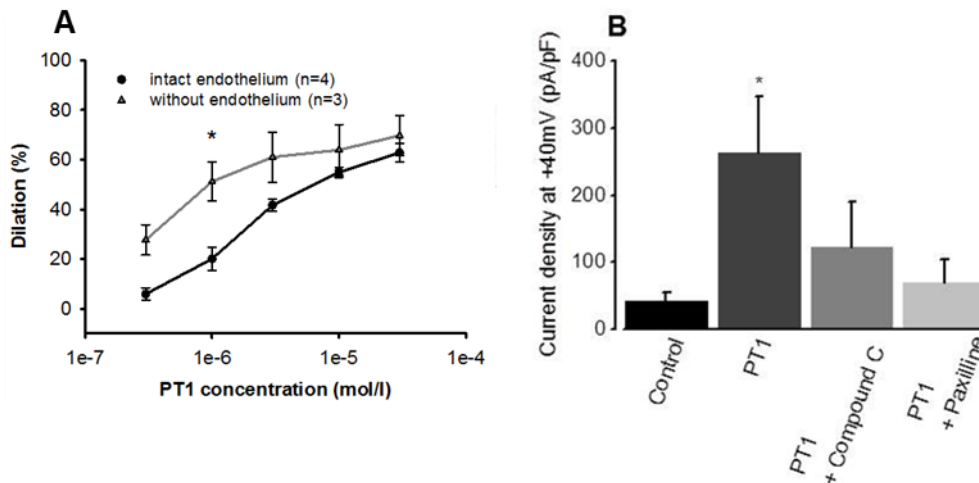
Fig. 3.4: A, The application of PT1 ($3*10^{-7}$ to $3*10^{-5}$ M) also caused dose-dependent and endothelium-independent vasodilation (n=3-4 per group). The dilatations were normalized to the maximal possible dilator responses of the pre-constricted vessels to nifedipine (*=P<0.05, intact endothelium vs. without endothelium, Two Way ANOVA, Tukey). **B,** PT1 (30mM) induced outward current was blocked by incubation with the BK$_{Ca}$-inhibitor paxilline, as well as with the AMPK-inhibitor Compound C. Modified from Schneider&Schubert et al.(Schneider et al., 2015)

3.5 Membrane potential in intact arteries

Measurements of membrane potential in isolated VSMC yielded a membrane potential of -52 ± 3 mV (n=8) under the influence of A76. This was reversed to -23 ± 2 mV by compound C (n=6, Fig. 3.5B). Likewise, impalement of murine mesenteric arteries smooth muscle cells in situ with sharp microelectrodes revealed a membrane potential of -34 ± 2 mV (n=6) after pre-constriction with norepinephrine, while under AMPK activation by A76 a mean of -60 ± 3 mV (n=6, Fig. 3.5C) was measured, a value that was comparable to isolated VSMC. This was consistent with BK$_{Ca}$ potassium channel activation by AMPK.
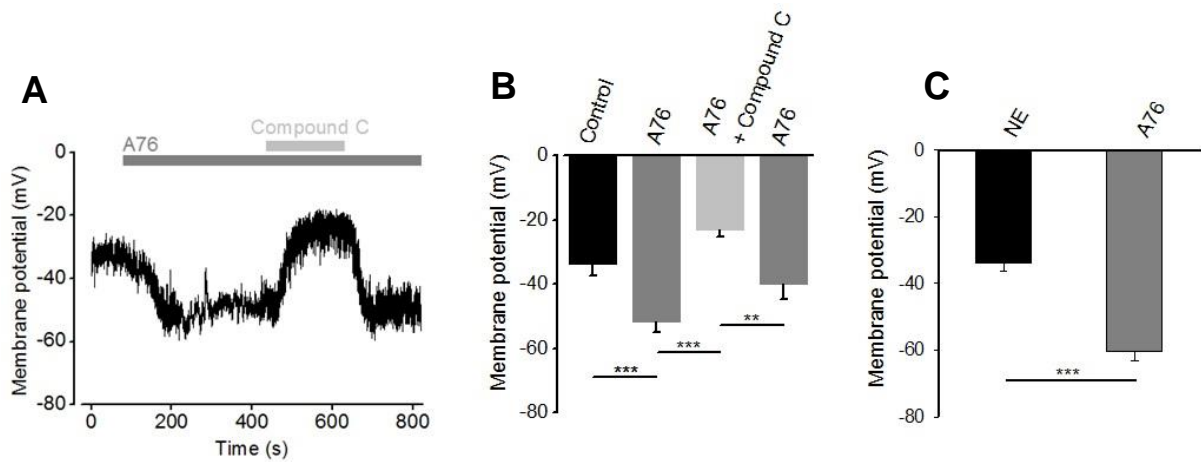
Fig. 3.5: A: Measurements in isolated VSMC confirmed hyperpolarization upon AMPK activation that was reversed by addition of compound C. **B**: Summary of the time series performed on single cells depicting reversible A76-induced hyperpolarization. **C**: Measurements of membrane potential with sharp microelectrodes showed a mean membrane potential of -34 ± 2 mV after preconstriction with norepinephrine (NE, 1 µM). A76 (30 µM) induced a hyperpolarization to -60 ± 3 mV (n=6, ***=P<0.001) Taken from Schneider&Schubert et al.(Schneider et al., 2015).

3.6 No changes by BK$_{Ca}$ channel inhibitors on AMPK-induced effects in intact vessels.

Despite the convinicing electrophysiological evidence from the BK$_{Ca}$-KO mice and outward current inhibition of AMPK-induced BK$_{Ca}$ activity by paxilline and iberiotoxin, these compounds showed only minor inhibitory effects on AMPK-mediated dilation of intact vessels and, in particular, did not affect the calcium decreases induced by A76 in intact arteries (Fig. 3.6A and 3.6C). Compatible with this, BK$_{Ca}$ gene-deficient mice showed no impairment of the AMPK-induced vasodilation, though VSMC from BK$_{Ca}$ gene-deficient mice showed no outward current upon AMPK activation as demonstrated in Fig 3.3C.

3.7 Significant impairment of dilation and of calcium decreases by SERCA inhibition.

We therefore conducted another series of concentration response curves (CRC) with AMPK stimulators in intact vessels to study the effects of the SERCA inhibitor thapsigargin (1 µM), with or without iberiotoxin or paxilline. Application of thapsigargin to vessels pre-constricted with norepinephrine gradually augmented VSMC cytosolic

Ca^{2+} throughout the incubation time (2 minutes) suggesting ongoing store depletion (not shown).

In sharp contrast to results obtained with BK$_{Ca}$ inhibition alone, pretreatment with thapsigargin alone substantially and significantly reduced the dilatory and calcium-decreasing effects of AMPK stimulation. The effects of thapsigargin could be reproduced with a second SERCA inhibitor, cyclopiazonic acid (10 µM, not shown). Combinations of thapsigargin with iberiotoxin or paxilline virtually abrogated the calcium decrease but still left a small dilator response (Fig. 3.6A).
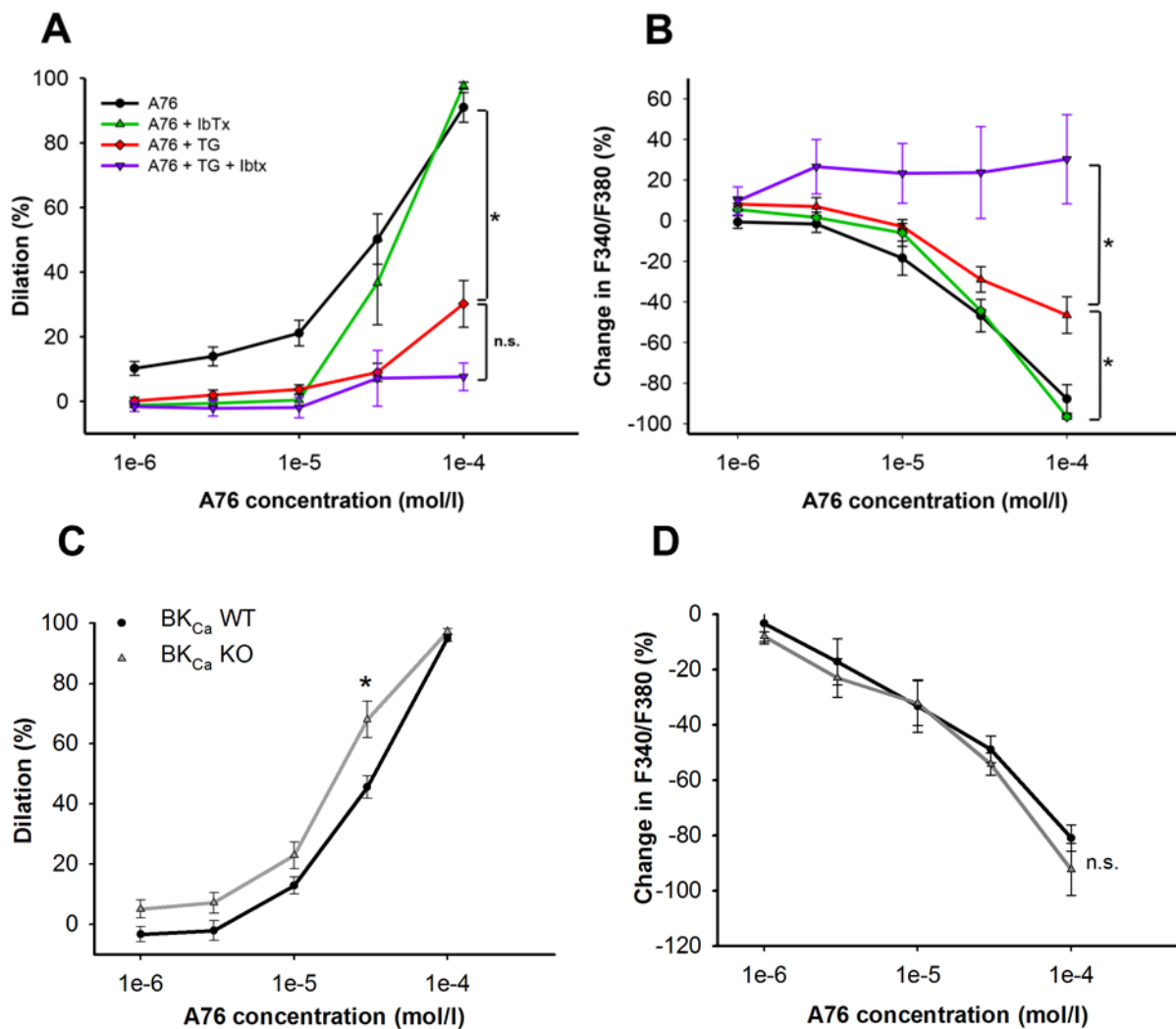
Fig. 3.6: Reduced AMPK effects under SERCA inhibition. Thapsigargin and iberiotoxin show inhibitory effects on the vasodilation (**A**) and calcium decrease (**B**) mediated by AMPK. The blockade of BK$_{Ca}$ channels with iberiotoxin (IbTx, 100 nM) caused no significant reduction of the AMPK induced vasodilator effects, contrary to SERCA inhibition with thapsigargin (TG, 1 µM). Simultaneous application of IbTx and TG virtually abolished the A76-induced calcium decrease and severely reduced dilation (n=4-6, *=P<0.05, Two Way ANOVA, Tukey). Little difference between BK$_{Ca}$ KO mice and WT littermates: mesenteric

44

arteries from BK_{Ca} KO mice showed no impairment in dilation **(C)** in response to A76. Rather, dilation was significantly higher at 30 µM A76. **D,** Likewise, the decrease in $[Ca^{2+}]_i$ was unaffected (n=4 each,*=P<0.05, Two Way ANOVA, Tukey). Taken from Schneider&Schubert et al.(Schneider et al., 2015)

3.8 Increased SERCA activity upon AMPK stimulation.

To further address the issue of an effect of AMPK on SERCA in intact vessels, we indirectly assessed smooth muscle sarcoplasmic reticulum (SR) calcium content by measuring the calcium transient upon application of caffeine (1 mM) (Potocnik & Hill, 2001). This transient was recorded in calcium-free buffer to avoid any confounding effects of channel-related influx. The relative height of the resulting calcium peak after caffeine application was taken as a measure of SR calcium content. Pretreatment with A76 indeed increased calcium transients in response to caffeine (Fig. 3-7A-C). In a separate set of experiments, voltage-gated calcium channels were blocked by nifedipine and again caffeine was applied in the absence or presence of A76. Pretreatment with A76 also enhanced the nifedipine-mediated basal $[Ca^{2+}]_i$ (Fig. 3.7D-F). Initially, the vessels were stimulated with norepinephrine (NE) to assess their calcium reactivity. After washout of NE, nifedipine with and without A76 was added to the organ bath and the resulting decrease of calcium was studied. Consistent with a higher activity of a second, probably SERCA mediated calcium removing mechanism, the calcium decrease after blockade of the calcium influx by nifedipine was significantly enhanced (Fig. 3.7 D-F).
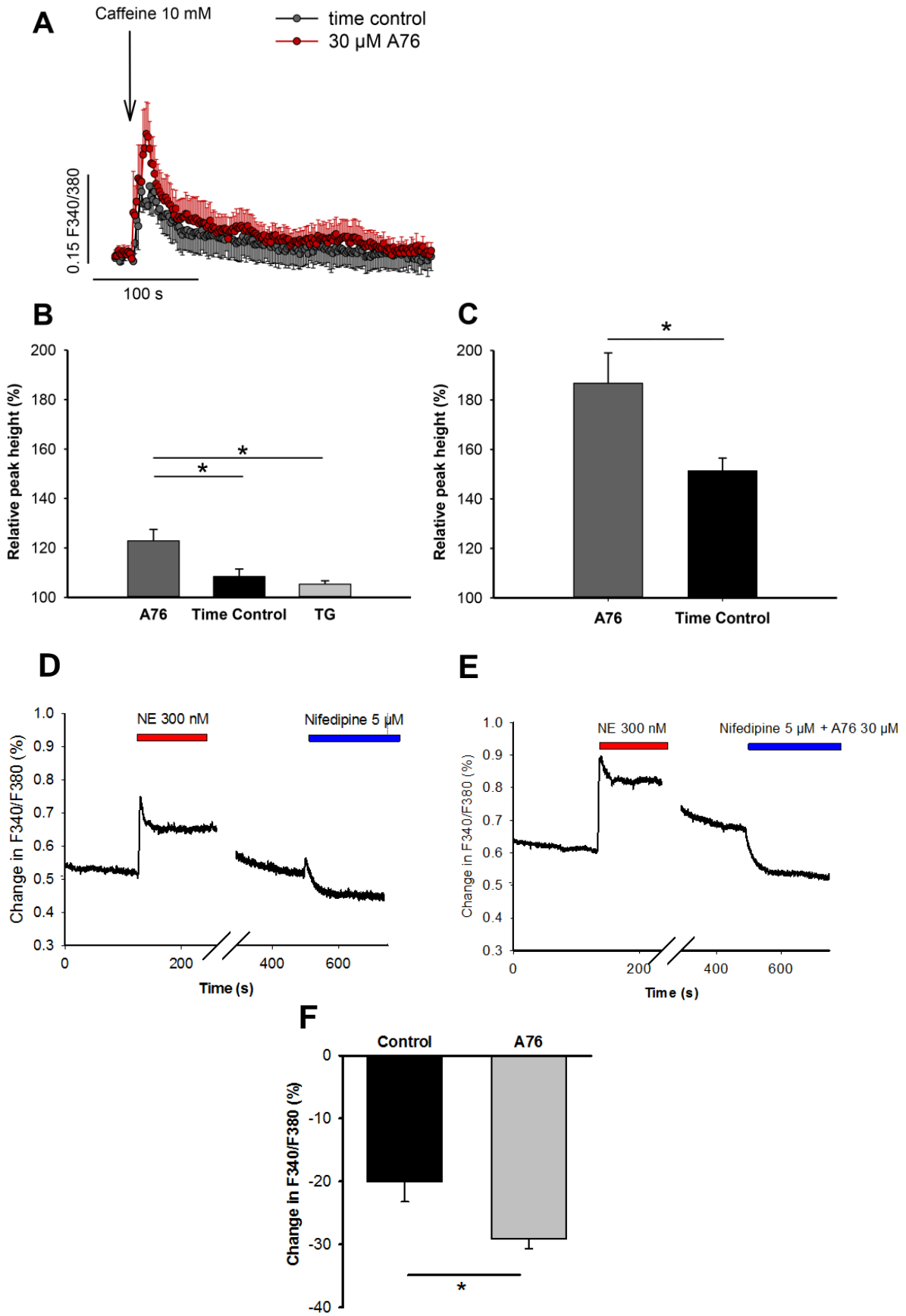
Fig. 3.7: A: **Increased SERCA activity upon AMPK stimulation**. **A**: Stimulation of calcium release *via* caffeine (10 mM) under calcium-free conditions elicited a smaller calcium transient in the time control vessels (dark triangles) compared to AMPK activated vessels (grey circles). **B**: In hamster arteries, as well as in mouse arteries (**C**), 1 mM caffeine and 10 mM caffeine, respectively, induced higher transients after A76 pretreatment than under control conditions. This transient could be inhibited by thapsigargin (TG, **B**). There was no statistically significant difference between the native state (time control) and thapsigargin, albeit the tendency suggests an intermediate store filling. **D, E**: Representative original registrations of intracellular calcium $[Ca^{2+}]_i$ in an isolated vessel. Nifedipine (Nif, 5 µM) was applied alone (**D**) or in combination with A76 (30 µM, **E**). The resulting reduction in $[Ca^{2+}]_i$ was calculated as percent of the maximum calcium reduction under calcium-free conditions. In both cases, the previous calcium response to norepinephrine (300 nM) is shown for comparison. **F**: Upon blockade of extracellular calcium influx by nifedipine (5 µM), AMPK stimulation with 30 µM A76 caused a significantly stronger $[Ca^{2+}]_i$ reduction. (**B:** n=5-9, *=$P<0.05$, Kruskal-Wallis test, Dunn's method, **C:** n=4 each, **D-F**: n=7-9,*=$P<0.05$, t-test). Taken from Schneider&Schubert et al.(Schneider et al., 2015).

3.9 Increased phosphorylation of the SERCA modulator phospholamban in microvascular smooth muscle after AMPK stimulation.

Since phospholamban is an important modulator of SERCA activity in many tissues(Eggermont, Wuytack, Verbist, & Casteels, 1990) we studied its expression and potential changes of its phosphorylation state in mouse microvessels. Quantitative PCR and Western blot experiments showed mRNA and protein expression of phospholamban in small mesenteric resistance arteries (Fig. 3.8). The protein was expressed in much smaller amounts than observed in cardiac muscle tissue (not shown) so that several vessel segments had to be pooled. After incubation with submaximal dilator doses of the AMPK activator A76, the phosphorylation of phospholamban at the regulatory Thr17 site (Fig. 3.8B) was significantly increased in vessels from both vascular regions.
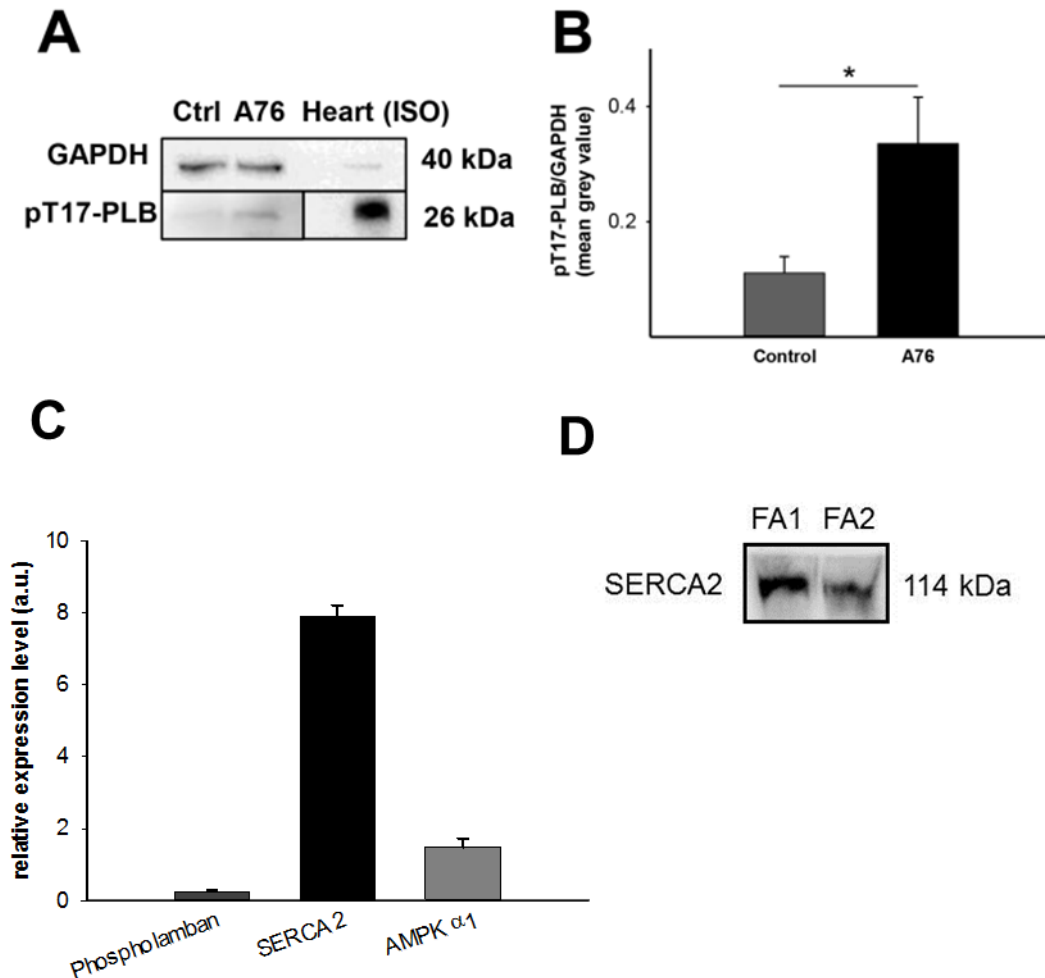
Fig. 3.8: Increased phosphorylation of the SERCA modulator phospholamban in vascular smooth muscle after AMPK stimulation. **A**: Representative Western blot from pooled femoral arteries to assess phosphorylation of phospholamban at threonine 17 (pT17-PLB, 24 kDa) in pooled arteries stimulated with norepinephrine and treated either with 30 µM A76 (A76) or with solvent only (0.03 ‰ DMSO, Ctrl). A76 increased PLB phosphorylation. Heart tissue ("Heart") stimulated with isoprenaline (ISO) was used as a positive control.
B: T17 phosphorylation in A76 stimulated arteries was 3-fold higher than in vehicle treated control (n=4, *=P<0.05, paired t-test).
C: Relative mRNA levels in mouse mesenteric arteries show comparably low quantities for phospholamban (pln) in contrast to SERCA 2 (atp2a2). For comparison with mRNA levels of an already confirmed transcript AMPK alpha 1 (prkaa1) was also amplified (n=3 qPCR reactions from 3 different cDNA isolates). **D**: Representative Western blot from 2 hamster femoral arteries (FA) which confirms the expression of SERCA2. Taken from Schneider&Schubert et al.(Schneider et al., 2015)

3.10 Small persistent remaining dilation after blockade of BK_{Ca}- and SERCA-mediated calcium decrease.

As shown in Fig. 3.6A, the combined inhibition of BKca channels and of SERCA largely abolished the acute dilator response and the calcium decrease induced by AMPK stimulation. However, since a small, obviously calcium independent dilation persisted, we analyzed this dilation further and over a longer time period. A longer exposure of de-endothelialized mouse arteries, pre-constricted with 125 mM K^+ (full inactivation of potassium channels) and pre-treated with the SERCA inhibitor thapsigargin induced a slowly developing dilation upon stimulation with PT1 (Fig. 3.9A) reaching a plateau (48 % of maximal dilation) after 35 min. This dilation was calcium independent as shown in Fig. 3.9B and 3.10B.
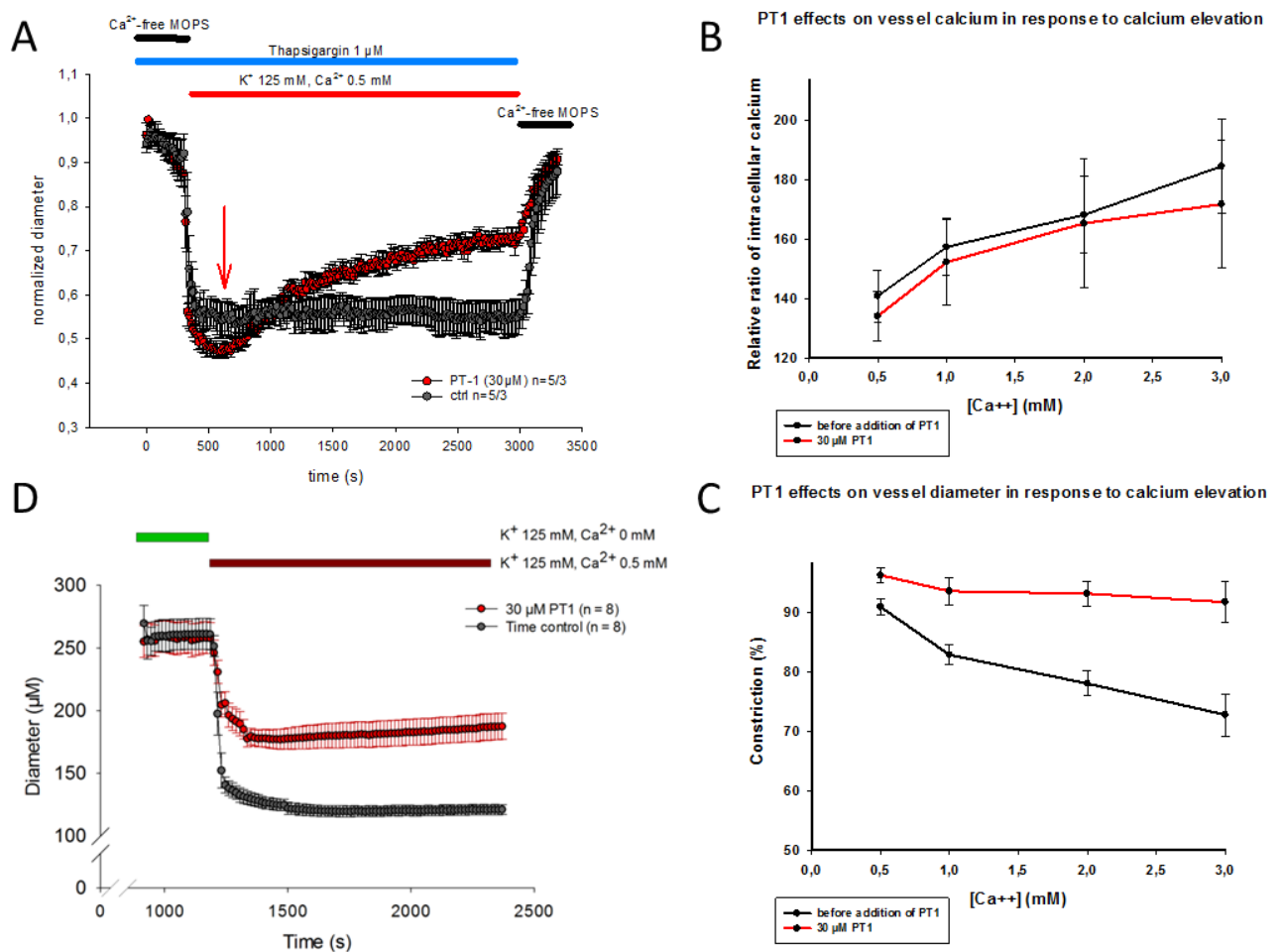
Fig. 3.9: Remaining dilation in de-endothelialized, Tharpsigargin and high potassium pre-treated vessels caused by AMPK activation. A, De-endothelialized arteries were pre-

incubated in Ca^{2+}-free MOPS buffer. Tharpsigargin followed by high potassium (125mM) MOPS were applied to inhibit SERCA and BK_{Ca} activity, respectively. After ten minutes (red arrow) PT1 (30 μM, red curve) or DMSO (0.03%, grey curve) were added to the organ bath and the diameter continuously recorded. Dilation after 40 minutes was 49 % ± 1.5% for PT1 and 0% ± 3.3% for control vessels (p=0.0212, t-test: AUC PT1 vs. AUC ctrl; 600-3000 s). Vessels were normalized to their initial maximal diameter in Ca^{2+}-free MOPS buffer. PT1 decreases Ca^{2+} sensitivity of mouse mesenteric arteries: Cannulated arteries were subjected to increasing concentrations of extracellular calcium in high potassium (125mM) MOPS buffer and their diameter (**B**) and intracellular calcium (**C**) continuously recorded. The graphs depict the constriction before (black) and after addition of PT1 (red) in the same artery. While the intracellular Ca2+ increase was the same before and after application of PT1, PT1 incubation caused a significant impairment of contractility starting from 1 mM extracellular Ca^{2+} concentration (**P<0.01; ***p<0.001 PT1 vs. before PT1 addition; Two Way ANOVA, Holm-Sidak). This change in contractility was absent in time control vessels which were treated with an identical protocol but without PT1 in the second step (not shown). Relative ratio was normalize to $[Ca^{2+}]_i$ values in Ca^{2+}-free MOPS (100%). **D,** Likewise, PT1 pre-incubation inhibited the constriction upon addition of high potassium by 52% compared to DMSO treated vessels. Modified from Schubert&Qiu et al. in revision.

3.11 Reduced Ca^{2+} sensitivity of VSMC after prolonged AMPK activation.

To further substantiate the calcium independent nature of the dilation, mesenteric arteries were depolarized by using high (125 mM) extracellular K^+ concentrations. Under these conditions of continuously opened voltage dependent calcium channels, increases of extracellular Ca^{2+} concentrations starting from zero Ca^{2+} induced respective changes in intracellular Ca^{2+} as measured by Fura2 ratios (Fig. 3.9B and 3.10B). Pre-incubation with the AMPK-activators PT1 and A76 significantly impaired the constriction induced by the elevations of cytosolic Ca^{2+} (Fig. 3.9C and 3.10A). PT1-induced impairment of constriction was stronger than in A76-treated arteries (not shown). The concentrations of both compounds used induced at least 60% acute dilation of arteries pre-constricted with norepinephrine (Fig. 3.2 C, E). Wash-out of the AMPK activators partly reversed their inhibitory effect (not shown). The $[Ca^{2+}]_i$ increases induced by the stepwise increase of extracellular Ca^{2+} concentrations were virtually the same under all three conditions, suggesting a reduction of Ca^{2+} sensitivity caused by AMPK activation (Fig. 3.9C and 3.10A). Likewise, PT1 pre-incubation reduced the ability of mesenteric arteries to constrict in response to potassium depolarization by ~50% compared to DMSO-incubated control vessels (Fig. 3.9D).
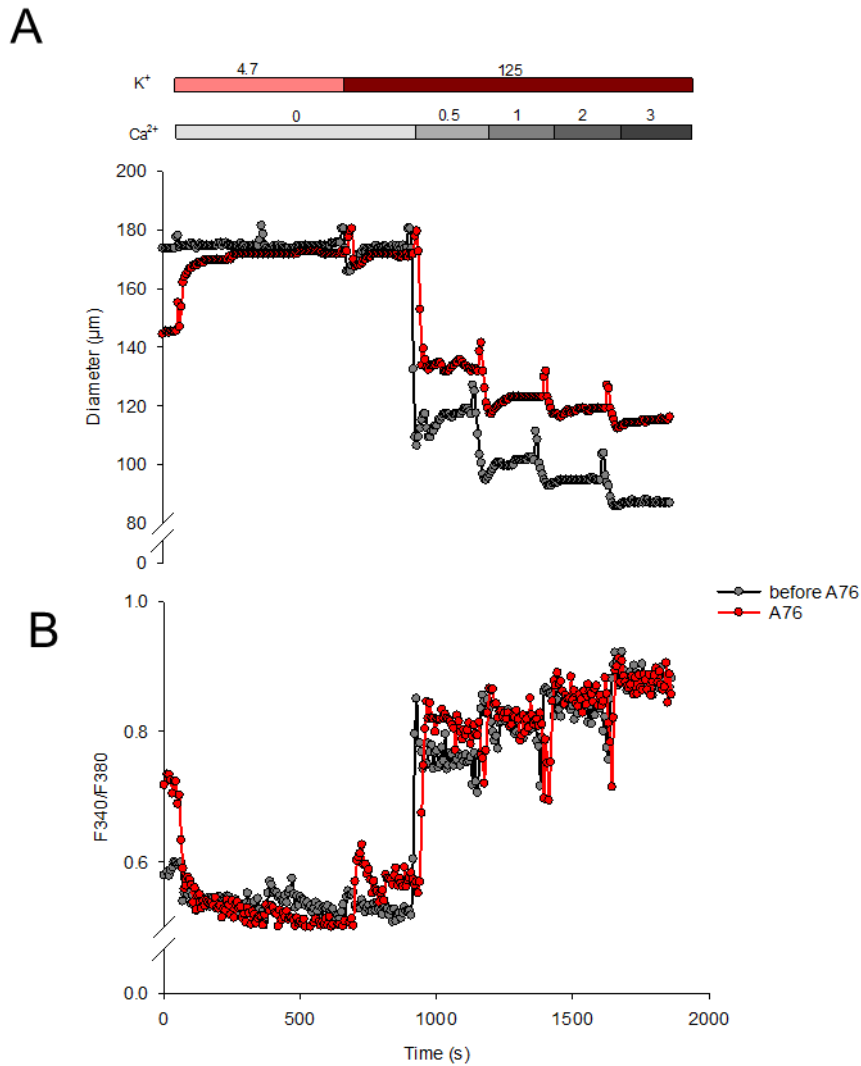
Fig. 3.10: Ca^{2+} sensitivity curves conducted on pressurized arteries. Typical experimental trace showing that A76 (red circles) caused a significant decrease in contractility **(A)** to increasing concentrations of extracellular Ca^{2+} while the intracellular Ca^{2+} increase was not significantly different **(B)**. Taken from Schubert&Qiu et al. in revision.

3.12 Unchanged MLC$_{20}$ and MYPT1 phosphorylation status after pre-activation of AMPK prior to constriction.

To study whether the reduced calcium dependency was due to an enhanced activation of myosin phosphatase, single mesenteric arteries pre-treated with high K$^+$ and thapsigargin in the presence or absence of the AMPK stimulator PT1 were snap frozen after 20 minutes incubation and processed as described. Neither the phosphorylation of MLC$_{20}$ nor the phosphorylation of regulator of from time controls in

51

spite of the fact that PT1 had induced a dilation of 48 % at this time point. In contrast, incubation with the Rho kinase inhibitor Y27632 (Y27, 10 µM), taken as positive control, caused a dephosphorylation of T853 as well as of MLC_{20} (not shown). T696 phosphorylation of MYPT1 by rho kinase inhibition was not affected. Similar results were obtained in a separate series on mouse tail arteries stimulated with PT1 under isometric conditions (not shown).
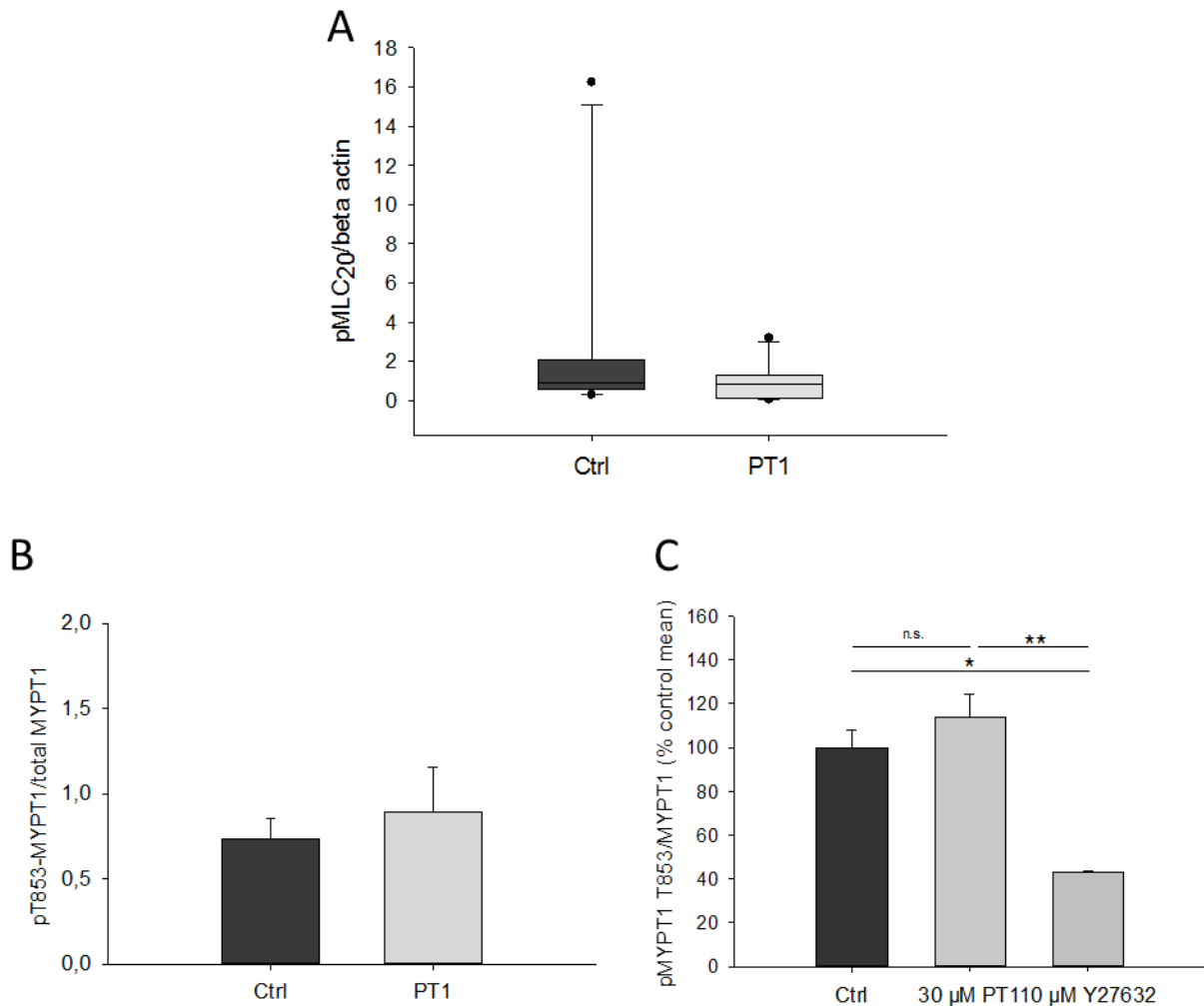
Fig. 3.11: AMPK does not change MLC_{20} or MYPT-phosphorylation status. A, MLC_{20} phosphorylation was not significantly different between control and AMPK stimulation by PT1. B, No differences in MYPT1- phosphorylation status (p=0.695, Signed Rank Test). C, These data were confirmed in an isometric setup on mouse tail arteries. ROCK-inhibition by Y27632 as a positive control caused a significant reduction on T853 of MYPT1. *p<0.05 vs ctrl and **p<0.01 vs. PT1, One Way ANOVA, Holm-Sidak. Taken from Schubert&Qiu et al. in revision.

3.13 No effect of PT1 on MLCK.

In order to test if AMPK causes vasodilation by inhibiting MLCK function, another important regulator of VSMC calcium-sensitivity, we incubated our arteries with the MLCK-inhibitor ML7 (10 µM) before adding 125 mM K^+. The constriction in the presence of ML7 had significantly prolonged constriction half-life compared to AMPK treated arteries, suggesting AMPK does not regulate Ca2+-independent vasodilation by inhibition of MLCK.
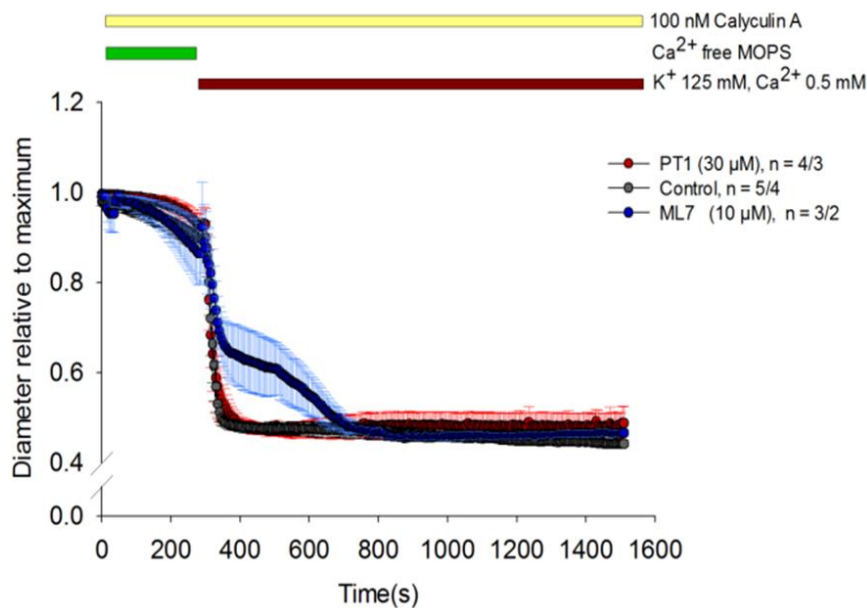
Fig. 3.12: Different dilation kinetics after PT1 and ML7. All arteries were pre-incubated with CalyculinA to block MLCP function and constricted with high extracellular potassium concentrations in the additional presence of DMSO (control group), PT1 or ML7 (MLCK inhibitor). While constriction kinetics of PT1-treated vessels do not differ from those of the control group, ML7-treated arteries depict substantial delay of full constriction. (PT1: n=4, Ctrl: n= 5, ML7: n=3).

3.14 Increased G-actin levels in intact arteries after prolonged AMPK activation.

Single cannulated arterial segments were snap-frozen after 20 min with high potassium (125mM) MOPS buffer in the presence of PT1 or solvent (DMSO). Arteries pre-treated with PT1 showed significantly higher G-actin levels compared to DMSO-treated ones (Fig. 3.13 A).

The AMPK-induced G-actin formation was compared with the effect of other compounds known to affect the actin cytoskeleton. In this series of experiments we

stained isolated and cannulated arteries with DNAseI and phalloidin to label G-actin and F-actin, respectively. All effects were compared to jasplakinolide, an agent that stimulates actin polymerization and hence maximizes F/G-actin ratio. The other end of the F/G-actin ratio spectrum was marked by stimulation with latrunculin A, an agent that inhibits actin polymerization. The F/G actin ratio observed after PT1 was close to the low values induced by latrunculin A. Of note, inhibition of LIMK with Limki3 led to similarly low F/G -actin ratios as PT1, suggesting LIMK itself or one of its downstream targets being involved in the AMPK-induced vasodilation (Fig. 3.13C). Inhibition of AMPK via compound C yielded ratios comparable to jasplakinolide despite concomitant stimulation with PT1. Also, in cultured human VSMC AMPK induced a decrease in the F/G-actin ratio when compared to control (not shown).
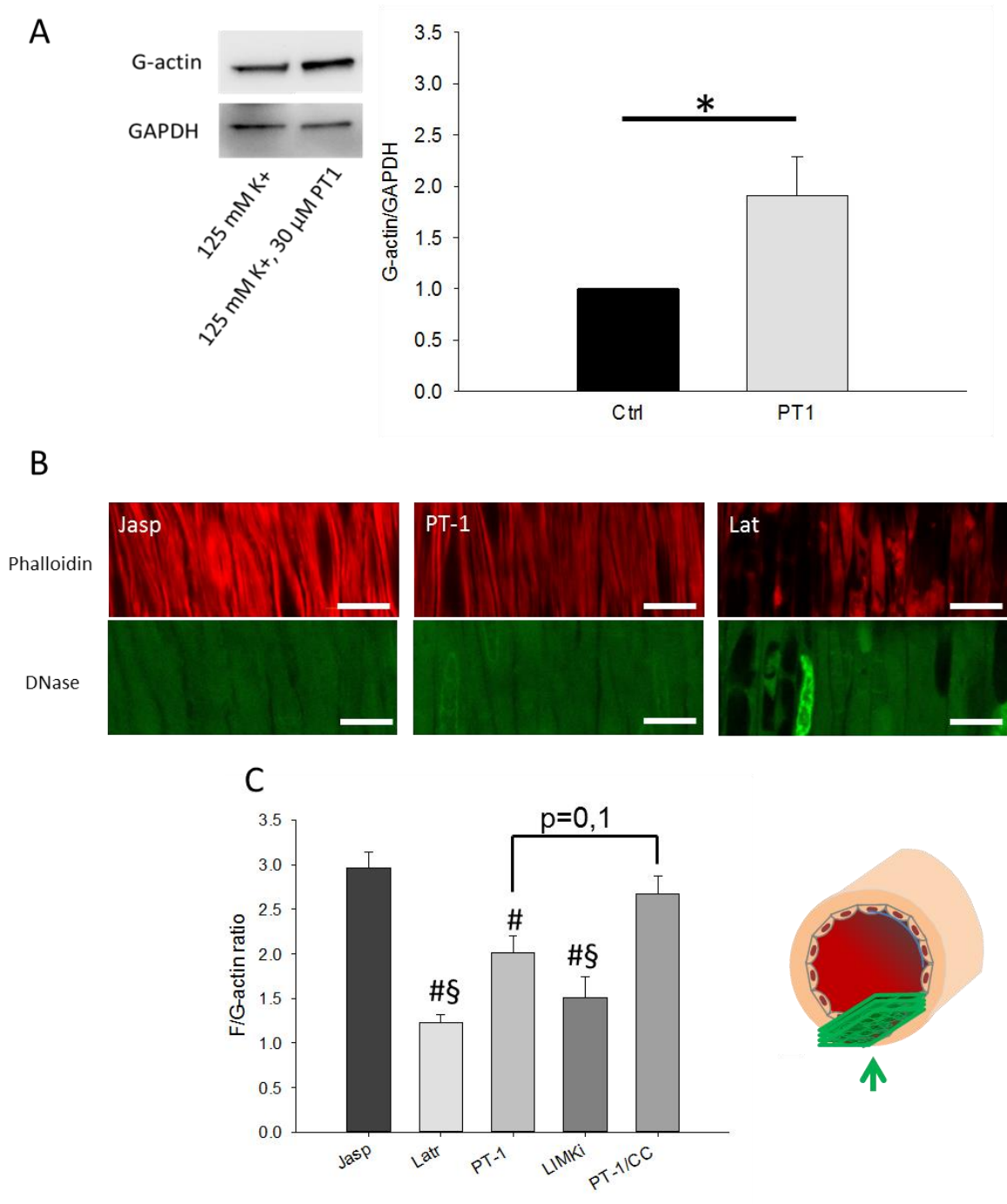
Fig. 3.13: A, G-actin content of single pressurized arteries was significantly enhanced in response to AMPK activation (*p<0.05, Mann-Whitney Rank Sum Test). Likewise, AMPK activation caused a decrease of F/G-actin levels as detected by immunofluorescence signals from isolated pressurized arteries. **B** shows representative images (z stacks, 3 μm depth) in VSMC of arteries stained with phalloidin (F-actin, red) and DNAse I (G-actin, green). Jasplakinolide (Jasp) and Latrunculin A (Lat) as respective enhancer and inhibitor of actin polymerization were chosen as positive and negative control. PT1 application showed a decrease in the F-actin signal while it increased the G-actin signal causing a lowering of the F/G-actin ratio. **C,** quantitative analysis of the images depicted in **B**. Interestingly, PT1 inhibition by Compound C increased the F/G-ratio to about the same degree as jasplakinolide, whereas LIMK inhibition by LIMKi3 as well as Y27632 (Y27) incubation changed the F/G-ratio to levels comparable to AMPK activation. # p<0.05 vs. Jasp; § p<0.05

vs. PT1/CC; One Way Repeated Measures ANOVA, Shapiro-Wilk. Taken from Schubert&Qiu et al. in revision.

3.15 Decreased mean actin filament thickness and filament network branching points in cultured human smooth muscle cells upon AMPK activation.

Confocal images of human umbilical artery smooth muscle cells (HUASMC) revealed that upon AMPK activation by PT1, actin filaments were significantly thinner by 7.4 ± 1.6 % (Fig. 3.14B). Moreover, AMPK activation increased the average length of filaments between branching points, suggesting reduced ramification (Fig. 3.14C).
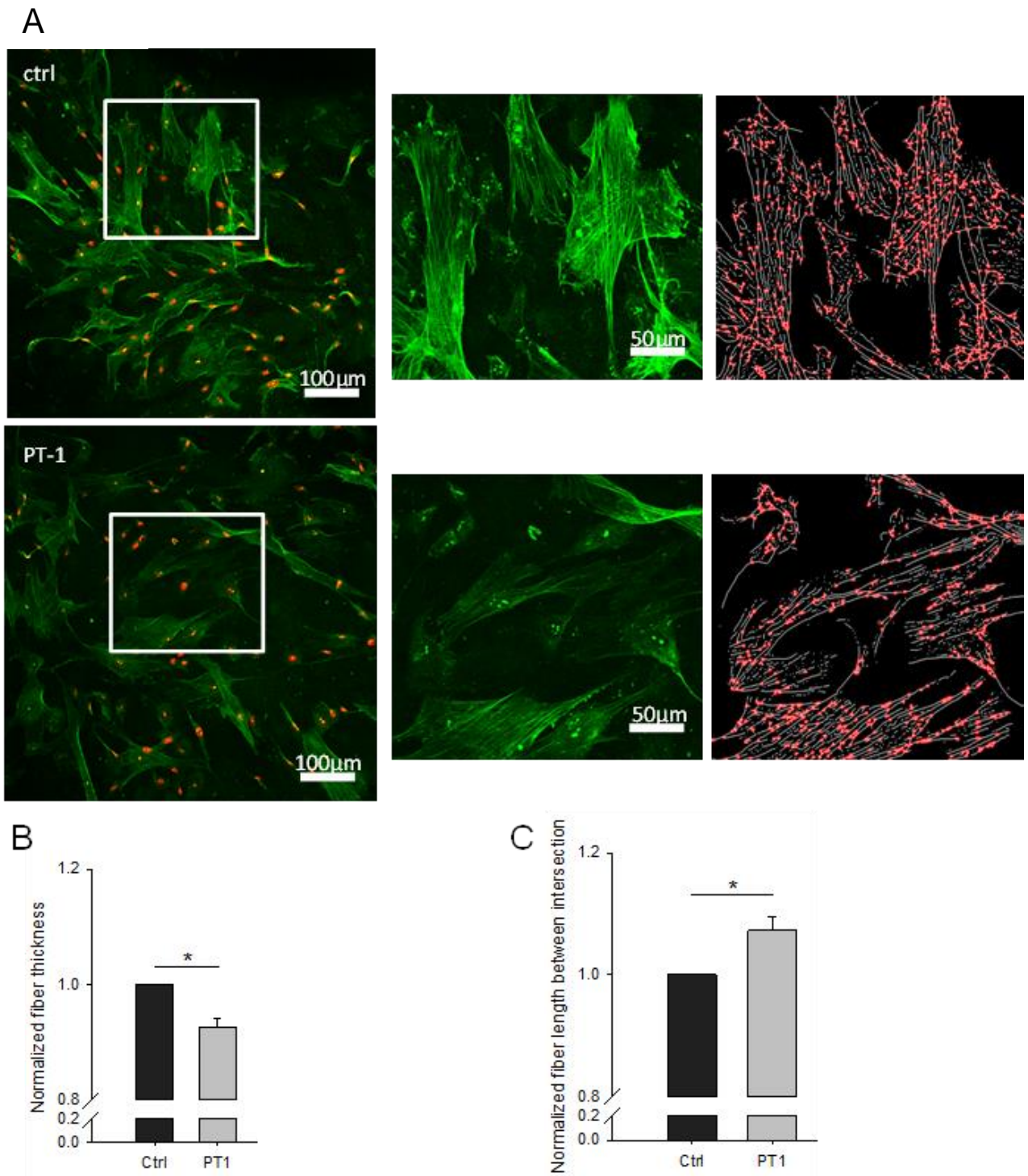
Fig. 3.14: A, representative images stained for alpha-actin (green) in cultured HUASMC (nuclei: red): areas with comparable nuclei count were chosen, pre-processed (for algorithm: see methods) and thereafter the filament thickness and intersection density (normalized by measuring the filament length between intersections) analysed. Left column: overview, second column: magnification of the marked fields in column 1(showing alpha actin only), right column: after pre-processing, mask for analysis of intersection points. HUASMC were stimulated, fixated and stained for alpha-actin and phalloidin. **B,** PT1 significantly decreased

filament thickness as compared to DMSO treated cells. **C,** indirect measurement of branching point density by calculating the filament length between intersections revealed an increase after PT1 incubation suggesting reduced intersections and branching points. *p<0.05 paired t-test. Modified from Schubert&Qiu et al. in revision.

3.16 AMPK-dependent rarefaction of F-actin in living arterial VSMC in situ.

Vessels from mice expressing LifeAct (Riedl et al., 2010) were used to test the effect of AMPK activation on dynamic changes of the actin cytoskeleton. The vessels were kept under isometric conditions in a wire myograph to avoid confounding effects by changes of vascular diameter and hence, muscle length and thickness. Vessels were first studied after stimulation with high K^+. Thereafter, PT1 was added to the organ bath. In a third step, the AMPK inhibitor compound C was added. PT1 led to a loss of the LifeAct/F-actin signal preferentially in the middle of the cells, an effect that was reversed upon addition of compound C in the continuous presence of PT1. The recovery of the signal in the center part excluded simple bleaching of LifeAct (Fig. 3.15B). In accordance with a change of filament arrangement the anisotropy of the actin signal increased after PT1 and decreased again after inhibition of AMPK (Fig. 3.15D). These findings were confirmed in an additional experimental series on pressurized arteries (Fig. 3.16). In these arteries, LIMK inhibition again mimicked the augmenting effects of PT1 on anisotropy. Likewise, compound C blunted AMPK-mediated filament anisotropy increase.
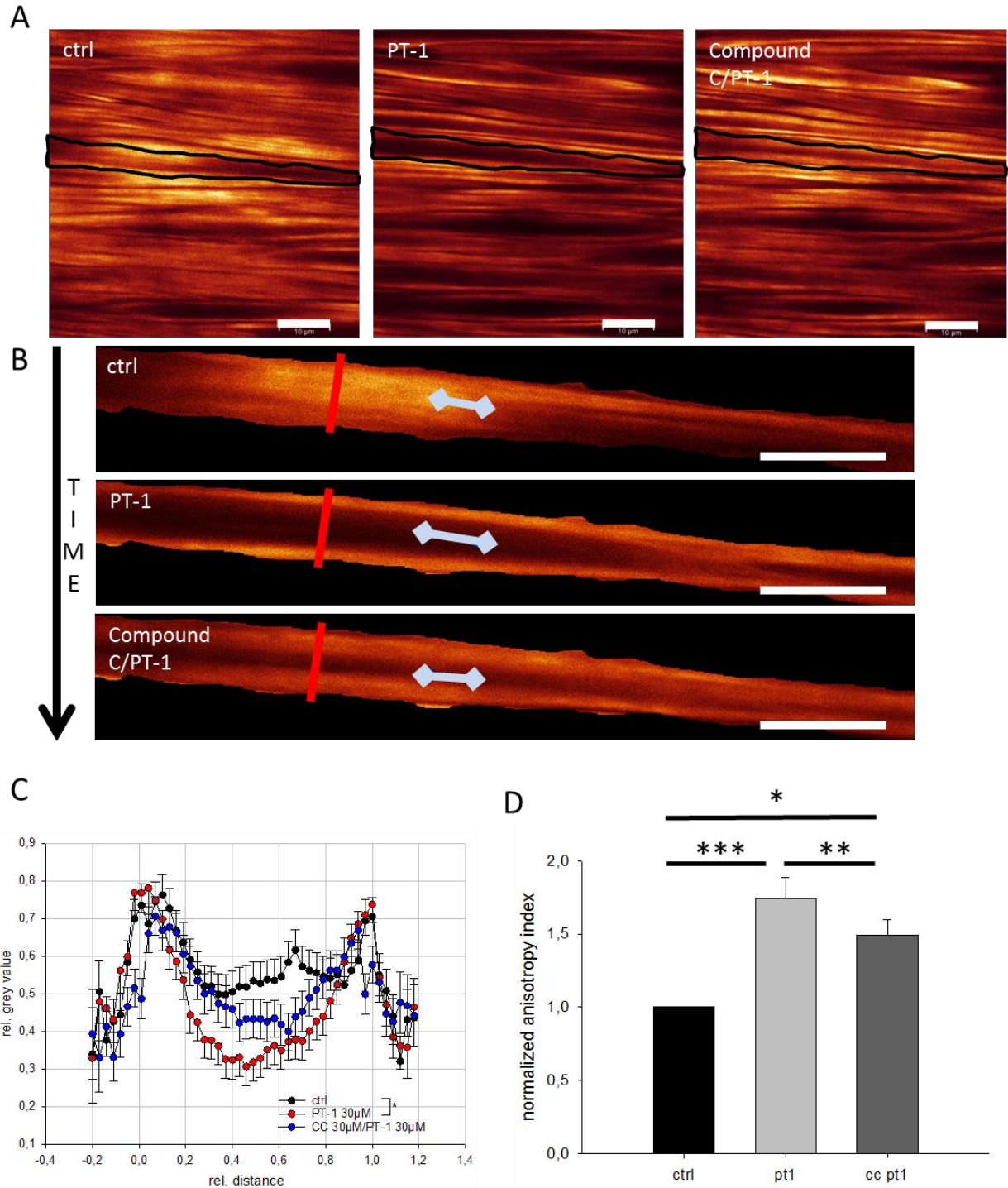
Fig. 3.15: Mesenteric arteries from LifeAct mice were fixed in an isometric setup and subsequently stimulated with high potassium (K$^+$ 125 mM) for ten minutes, followed by PT1 (30 μM) for 90 minutes and compound C/PT1 (15 μM/30 μM) for additional 30 minutes. **A,** PT1 causes a decrease in LifeAct signal intensity which was most notably in the center part of the VSMCs. This decrease was partly reversible after compound C incubation. **B,** shows a representative cell highlighted in **A**. The surrounding cells are cleared for better detection of the cell borders and clarification of the quantitative analysis in the artery samples: The red line represents a typical cross-section for grey value calculation via plot profile analysis and the length of the blue line is a graphical representation of the calculated anisotropy. AMPK

activation causes a central darkening which could be stopped and led even to the restoration of central F-actin signal after application of compound C. All scale bars 10 µm. **C**, summary of plot-profiles depicting the significant mid-central darkening after PT1 application (*p=0.019 AUC PT1 vs. AUC ctrl) which is partly reversed after AMPK inhibition with Compound C. p=0.259 AUC CC vs. ctrl, Repeated Measures ANOVA, Holm-Sidak. **D,** quantitative analysis of the anisotropy index of individual VSMCs (9 cells per artery) followed over time from isometric LifeAct mice (n = 3). Anisotropy values of each individual VSMC were normalized to their initial values under high K$^+$ conditions (125mM, ctrl). * $p<0.05$, ** $p<0.01$, ***$p<0.001$ (Friedman Repeated Measures ANOVA on Ranks, Tukey). Modified from Schubert&Qiu et al. in revision.
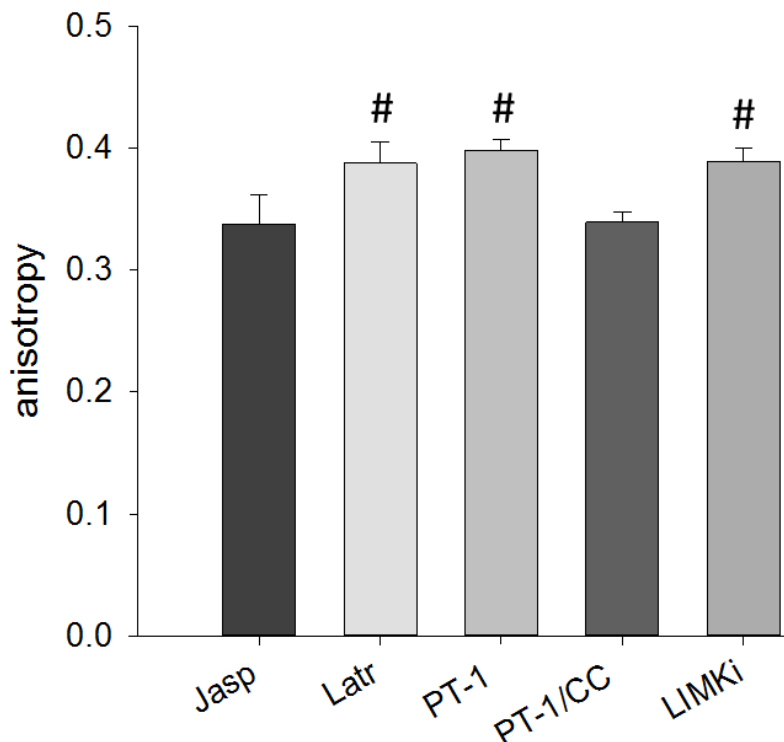
Fig. 3.16: VSM F-actin anisotropy in pressurized arteries. Cannulated arteries were stimulated with high K$^+$ in the presence of either jasplakinolide, an F-actin stabilizing agent, latrunculin A, an actin polymerization inhibitor, PT1, PT1 plus AMPK inhibitor compound C and Limki3, a LIMK inhibitor. Of note, PT1 induced the same anisotropy values as did the actin polymerization inhibitor and the LIMK inhibitor. The PT1-induced effect was reversible by parallel inhibition of AMPK. (Jasp: n= 3, Latr: n= 3, PT1: n= 3, PT1/CC: n=4, Limki: n=3; #p<0.05 vs. Jasp, One Way Repeated Measures ANOVA, Holm-Sidak).

3.17 Decreased cofilin phosphorylation after AMPK activation.

In search for a mechanism by which AMPK could cause actin disassembly we conducted a phosphorylation array of proteins relevant for the actin cytoskeleton in

porcine femoral artery (not shown) and found a reduced phosphorylation status of the actin severing protein cofilin after stimulation with PT1. Since cofilin is known to be inhibited by LIMK-mediated phosphorylation and LIMKi3 treatment mimicked the effect of PT1, further studies were performed in pooled mesenteric arteries. Western blots showed cofilin dephosphorylation after incubation of these arteries with PT1 (Fig. 3.17A). Likewise, immunofluorescence staining of phospho cofilin in pressurized, PT1-treated arteries was reduced as compared to DMSO-treated arteries (Fig. 3.17B-D).
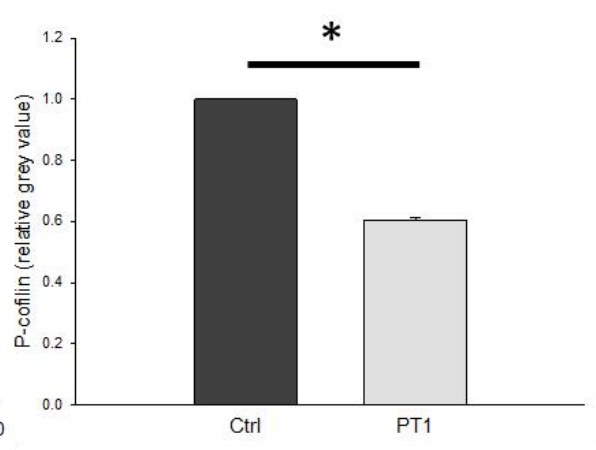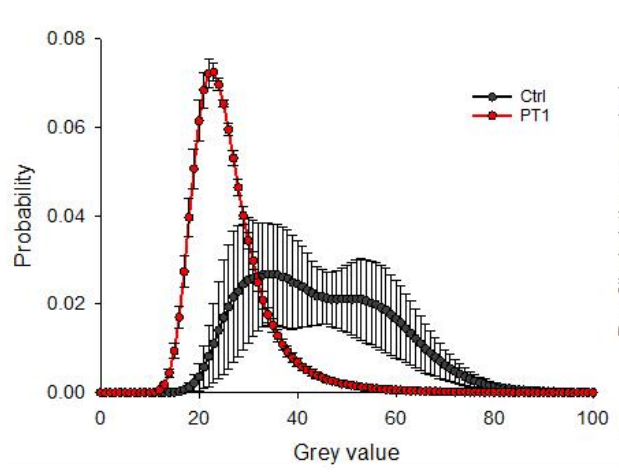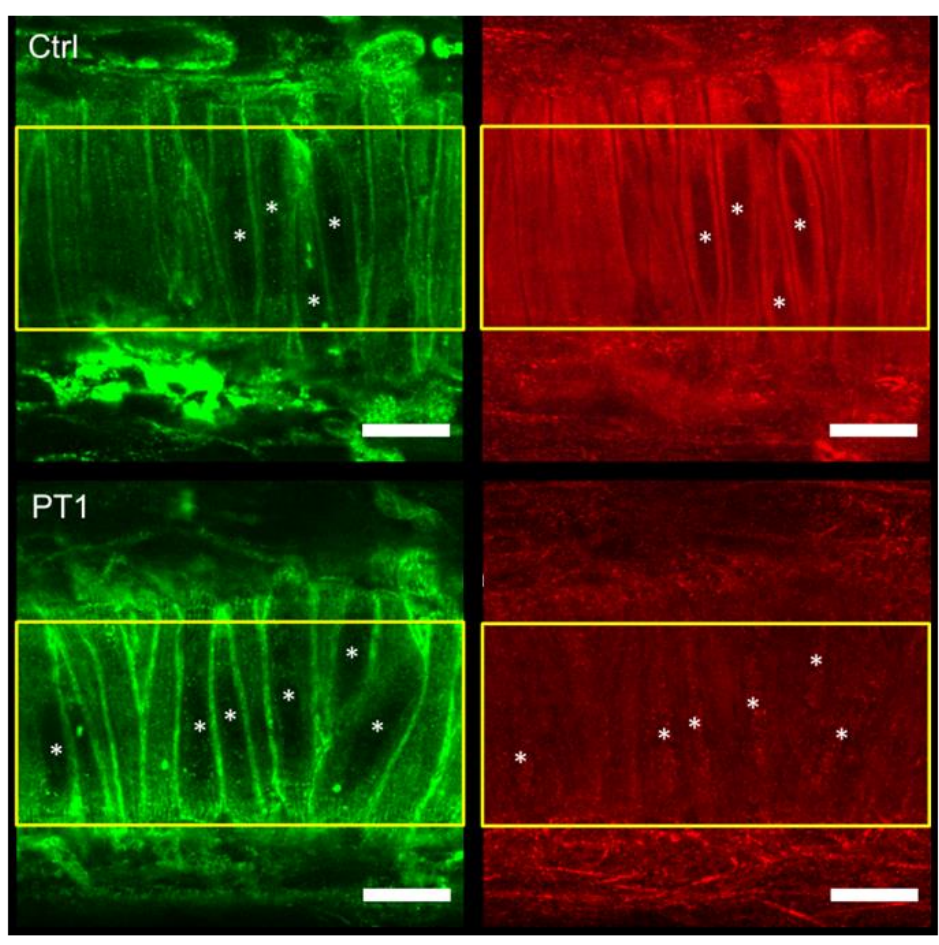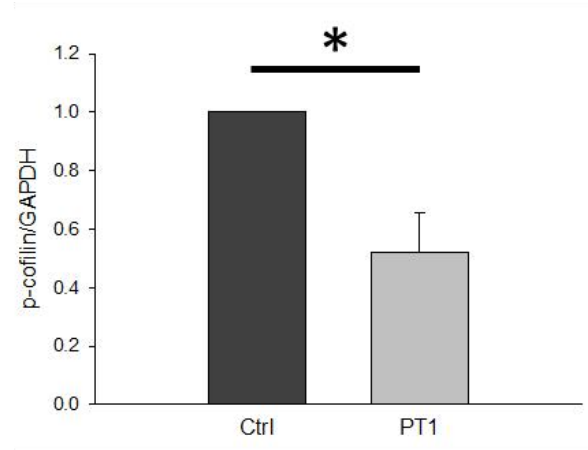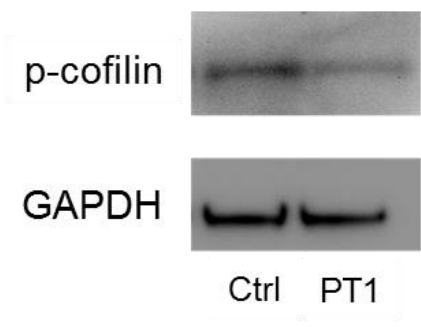
Fig. 3.17: A, Western-Blots conducted in arterial samples showed a significant dephosphorylation of cofilin in PT1 treated mesenteries. *p<0.05, paired t-test. **B**, pressurized arteries which were stained for paxillin (green) as well as for phospho-cofilin (S3, green) showed less phospho cofilin signal after AMPK activation with PT1 compared to DMSO-treated vessels. Comparable paxillin staining between both groups showed sufficient permeabilization and delineated the cell margins and nuclei (white asterisks). **C**, A histogram for quantitative analysis of grey values from indicated central regions of interests (yellow rectangles from Fig. 3.17B) revealed a leftward shift in PT1 treated arteries and a significant reduction in the mean grey value **(D)** *p<0.05, Mann-Whitney Rank Sum Test. Taken from Schubert&Qiu et al. in revision.

3.18 AMPK leads to liberation of Cofilin from 14-3-3

As AMPK as a kinase cannot directly dephosphorylate cofilin we studied a potential mechanism controlling cofilin activity and phosphorylation status. Lysates from porcine coronary artery smooth muscle cells were subjected to co-immunoprecipitation for 14-3-3 and cofilin. AMPK activation led to a significant reduction in 14-3-3-bound cofilin (Fig. 3.18B). This suggests that AMPK could mediate the liberation of cofilin from 14-3-3, hence increasing its free cytosolic fraction exposing it to the influence of an yet unknown phosphatase.
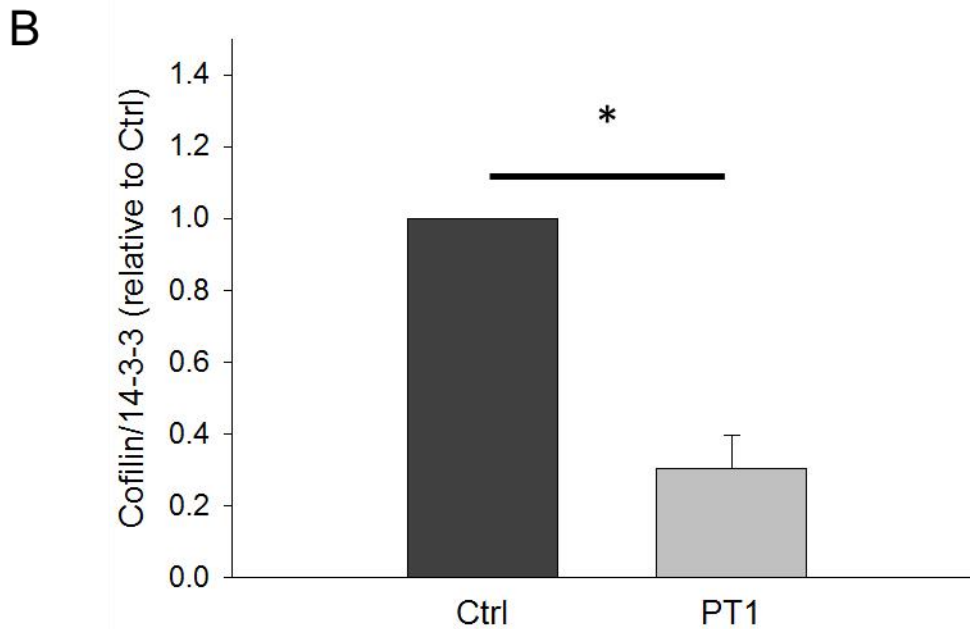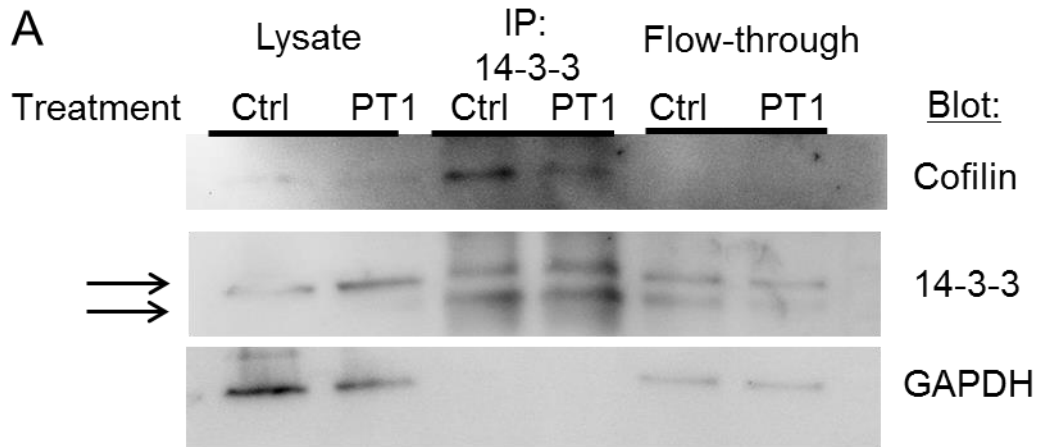
Fig. 3.18: AMPK induces displacement of cofilin from 14-3-3 protein. A, representative Western blot from PCASMC showing that in PT1-treated cells less cofilin co-immunoprecipitates with 14-3-3 protein. Arrows indicate two different molecular weight isoforms of 14-3-3 which were both pulled down by the pan-14-3-3 antibody. Note the enrichment of the lower molecular weight band in the IP groups. B, Quantification of cofilin protein bound to 14-3-3 reveals significantly less bound cofilin in the AMPK-activated state (*p<0.05, paired t-test, n=3). Modified from Schubert&Qiu et al. in revision.

4. Discussion

The main aim of this thesis was the characterization of AMPK as a potential central regulator of microvascular tone. Indeed, we found that AMPK can induce vasodilation of arterial microvessels by causing a substantial decrease of $[Ca^{2+}]_i$ ("Ca^{2+}-dependent dilation") as well as by changing the calcium sensitivity of the contractile apparatus ("Ca^{2+}-independent dilation"). "Ca^{2+}-dependent" vasodilation was found to be due to activation of BK_{Ca} channels and activation of SERCA via PLN Thr17 phosphorylation while "Ca^{2+}-independent" vasodilation is caused by remodeling of the actin cytoskeleton. The latter is achieved via dephosphorylation of actin severing protein cofilin which probably occurs after AMPK-dependent liberation of cofilin from its binding partner, protein 14-3-3.

4.1 Principles of VSMC Signal Tranduction

4.1.1 Regulation of MLC_{20} Phosphorylation

The two key enzymes in the regulation of the MLC_{20} phosphorylation are MLCK and MLCP. The activity of MLCK on the one hand mainly depends on $[Ca^{2+}]_i$ levels and their spatiotemporal distribution (Amberg & Navedo, 2013). While influx of extracellular Ca^{2+} is primarily regulated by the activity of L-type Ca^{2+} channels (LTCC) (Navedo & Amberg, 2013) and some transient receptor cation channel subtypes (TRPs) (Earley & Brayden, 2015) the intracellular calcium concentration is also determined by Ca^{2+} removal from the cytosol as achieved by SERCA and potentially, the activity of the sodium/calcium exchanger. Although $[Ca^{2+}]_i$ is predominantly associated with contraction processes of VSM it also controls numerous enzymes and transcription factors and therefore, ultimately, the VSM phenotype. Calcium handling in VSM is highly compartmentalized and requires a highly orchestrated network of several channels and regulating proteins to produce calcium sparklets, sparks, waves or store operated calcium entry (SOCE) (Brozovich et al., 2016). Local transient increases in cytoplasmic Ca^{2+} resulting from influx through single or small clusters of LTCCs are defined as Ca^{2+} sparklets and are closely coupled to changes

in membrane potential. LTCC Ca^{2+} sparklets require a pentadic complex involving the plasmalemmal anchor protein and LTCC-regulator AKAP150, the protein kinases PKC and PKA, and the counteracting phosphatase calcineurin (Navedo & Amberg, 2013). The LTCC-containing microdomains closely interact with several TRP-channels of which TRPV4 and TRPM4 have been best described so far (Earley & Brayden, 2015). Highly restricted, large amplitude Ca^{2+} release events through SR RyRs are defined as Ca^{2+} sparks and can be divided into sparks coupled to Ca^{2+} gated K^+ channels on the one side and Cl^- channels on the other side. The central player of the Ca^{2+} gated K^+ channel-coupled sparks is the large conductance potassium channel (BK_{Ca}) whose changes in expression and function have been linked to pathogenesis as well as to compensatory alterations in hypertensive disease (Cox & Rusch, 2002; Nieves-Cintron, Amberg, Nichols, Molkentin, & Santana, 2007). BK_{Ca} channel expression and splice variants differ between vascular beds and contribute to functional distinctions between them (Nourian et al., 2014). Further channels involved in the generation of Ca^{2+} sparks belong to the Cl^- channel family (CACC: TMEM16 and bestrophins) and are rather poorly described due to their still unknown molecular identity and lack of specific targeting compounds (Matchkov, Boedtkjer, & Aalkjaer, 2015). Ca^{2+} waves are Ca^{2+} signals triggered by the opening of sarcoplasmic reticulum IP3Rs and RyRs which causes a self-renewing wave of Ca^{2+} release events across the entire length of VSMC, usually close to the plasma membrane. Eventually, waves contribute to the so-called calcium induced calcium release (CICR) and allow for a more homogenous contraction of VSM. They depend on the activity of phospholipase C (PLC) and its upstream activators like endothelin or norepinephrine (Amberg & Navedo, 2013; Lamont, Vainorius, & Wier, 2003). The SR Ca^{2+} sensor STIM1 (stromal interaction molecule) and certain TRP channels (TRPC1,3,6) are associated with Orai [CRAC (calcium release activated calcium channel)] and can influence SOCE and SR calcium handling. Although under physiologic conditions these molecular interactions seems to be of minor importance they appear to be involved in certain forms of hypertension due to VSM phenotype switches (Beech, 2013; Trebak, 2012).

MLC_{20} dephosphorylation on the other hand is catalyzed by MLCP which in turn is regulated by numerous signaling pathways. MLCP is a holoenzyme consisting of a catalytic subunit (PP1c-δ), a 20-kDa subunit of unknown function (M20), and a myosin targeting subunit (MYPT1) (Hartshorne, Ito, & Erdödi, 1998). Major regulators

of MLCP activity include small GTPases, such as Rho, and PKC. Rho activity is controlled by a multitude of guanine nucleotide exchange factors (GEFs), GTPase activating proteins (GAPs), and guanine dissociation inhibitors (GDI) which are all expressed in a tissue-specific manner (Puetz, Lubomirov, & Pfitzer, 2009). When activated Rho can phosphorylate CPI-17 at Thr38, PHI-1 at Thr57 and MYPT1 at both Thr696 and Thr850 (El-Toukhy, Given, Ogut, & Brozovich, 2006; Kitazawa & Kitazawa, 2012; Murányi et al., 2005). Likewise, PKC can phosphorylate CPI-17 at Thr38 and PHI-1 at Thr57 (M Eto, Ohmori, Suzuki, Furuya, & Morita, 1995; Masumi Eto, Karginov, & Brautigan, 1999). Other less well understood kinases which are involved in the regulation of MLCP activity comprise ZIP kinase (ZIPK) and integrin-linked kinase (ILK). All these phosphorylation events inhibit MLCP activity and thus induce vasoconstriction. Because these pathways do not require Ca^{2+} as transmitter they are considered to be calcium-independent (i.e. independent of changes of Ca^{2+}_i) but are able to alter the apparent calcium-sensitivity of the contractile apparatus (Somlyo & Somlyo, 2009).
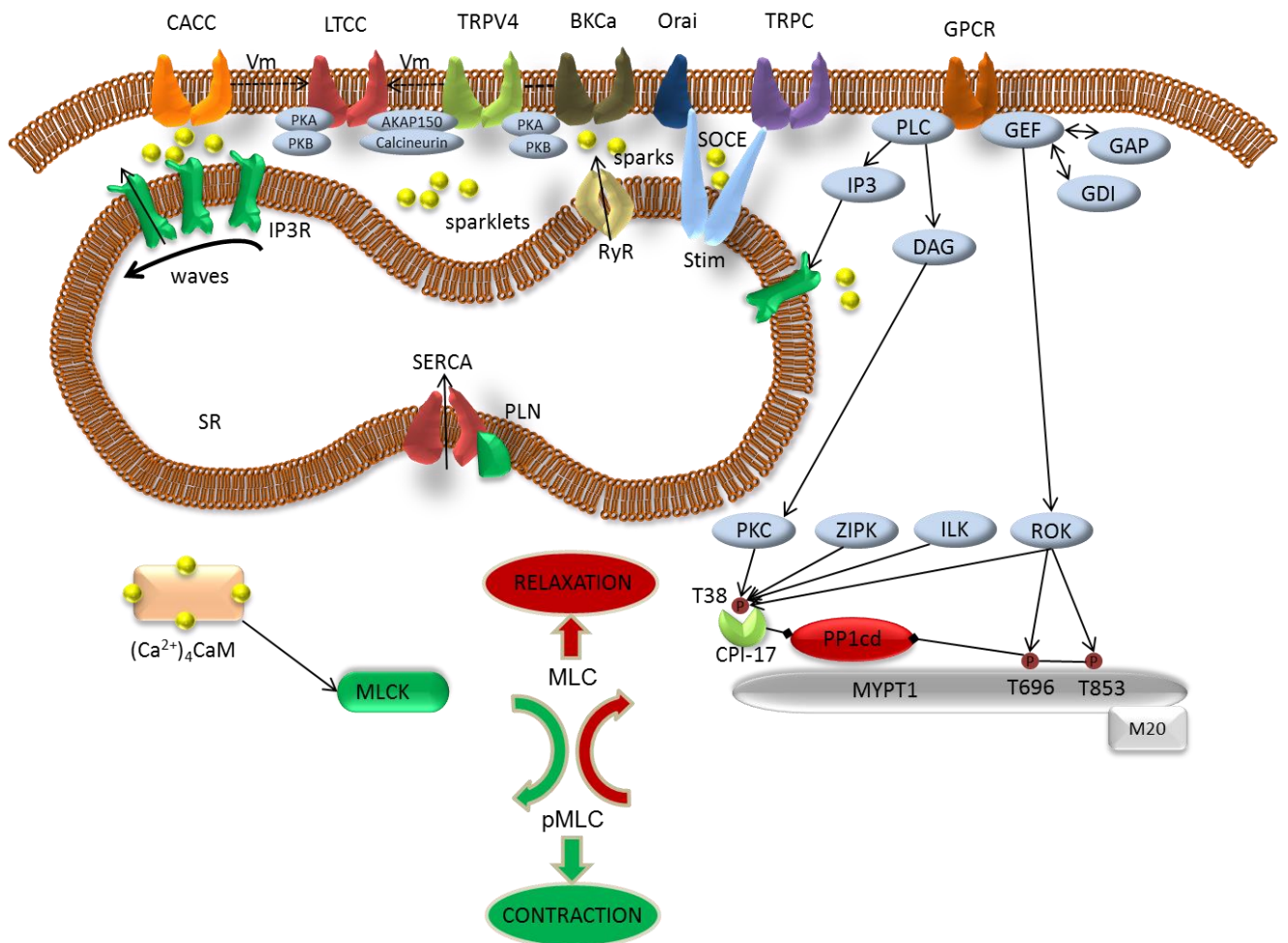
Fig. 4.1: Signaling pathways for regulation of MLC$_{20}$ phosphorylation: The balance of MLCK and MLCP activities defines the level of MLC$_{20}$ phosphorylation and force generation. MLCK is activated by the binding of (Ca^{2+})$_4$ CaM leading to the phosphorylation of MLC$_{20}$ at serine 19 that permits myosin-actin interaction, cross-bridge cycling and contraction. Therefore, MLCK is mainly regulated by VSM calcium handling which is controlled by a highly organized network of receptors, ion channels and their regulating proteins. MLC$_{20}$ is dephosphorylated by MLCP. The activity of the latter is controlled by a handful of kinases which integrate the signals of several signalling cascades and is mostly independent of acute changes of intracellular free calcium.

Abbreviations: CACC (Ca^{2+} gated Cl2 channels), LTCC (L-type calcium channels), TRPV4 (transient receptor potential cation channels vanilloid subfamily member 4), BKCa (large conductance calcium-activated potassium channel), guanine nucleotide exchange factors (GEFs), GTPase activating proteins (GAPs), and guanine dissociation inhibitors (GDI), STIM (stromal interaction molecule), Orai [CRAC (calcium release activated calcium channel)], PKA (protein kinase A), PKB (protein kinase B), AKAP150 (A-kinase anchoring protein 150), IP3R (inositol 1,4,5-trisphosphate receptor), SOCE (store operate calcium entry), MLCK (myosin light chain kinase), MYPT1 (myosin phosphatase-targeting subunit 1), CPI-17 (protein kinase C-potentiated inhibitor protein of 17 kDa), ZIPK (zipper-interacting protein kinase), ILK (integrin linked kinase), ROK (rho associated coiled-coil containing protein kinase 1), DAG (diacylglycerol), IP3 (inositol 1,4,5-trisphosphate), PLC (phopholipase C), SR (sarcoplasmatic reticulum), SERCA (sarcoplasmic/endoplasmic reticulum Ca^{2+} ATPase), PLN (phospholamban).

4.1.2 Cytoskeletal Regulation in contractile VSMC

For a long time neglected because of their apparent mere structural role for VSM, cytoskeletal proteins have recently gained attention because researchers became aware of their implication in fields such as cell migration and vascular remodeling (Brozovich et al., 2016; Gerthoffer, 2005; D D Tang & Anfinogenova, 2008; Yamin & Morgan, 2012). The major types of filaments in cytoskeletal networks besides myosin are: intermediate filaments, microtubules and actin. Studies about the role of intermediate filaments, dystrophin, utrophin, and microtubules in the control of vascular tone are relatively sparse. Nonetheless, they form a cable-like network in VSM connecting non-contractile actin in cytoplasmic dense bodies to membrane-bound focal adhesions. They can dynamically adjust their length and also serve as scaffolds for proteins controlling the tone of VSM (Yamin & Morgan, 2012; J. Zhang, Herrera, Paré, & Seow, 2010).

Actin architecture also undergoes dynamic reorganization via polymerization and depolymerization. A pool of 25-30% of non-sequestered globular actin (G-actin) can undergo polymerization to filamentous (F-actin) in response to pharmacological and mechanical stimuli which can go along with changes of vascular tone (Moreno-Domínguez et al. 2014; D. D. Tang and Tan 2003; D. D. Tang and Tan 2003). Actin assembles at its barbed ends near the membrane while it disassembles on pointed ends on the opposite side (D D Tang & Anfinogenova, 2008). Findings that actin stabilization (e.g. via the compound jasplakinolide) and actin destabilization (e.g. via the compounds latrunculin or cytochalasin D) can go along with VSM contraction warrant investigations of proteins which control actin dynamics. Focal adhesions (membrane dense bodies) in particular have been suggested as the sites of actin dynamics and force transmission for the following reasons: they are highly organized protein-rich domains connecting the actin cytoskeleton via vinculin/talin "force transduction anchors" and integrins to the extracellular matrix and they are the sites where actin filament polymerization is initiated and regulated (Brozovich et al., 2016; Kanchanawong et al., 2010; Poythress, Gallant, Vetterkind, & Morgan, 2013; D D Tang & Anfinogenova, 2008). Cellular proteins described to be involved in VSM actin dynamics in VSM can be divided in protein kinases associated with integrins and/or membrane receptors (Abl, Src, FAK, PAK, MAK), the small RhoGTPases (Rac, Cdc42 and Rho) and actin regulating proteins as effectors of the upstream signaling

pathways (VASP, N-WASP, Arp2/3 complex, cofilin, profilin, HSP family) (Brozovich et al., 2016; Gerthoffer, 2005; Gunst & Zhang, 2008; D D Tang & Anfinogenova, 2008; Yamin & Morgan, 2012). An interesting but largely unknown role in the regulation of the cytoskeleton has been proposed for phosphatases and 14-3-3 adapter proteins (Freeman & Morrison, 2011; Rubio et al., 2004; Sluchanko & Gusev, 2010). Human tissues contain seven 14-3-3 isoforms which interact with more than 300 targets. Whereas their role in carcinogenesis and neurodegenerative diseases due to regulation of apoptosis, cell cycle, proliferation, transcription, replication, functioning of ion channels and organization of cytoskeleton is increasingly valued, their function in VSMC remains largely uninvestigated.
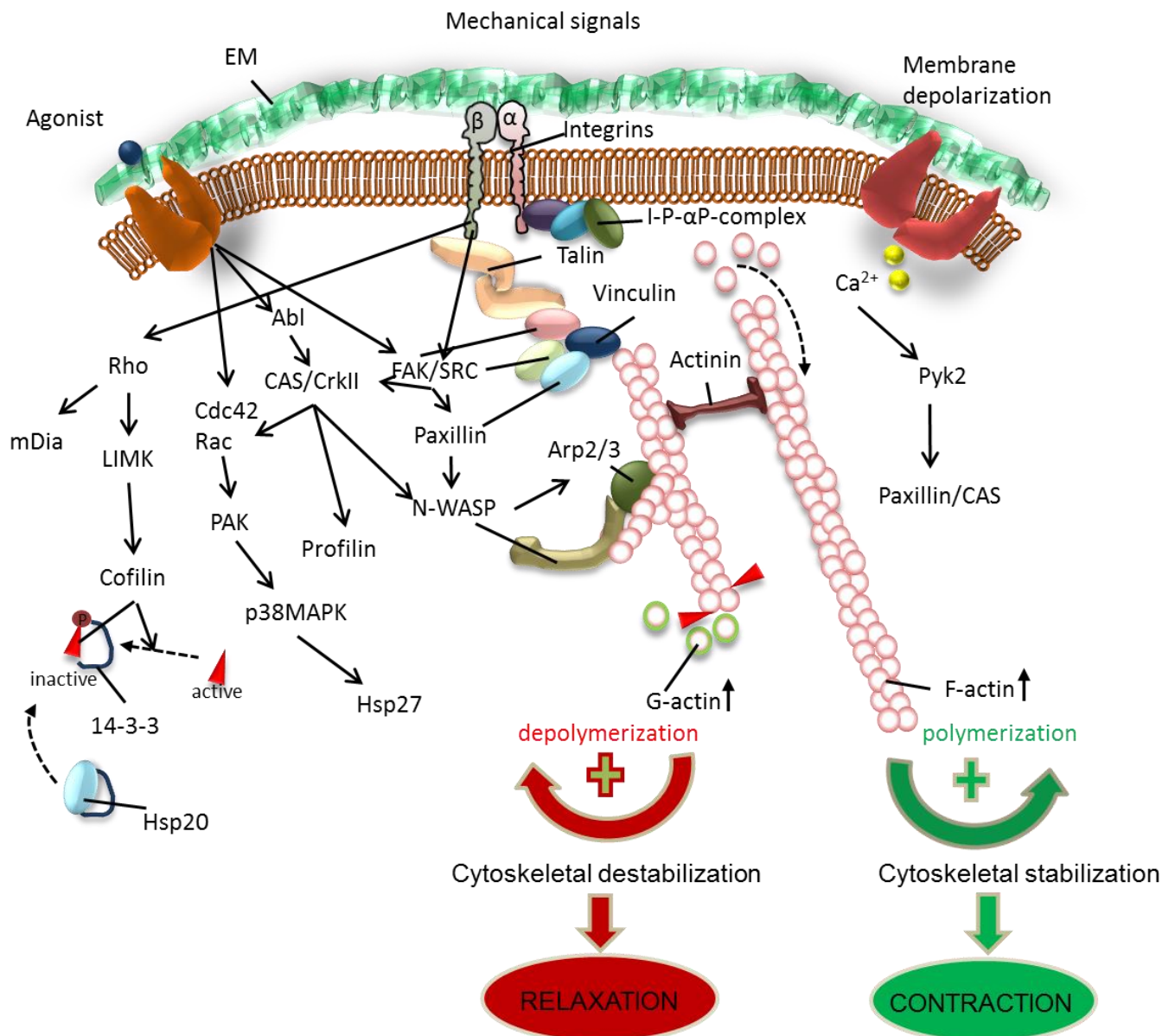
Fig. 4.2: Molecular organisation and signalling cascades for actin polymerization and depolymerisation in VSM: Actin filaments are linked to integrin proteins via actin cross-linking proteins (talin, actinin, paxillin) that bind to the cytoplasmic tails of integrin proteins. Scaffolding proteins regulate the assembly of protein complexes at adhesion junctions (vinculin, α-Parvin, PINCH, ILK). Contractile agonist and mechanical signals activate protein kinases (abl, FAK, src, MAPK, etc.) and small GTPases (Rho, Cdc42 and Rac) especially at sites of integrin clusters in interaction with the scaffolding proteins. Kinase activity regulates the downstream effectors (CAS/CrkII, N-WASP, the Arp2/3 complex, profilin, paxillin/Hic-5, HSP27, cofilin, VASP, etc.) and thus actin polymerization, cytoskeletal stability and VSM contractility. Intracellular Ca^{2+} modulated by electric signals (changes in membrane potential), receptor dependent pathways or FAK/Src may also mediate actin dynamics by regulating the PYK/paxillin/CAS pathway.

Abbreviations: EM (extracellular matrix), I-P-αP (ILK[integrin linked kinase]-PINCH[particularly interesting new Cys-His protein]-α-Parvin-complex), LIMK (LIM domain kinase), Cdc42 (cell division cycle 42), PAK (P21 protein (cdc42/rac)-activated kinase), p38MAPK (P38 mitogen activated protein Kinase), CAS (Crk-associated substrate), Arp2/3 (Actin related protein 2/3), HSP (heat shock protein), Pyk2 (protein tyrosine kinase 2).

4.1.3 AMPK effects on vascular tone in EC and VSMC

There are conflicting results how AMPK influences vascular tone via actions in EC and/or VSMC. This is probably not only due to the known differences between large and small vessels and cell cultures but also due to the differences between organs and species from which the vessels or cells originated as well as the AMPK stimulator used (see section 1.3 and Table 4.1).

reference	vessel/cell model	AMPK stimulator	effector
(Ford et al., 2011)	Aorta from WKY and SHR rats	AICAR	Endothelium: NO, EDCF
(Ford et al., 2012)	Thoracic aorta and mesenteric artery from WKY and SHR rats	AICAR	Endothelium: NO, mean arterial pressure (MAP) decrease in SHR but not in WKY
(Enkhjargal et al., 2014)	Mesenteric arteries from endothelial AMPKα1 single/AMPKα2 single /AMPKα1+2 double KO mice	KO models	Endothelium: inhibited EDH and hyperpolarization in eAMPKα1 and eAMPKα1/2-KO
(Bradley et al., 2010)	Cremaster muscle arteries ex vivo and hindlimb arteries in vivo from rats	AICAR	Endothelium: NO
(Zhao et al., 2014)	Mesenteric arteries from rats, HUVECs	Metformin	Endothelium: IKCa and SKCa
(Weston et al., 2013)	Mesenteric arteries from mice	Adiponectin, ADHF from PVAT	VSM: BKCa

(Zaborska, Wareing, Edwards, & Austin, 2016)	Mesenteric arteries from HFD or control Sprague–Dawley rats	A769662	Reduced anti-contractile effect in HFD rats
(Horman et al., 2008)	rat aortic smooth muscle cells	Vasopressin and A23187	VSM: MLCK
(S. Wang, Liang, Viollet, & Zou, 2011b)	HSMCs and cultured MSMC from global AMPKα1/AMPKα2 KO mice	AICAR, KO models	VSM: MYPT1 via p190RhoGAP
(Rivera, Morón, Zarzuelo, & Galisteo, 2009)	Obese and lean Zucker rats	Resveratol	Systolic BP decrease
(Yiqun Wang et al., 2009)	HUVECs and aorta from Sprague–Dawley rats	Berberine	Endothelium: eNOS
(Goirand et al., 2007)	Aortic rings from global AMPKα1/AMPKα2 KO mice and control littermates	AICAR	Endothelium-independent dilations abolished in AMPKα1 KO
(Woollhead, Scott, Hardie, & Baines, 2005)	H441 lung cells	Phenformin and AICAR	inhibition of both apical Na+ entry through ENaC and basolateral Na+ extrusion via the Na+,K+-ATPase
(Hallows et al., 2003)	polarized T84 cells	AICAR	inhibited forskolin-stimulated CFTR-dependent short-circuit currents
(Aziz, Thomas, Khambra, & Tinker, 2010)	Mouse aortic smooth muscle cells	Phenformin	Kir6.1/SUR2B channels (KATP)
(Cao, Luo, Luo, & Tang, 2014)	HVSMC, AngII induced hypertensive mice	Resveratol	Decreased AngII induced MYPT1 phosphorylation via p190RhoGAP and alleviated AngII induced hypertension
(Sun, Li, Du, & Meng, 2015)	DOCA-hypertensive mice (AMPKα2 KO), aorta of mice and cultured VSMC	Resveratol	lowers BP in DOCA-hypertensive mice through an AMPK/RhoA/ROCK2/MLCP /MLC pathway
(Omae, Nagaoka, Tanano, & Yoshida, 2013)	Porcine retinal arterioles	Adiponectin	Endothelium: NO

Table 4.1: Effects of AMPK-stimulators on vascular tone

With regard to small arteries it has been shown that the microvascular endothelium mediates its endothelial vasorelaxant effects mainly by endothelium-derived hyperpolarizing factor (EDHF)-related mechanisms (Bolz et al., 1999), which involves stimulation of smooth muscle BK_{Ca} channels (Félétou & Vanhoutte, 2009). This EDHF-mediated mechanism is not hampered in our vessels though an inhibitory effect of AMPK on BK_{Ca} channels has been described in oxygen-sensing carotid body cells (F. A. Ross et al., 2011). Data from large vessels demonstrate that AMPK may have significant dilator effects by stimulating endothelial nitric oxide (NO) production (Bradley et al., 2010; Ford et al., 2011, 2012; Yiqun Wang et al., 2009), though data are conflicting (Fisslthaler & Fleming, 2009) and could not be confirmed in our studies in small vessels . Studies in large vessels also report direct vasodilator effects of AMPK in VSM. Unfortunately, they differ to a substantial amount in their results and may not be transferable to small vessels. While Goirand et al. reported that AMPK dilation depends on expression of the alpha 1 subunit (Goirand et al., 2007), Wang et al. argued that AMPK mainly controls MLCP via the alpha2 subunit in aortic VSM (S. Wang et al., 2011b). A further Ca^{2+}-independent desensitization mechanism via inhibition of MLCK was shown indirectly by Horman et al. in cultured aortic VSM (Horman et al., 2008). Some studies have focused on the role of AMPK and ion channel function on VSM tone. In VSMC, AMPK has been found to inhibit ATP-sensitive K+ channels (KATP) after stimulation by phenformin and AICAR, which would cause VSM depolarization and contraction (Aziz et al., 2010). Weston et al. reported AMPK activation via perivascular adipose tissue, suggesting that this was due to adiponectin release which can activate AMPK and enhance the activity of BKCA channels in mouse mesenteric arteries (Weston et al., 2013) which support our own findings. Since Weston was studying vessels without tone, he could not evaluate the effective vasodilator potency of this mechanism. In epithelial and endothelial cell models activation of AMPK inhibits apical Na^+ entry and basolateral extrusion via the Na^+/K^+ ATPase, regulates the cystic fibrosis transmembrane conductance regulator (CFTR) and restores IKCa and SKCa-dysfunction caused by Advanced Glycation End Products (AGEP) (Hallows et al., 2003; Woollhead et al., 2005; Zhao et al., 2014). These effects were not studied in our experiments.

Numerous reports underpin that AMPK is also involved in pathways regulating cell migration and polarity (Bettencourt-Dias et al., 2004; Giet et al., n.d.; J. H. Lee et al.,

2007; Vazquez-Martin, Oliveras-Ferraros, & Menendez, 2009; Zheng & Cantley, 2007). These pathways have been shown to have much in common with the cytoskeletal dynamics triggered during contraction and relaxation of vascular smooth muscle cells (Brozovich et al., 2016; Gerthoffer, 2005; Gunst & Zhang, 2008; D D Tang & Anfinogenova, 2008; Yamin & Morgan, 2012). Furthermore AMPK has been described as a major regulator of actin cytoskeleton and membrane integrity in high throughput screenings (Marin et al., 2015; Moon et al., 2014; E. Ross et al., 2015; Schaffer et al., 2015).

Nonetheless little is known about cytoskeletal impacts of AMPK in EC and VSMC. Blume et al. reported that Thr-278 phosphorylation of VASP in endothelial cells modulates F-actin binding and reduces VASP actin polymerization-promoting activity (Blume et al., 2007). This findings could be reproduced in VSMC with a focus on anti-proliferative and anti-migratory effects of AMPK (Stone et al., 2013). These effects went along with an increase in G/F-actin ratio, abrogated PDGF-stimulated Ser397 autophosphorylation of focal adhesion kinase and decreased promigratory cytoplasmatic accumulation of paxillin (Stone et al., 2013).

Another mechanism how AMPK might alter migrational behavior of VSMC is phosphyorylation of PDLIM5 at Ser177 and subsequent suppression of the actin-stabilizing Rac1-Arp2/3 signaling pathway (Yan et al., 2015). It has also be shown that AMPK can influence VSMC migration by influencing microtubule polymerization via phosphorylation of the cytoplasmic linker protein CLIP-170 (Nakano et al., 2010). Fig. 4.3 and Table 4.1 summarize some of the major findings on AMPK effects on EC and VSMC.
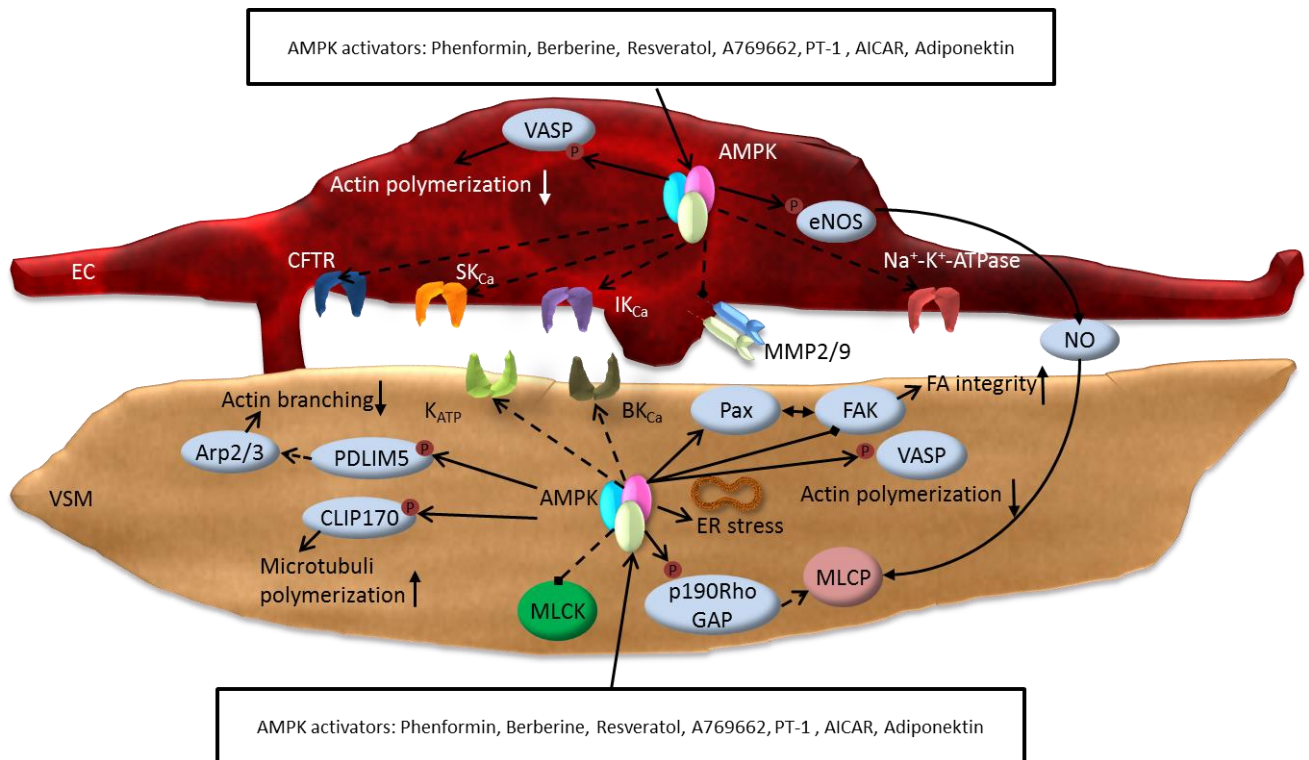
Fig. 4.3: AMPK effects on vascular tone in EC and VSMC: In EC primarily NO synthesis by phosphorylation and activation of eNOS has been described. Furthermore AMPK is reported to regulate certain channels in ECs. Moreover Blume et al. reported inhibition of actin polymerization due to VASP phosphorylation in ECs.

In VSMC AMPK was reported to influence MLCP via the p190RhoGAP/Rho/ROK/MYPT1-pathway as well as MLCK by inhibitory phosphorylation, thereby reducing sensitivity to Ca^{2+}. The activation of potassium channels K_{ATP} and BK_{Ca} hyperpolarize VSM membrane potential after AMPK activation. AMPK induced reduction of actin branching was reported to occur via a PDLIM5/Rho/ROK/Arp2/3-pathway, and reduced actin polymerization via VASP phosphorylation.

Abbreviations: VASP (vasodilator-stimulated phosphoprotein), AMPK (AMP-activated protein kinase), eNOS (endothelial nitric oxide synthase), EC (endothelial cell), VSM (vascular smooth muscle), CFTR (Cystic Fibrosis transmembrane conductance regulator), SK_{Ca}, IK_{Ca}, BK_{Ca} (small, intermediate, big conductance Ca^{2+}-activated potassium channel), K_{ATP} (ATP-sensitive potassium channel), Arp2/3 (actin related protein 2/3), FAK (focal adhesion kinase), Pax (paxillin).

4.2 Ca2+-dependent vasodilation

4.2.1 AMPK and endothelium-independent dilation

Two mechanisms appear to be involved in Ca^{2+}-dependent vasodilation caused by AMPK activation: Hyperpolarization induced by stimulation of BK_{Ca} channels and a

stimulation of SERCA via phosphorylation of PLN at Thr17. Both mechanisms act independently of the endothelium at the level of vascular smooth muscle, since removal of the endothelium (and thereby removal of all endothelium-derived vasoactive factors) did not abolish or reduce the dilatory and $[Ca^{2+}]_i$-decreasing effects of AMPK stimulation. Rather, a leftward shift of the concentration response curves for both compounds after endothelium removal suggests that the endothelium may release a factor that exerts an inhibitory function on the AMPK effects in these small vessels. From the comparison of arteries incubated with L-NAME, indomethacin, L-NAME + indomethacin or deendothelialized vessels (not shown), we speculate that this factor is a cyclooxygenase (COX) product. AMPK has been shown to downregulate COX expression (Y. K. Lee, Park, Kim, Lee, & Park, 2009). A reduced COX activity which is believed to be the major generator of the vasodilator PGI_2 in endothelium (Félétou, Huang, & Vanhoutte, 2011), could explain the observed effects.

Our finding that AMPK induces endothelium-independent vasodilation contrasts with earlier reports describing activating effects of AMPK on endothelial NOS after indirect stimulation of AMPK using AICAR, as originally reported in rat cardiac endothelial cells (Chen et al., 1999; Fryer et al., 2000). NO-mediated, endothelium-dependent dilation has been described in rat microvessels after stimulation with AICAR (Bradley et al., 2010) as well as in porcine arterioles after stimulation with adiponectin (Omae et al., 2013). However, AICAR is not only known to be an indirect activator of AMPK (Bryan & Marshall, 1999; Gruber et al., 1989), but also enhances endothelial adenosine release which secondarily can induce NO-dependent vasodilation (Bryan & Marshall, 1999; Gadalla et al., 2004; Gruber et al., 1989). Moreover, endothelium-independent vasodilator effects of AICAR have been reported (Goirand et al., 2007). In hamster microvessels, as used in the present study, the endothelium mediates dilation not primarily by NO but rather by EDHF (Bolz et al., 1999), an observation which we also made in mouse microvessels of that size (not shown). It must be stated that the interrelationship between NO and AMPK is not yet entirely clear. For example, in human endothelial cells, NO seems to activate AMPK rather than AMPK enhancing NO production (Bess, Fisslthaler, Frömel, & Fleming, 2011). Other groups have shown that AMPK elicits Endothelium-derived hyperpolarization (EDH) (Enkhjargal et al., 2014; Ford et al., 2011). While Ford et al. used again the highly

unspecific AMPK activator AICAR, Enkhjargal et al. created endothelial specific AMPKα1, α2-KO or α1-α2-KO mice and proposed that eAMPK α1 substantially mediates EDH. Several publications have questioned the role of endothelium-dependent dilation by AMPK and shown that removal of the endothelium still causes potent vasodilations, pointing – in agreement with our findings - towards a predominant role of smooth muscle AMPK in the control of vascular tone (Goirand et al., 2007; Horman et al., 2008; S. Wang, Liang, Viollet, & Zou, 2011a).

4.2.2 AMPK and potassium channels

Dilation as well as calcium decrease were observed as common responses to two structurally unrelated AMPK stimulators. We have confirmed the expression of the AMPK subunits which are required for the stimulator effects of A76 and PT1 (Pang et al., 2008; Scott et al., 2008). We did not study the effect of acute pharmacological AMPK inhibition on vascular responses to A76 and PT1, since the best known AMPK inhibitor, compound C, has not only poor selectivity for AMPK (Bain et al., 2007) but in our hands also elicited an acute and almost maximal vasodilation by itself, thus precluding any assessment of short term AMPK-mediated vasodilator effects in isolated vessels. Nevertheless, compound C did block the effects of both AMPK stimulators on BK_{Ca} channels in freshly isolated smooth muscle cells, thereby further supporting that this effect was AMPK-dependent.

Our finding of an AMPK-induced reduction of SMC $[Ca^{2+}]_i$ is in accordance with a recently published study in neurons, reporting both a decrease in the calcium peak in response to glutamate as well as a reduced spontaneous calcium oscillation when the neurons were treated with the putative AMPK activator latrepirdine (Weisová et al., 2013).

The increase in smooth muscle $[Ca^{2+}]_i$ in response to norepinephrine in our vessels could be completely prevented or reversed by nifedipine, indicating that under the conditions chosen an influx of calcium *via* voltage-dependent L-type calcium channels ($Ca_v1.2$) played an important role for the control of $[Ca^{2+}]_i$. However, a direct inhibitory effect of AMPK on Ca_v channels can be ruled out in these vessels,

since in potassium-depolarized vessels (whose smooth muscle Ca_v channels are thus highly activated) AMPK stimulation did not alter increases of intracellular calcium in response to stepwise augmentation of the extracellular calcium concentration (Fig. 3.9 C and 3.10B). Therefore, we investigated whether AMPK induces changes in membrane potential to an extent that could affect Ca_v activity "indirectly". Indeed, we observed a significant smooth muscle hyperpolarization in intact vessels in response to the AMPK stimulator A76, consistent with an activation of potassium channels. The magnitude of hyperpolarization was in accordance with previous observations made by Weston and colleagues on AMPK-induced BK_{Ca}-mediated hyperpolarization in rat and mouse mesenteric arteries (Weston et al., 2013). In our electrophysiological patch clamp studies in smooth muscle cells (freshly isolated from the same type of vessels as used for our functional studies) both PT1- and A76-elicited outward currents whose magnitudes were characteristic for BK_{Ca} channels (Mistry & Garland, 1998), a conclusion further supported by the measured I/V relationships (Mistry & Garland, 1998). Consistent with a role of BK_{Ca} channels, the currents were sensitive to inhibition by the specific channel inhibitors paxilline and iberiotoxin (Galvez et al., 1990; Sanchez & McManus, 1996). Furthermore this activation was AMPK dependent, since, they could be suppressed by the AMPK inhibitor compound C. It has been already shown in other cells that AMPK can directly phosphorylate BK_{Ca} channels and increase or decrease (Wyatt et al., 2007) their conductance, depending on the specific splice variant expressed by the tissue under investigation (F. A. Ross et al., 2011). Hyperpolarization in response to AMPK activation was also seen in a study on neurons (Weisová et al., 2013).

Surprisingly, and partially in contrast to what could be expected from our findings on isolated cells, treatment of intact resistance arteries with the BK_{Ca} channel blockers iberiotoxin or paxilline only partially reduced both, the $[Ca^{2+}]_i$ decrease and the dilation in response to AMPK stimulation. The blockers were given in sufficient concentrations to affect BK_{Ca} channels as indicated by an increase in resting vascular tone and by the occurrence of rhythmic oscillations in $[Ca^{2+}]_i$ and diameter, i.e. in vasomotion. The limited effect of BK_{Ca} channel inhibitors is consistent with our observations that mesenteric arteries of BK_{Ca} gene-deficient mice still showed AMPK-induced dilation, as well as decreases in $[Ca^{2+}]_i$. These observations suggested that in the intact vessels at least one additional AMPK-dependent

mechanism must have been involved in the AMPK-dependent induction of $[Ca^{2+}]_i$ decrease and vasodilatation.

4.2.3 AMPK, PLN and SERCA

The sarcoendoplasmic reticulum Ca^{2+}-ATPase (SERCA) is a well-known and potent modulator of smooth muscle $[Ca^{2+}]_i$ (Sanders, 2001). The magnitude of calcium sequestration from the cytosol by SERCA dominates over alternative mechanisms to remove free calcium from the cytosol such as plasmalemmal Ca^{2+}-ATPases (PMCA) or sodium/calcium exchanger(s) (NCX1) in vascular smooth muscle (Szewczyk et al., 2007). In the present study we show for the first time that AMPK stimulation rapidly increased SERCA-dependent calcium lowering mechanisms to an extent that potently reduced VSMC $[Ca^{2+}]_i$. Several lines of evidence allow us to conclude that the $[Ca^{2+}]_i$ lowering effect of AMPK stimulation is dependent on SERCA. Firstly, the effects of AMPK stimulators were greatly reduced after selective inhibition of SERCA with thapsigargin or cyclopiazonic acid. Secondly, caffeine (which was used to evoke calcium release from intracellular stores (Potocnik & Hill, 2001)) induced higher calcium peaks in cells pretreated with an AMPK stimulator than in control cells, suggesting that the stores were more filled, probably due to a higher SERCA activity. This was observed in the absence of extracellular calcium, which excludes involvement of an altered store-operated calcium entry. Thirdly, the $[Ca^{2+}]_i$ decrease following the transient, caffeine-induced calcium peak was more pronounced in cells pretreated with an AMPK stimulator, again suggesting a higher store content due to a more efficient removal of $[Ca^{2+}]_i$ into internal stores. In line with this interpretation, we also observed a stronger decrease of $[Ca^{2+}]_i$ immediately after blockade of Ca_v channels when an AMPK stimulator was present. Our observations are in agreement with recent publications that described impaired calcium handling in endothelial cells and VSMC from AMPK-α2-deficient mice (Dong et al., 2010; Liang et al., 2013). Chronic AMPK-α2 deficiency went along with increased $[Ca^{2+}]_i$, reduced SERCA activity (Dong et al., 2010) and decreased calcium content of the sarcoplasmic reticulum (SR), respectively (Liang et al., 2013) All of the effects were ascribed, however, not to a direct effect of AMPK on SERCA but to an increased reactive

oxygen species (ROS) activity and to a resulting ER stress in the absence of the AMPK-α2 subunit.

As a mechanism how AMPK can induce SERCA-dependent calcium lowering of the VSMC we found that AMPK can enhance phospholamban phosphorylation at the regulatory Thr17 site in isolated mesenteric and femoral arteries of mice. PLN phosphorylation has been shown to increase SERCA activity (Tada, Kirchberger, & Katz, 1975) and thus could explain the stimulatory effect of AMPK on SERCA. PLN activity can be regulated on another regulatory site, Ser 16. Protein kinase A (PKA) can phosphorylate both sites, Ser 16/Thr 17, while stimulation of calcium-calmodulin-dependent protein kinase II (CaMKII) –an upstream regulator of AMPK – leads to phosphorylation only of Thr 17. Both phosphorylations cause a disinhibition of SERCA (Kranias & Hajjar, 2012). We focused on Thr 17 as implied by sequence analysis of AMPK recognition sites. It has been shown that smooth muscle cells of the mouse aorta can express phospholamban (Lipskaia et al., 2013; Raeymakers & Jones, 1986) and that its knockout altered vascular reactivity and calcium handling (Lalli, Harrer, Luo, Kranias, & Paul, 1997). However, these results do not exclude other mechanisms that may be involved in AMPK-mediated stimulation of SERCA. We studied the phospholamban phosphorylation only in two different vascular beds of the mouse. Furthermore, while the SERCA:PLB protein ratio reportedly covers a range between 1:2 and 1:1 in heart ventricle which seems essential for the mediation of the PLB effects (Colyer & Wang, 1991; Koss, Grupp, & Kranias, 1997) the measured mRNA extracted from the microvessels in our experiments were roughly 1:100 (not shown). Whether SERCA activity in hamster vessels is regulated in a similar manner as we found in mouse vessels was not studied in our project. NO- and O_2^--mediated, peroxynitrite-induced S-glutathionylation of SERCA has been shown to enhance SERCA function in a Cys674-dependent manner (Adachi et al., 2004). It is unlikely that the vasodilator effect of AMPK can be explained by a stimulation of this pathway, since NO could not be generated due to pretreatment of the vessels with the NOS inhibitor L-NAME. In contrast, high levels of ROS have been shown to inhibit SERCA activity due to SERCA oxidation (sulfonylation) (Adachi et al., 2004). Since this oxidation is thought not to be readily reversible, if not irreversible (Adachi et al., 2004; Sharov, Dremina, Galeva, Williams, & Schöneich, 2006) it seems also unlikely that the AMPK effect was due to an acute reversal of pre-exisiting inhibitory

SERCA oxidation. Other AMPK mechanisms such as SERCA activation by phosphorylation of SERCA itself, or of one of the modulator proteins located within the ER (Wray & Burdyga, 2010) cannot be excluded. The γ-subunit of the AMPK has been found to partly colocalize with SERCA 2 in skeletal as well as in cardiac muscle, which points to a localized and so far unknown mechanism by which AMPK could alter the functional status of SERCA or SERCA-associated proteins (Pinter, Grignani, Watkins, & Redwood, 2013).

SERCA can cause fast relaxation of VSM due to different pathways: 1) lowering $[Ca^{2+}]_{i, and}$ 2) modulating membrane excitability (calcium sparks and spontaneous transient outward currents (STOCs; Cheranov and Jaggar 2002)) through activation of Ca^{2+}-sensitive ion channels and 3) contributing to the efficacy of plasma membrane Ca^{2+} extrusion mechanisms by vectorially releasing Ca^{2+} to them (Wray & Burdyga, 2010). It would be interesting to determine the mechanism of all these processes interact in detail and promote AMPK mediated vasodilation. Unfortunately we were not able with the calcium imaging technique used here to resolve compartmentalization of calcium events (i.e. sparks, sparklets etc.) and their changes due to AMPK/SERCA activity. This would help to understand the interaction between SR calcium handling and BK_{Ca} channel function. Wellman et al. showed that spark frequency and thus BK_{Ca} activity is increased in cerebral arteries from PLN-KO mice (Wellman, Santana, Bonev, Nelson, & Nelson, 2001). If this is also true in AMPK-KO and if the two mechanisms found in this study can be attributed to one of the two catalytic subunits α1 or α2 of the AMPK needs to be tested in subsequent projects.
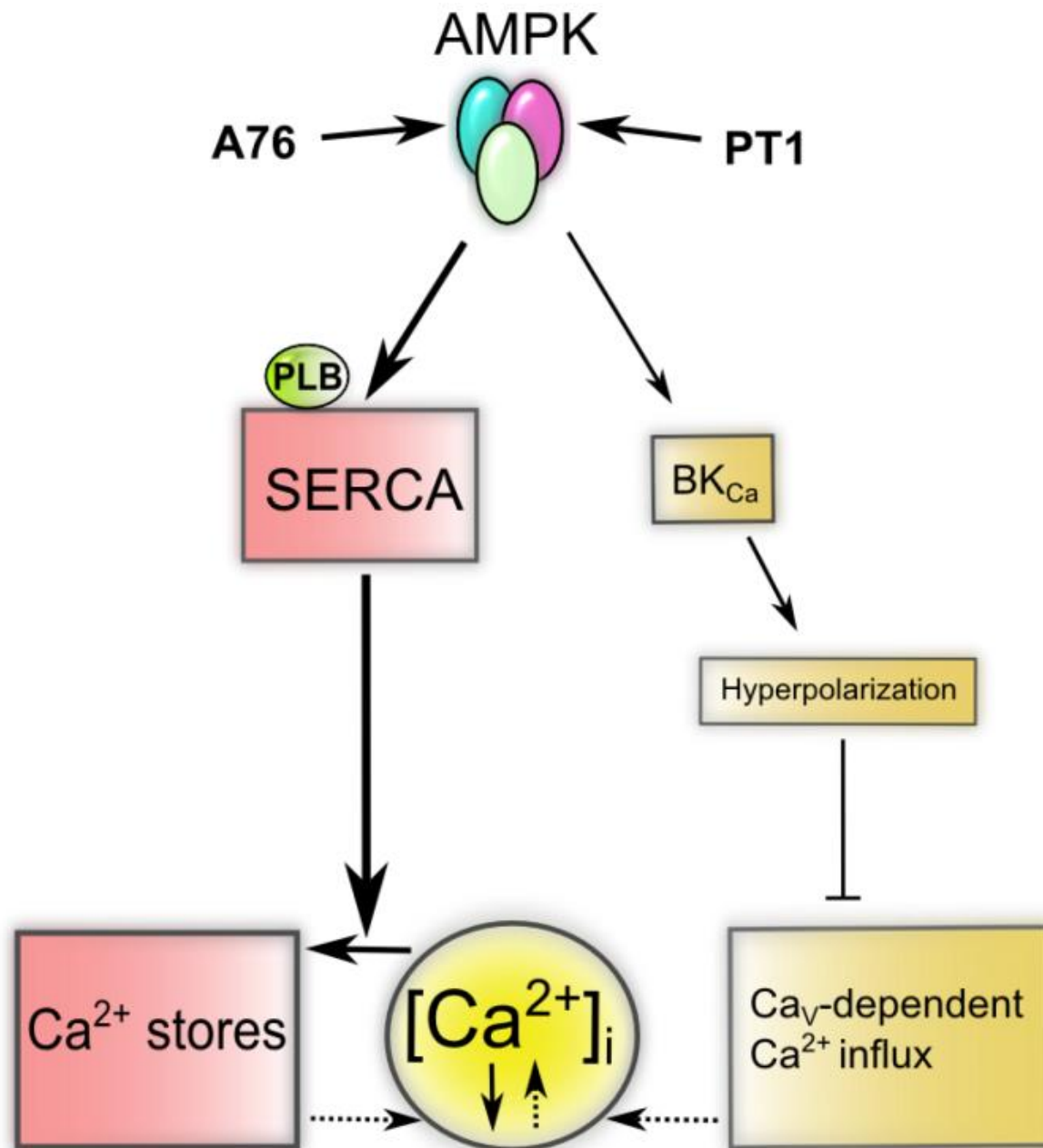
Fig. 4.4: Proposed model of AMPK-mediated Ca^{2+}-dependent effects in VSMC. AMPK activates BK$_{Ca}$ channels leading to hyperpolarization and (partial) closure of Ca$_V$ channels. Additionally, AMPK increases SERCA activity involving phospholamban (PLB) phosphorylation. Both mechanisms result in a reduced [Ca^{2+}]$_i$ which ultimately leads to relaxation of VSMC. Though both mechanisms are activated, SERCA stimulation alone already is sufficient for the AMPK-mediated [Ca^{2+}]$_i$ reduction and vasodilation. Taken from Schneider&Schubert et al.(Schneider et al., 2015).

Under the conditions studied here, the two mechanisms by which AMPK potentially reduces [Ca^{2+}]$_i$ and consequently induces vasodilation do not seem to be equipotent in microvascular smooth muscle. The limited effect of BK$_{Ca}$ channel inhibitors and the

persistent AMPK induced dilation in BK_{Ca} knockout mice suggest a significant role for an additional calcium lowering mechanism. This was surprising since at the more negative membrane potential observed in our vessels under AMPK stimulation, we expected Ca_v channels to be mainly in the closed state, in particular of the isoform $Ca_v1.2$ (Moosmang et al., 2003). At a membrane potential of -60 mV no current through $Ca_v1.2$, the main isoform in vascular smooth muscle, could be detected in tibial artery VSMC (Moosmang et al., 2003). We have also shown previously, in the same type of vessels studied here, that maximal pharmacologic stimulation of BK_{Ca} channels induced pronounced $[Ca^{2+}]_i$ decreases (Bolz, Fisslthaler, et al., 2000). It is therefore conceivable that the BK_{Ca} channel stimulation by AMPK may have been incomplete in our intact vessels. In accordance with this explanation, the A76-induced calcium decrease that we observed after SERCA inhibition could be further enhanced by additional dihydropyridine treatment, i.e. blockade of Ca_v channels in most experiments. As a result, the AMPK effects on SERCA (as observed in the presence of BK_{Ca} inhibitors or vessels from knockout mice) with regard to cellular calcium homeostasis prevailed in our setting over BK_{Ca} channel dependent effects. Accordingly, the activity of SERCA2b, which is the major isoenzyme in VSMC (K. Wu et al., 2001), can increase several fold upon stimulation (Chandrasekera, Kargacin, Deans, & Lytton, 2009). We conclude that AMPK is a novel and potent stimulator for SERCA-dependent calcium lowering via phosphorylation of PLN at Thr17. Therefore enabling the cell to reduce $[Ca^{2+}]_i$ even in the absence of functional BK_{Ca} channels. This potent role of SERCA in the control of $[Ca^{2+}]_i$ in smooth muscle may be one explanation for the surprisingly mild vascular phenotype of BK_{Ca} knockout mice (Sausbier et al., 2005).

4.3 Ca^{2+}-independent vasodilation

Since prolonged exposure to AMPK stimuli induced a slowly developing relaxation of vessels despite intracellular calcium levels did not change, we inferred that AMPK may, in addition to its calcium reducing effects desensitize the contractile apparatus to calcium within vascular smooth muscle. The remaining dilation after blockade of BKCa- and SERCA-mediated calcium decrease and earlier observations from other research groups (Cao et al., 2014; S. Wang et al., 2011a) pointed to AMPK acting

through MLCP activation and calcium desensitization. However, thorough investigation of MLC_{20} phosphorylation and the main regulatory phosphorylation sites of MYPT1, which determine MLCP activity, did not reveal significant differences to the control group under 30 minutes of AMPK stimulation except a transient decrease of MLC_{20} phosphorylation (not shown) at a time point where no vasodilation could be observed (in the presence of high K^+). When investigating MLC_{20} phosphorylation at a later time point where the calcium independent dilation reached its plateau (20 min) the MLC_{20} phosphorylation showed no difference from control values. Furthermore, the differing constriction kinetics induced by high K^+ Mops in the presence of a MLCK inhibitor (ML7) compared with constrictions in the presence of PT1 (Fig. 3.12) argue against an involvement of the second modulator of calcium sensitivity, MLCK as reported previously by Horman et. al. (Horman et al., 2008).

Given these findings, we chose to shift our focus to AMPK effects on actin in the control of vascular tone. As evidenced by two independent methods, the VSM F-actin/G-actin ratio was significantly decreased by PT1. Immunoblotting indicated that AMPK induces dephosphorylation of cofilin, hence promoting its actin severing capability. Ultrastructural investigations yielded AMPK-dependent increases in the anisotropy of actin filaments, arguing for less complex structure and, hence, weakened force transmission. Likewise, a vanishing of mid-cellular F-actin upon AMPK stimulation was observed in smooth muscle of intact arteries from LifeAct mice. In cultivated HUASMC, actin filament thickness decreased as well as the number of actin filament branching points.

4.3.1 AMPK and actin dynamics

When smooth muscle contracts, the actin cytoskeleton does not only work as a passive scaffold to permit myosin filament sliding. Exposure to contractile stimuli can also trigger actin polymerization (Brozovich et al., 2016; Gerthoffer, 2005; D D Tang & Anfinogenova, 2008) This may enable smooth muscle to maintain a shorter cell length without the need for extensive myosin actin interaction (Rembold, Tejani, Ripley, & Han, 2007). In addition, a rearrangement of the cortical actin cytoskeleton is thought to allow for better transmission of force to the extracellular matrix *via*

integrins (Walsh & Cole, 2013) and has also been linked to artery inward remodeling as observed in hypertension (Staiculescu et al., 2013). *Vice versa*, it is conceivable that a reduction of the number and structure of the meshwork of actin filaments by inhibiting actin polymerization, contractile processes are hampered despite unaltered MLC_{20} phosphorylation levels (Moreno-Domínguez et al., 2014; Saito, Hori, Ozaki, & Karaki, 1996). Activation of smooth muscle leads to the recruitment of N-WASP and Arp2/3 to the cell membrane, indicative of the formation of new actin filaments at the cell cortex (Wenwu Zhang, Wu, Du, Tang, & Gunst, 2005). The aforementioned phenomena have been reviewed in great detail (Gunst & Zhang, 2008). Also, so-called "stimulated actin polymerization" is presumed to mediate a 15% gain in arterial constriction after prior submaximal stimulation when a second stimulation is applied (Tejani, Walsh, & Rembold, 2011). Actin availability hence has proposed as an alternative or supportive pathway of smooth muscle contraction in a recent review (Brozovich et al., 2016).

Studying primarily migration processes of cultured VSMC, Stone and colleagues have indeed described that activation of AMPK can lead to depolymerization of F-actin and consequently an increase of G-actin, thereby hampering VSMC migration (Stone et al., 2013).

4.3.2 AMPK and cofilin dephosphorylation by liberation from protein 14-3-3

Cofilin has been implicated in the regulation of smooth muscle contraction *via* controlling its actin polymerization state in various studies. However, there is conflicting evidence as to whether contraction is paralleled by cofilin phosphorylation or dephosphorylation. Confusion arises also from two opposing models of cofilin function for the generation of smooth muscle tone: (1) Actin depolymerization by cofilin abolishes mechanical support for maintenance of smooth muscle tone and leads to relaxation. (2) Actin depolymerization by cofilin provides the necessary G-actin monomers for de novo F-actin polymerization and new ends for actin filament nucleation and leads to contraction.

Apart from these theoretical considerations, if only studies with vascular smooth muscle are taken into account, then five studies report increased cofilin phosphorylation in response to contractile stimulation (Albinsson, Nordström, & Hellstrand, 2004; Dai, Bongalon, Mutafova-Yambolieva, & Yamboliev, 2008; Hocking

et al., 2013; Moreno-Domínguez et al., 2014; Nour-Eldine et al., 2016) as opposed to one study reporting decreased phosphorylation (Tejani et al., 2011) arguing in favour of of a causal relation between - cofilin dephosphorylation and vasodilation.

It seems at first glance odd, that a kinase should be involved in dephosphorylation of cofilin. However, we were able to show with three independent techniques that AMPK stimulation induces cofilin S3 dephosphorylation in intact as well as cultured VSMC. Cofilin dephosphorylation and activation has been shown to depend on its interaction with the scaffolding protein 14-3-3 (Dreiza et al., 2005). Displacing cofilin from 14-3-3 allows for cofilin dephosphorylation and its activation (Dreiza et al., 2005). Interestingly AMPK and 14-3-3 show a functional overlap at their respective phosphorylation or binding sites on proteins (Hardie, Schaffer, & Brunet, 2016). Thus, AMPK has been shown to phosphorylate a number of 14-3-3 binding partners (Short et al., 2010; Weerasekara et al., 2014; Xie & Roy, 2015) which then can bind to 14-3-3. By such a mechanism, cofilin could be relocated away from 14-3-3 and undergo dephosphorylation consistent with a competitive replacement of cofilin by an unknown protein which is phosphorylated by AMPK thus enabling it 14-3-3 binding. Indeed, we were able to demonstrate that AMPK stimulation leads to the displacement of cofilin from 14-3-3.

It must be emphasized, however, that in a number of cell lines other than VSMC it was reported that AMPK stimulation lead to cofilin phosphorylation (Miranda et al., 2010; Onselaer et al., 2014; Palanivel, Ganguly, Turdi, Xu, & Sweeney, 2014). At present, we can only speculate about possible explanations for this discrepancy. First, it should not be neglected that in our experimental setting we did not assess the effect of AMPK activation compared to a baseline situation. Rather, we performed our studies in vessels pre-activated with high extracellular K^+ concentrations and thus high phosphorylation status of LIMK and cofilin (Ren, Albinsson, & Hellstrand, 2010). Under these conditions it seems plausible that cofilin may be mainly phosphorylated since it would otherwise inhibit the K^+ induced vasoconstriction. Starting from such a high phosphorylation level one would expect to see a dephosphorylation which one could not detect if the phosphorylation level was low. A second explanation could be that smooth muscle specific translational regulation by miRNA might account for differences between SMC and non-SMC (in which many cofilin studies were performed). Smooth muscle cells are the only cell type in which the promoter of miR-

143 and miR-145 are expressed and active (Boettger et al., 2009). These miRNAs not only regulate differentiation to the contractile phenotype, they also control the expression of multiple actin-related proteins, such as Arp2/3 subunit 5, β-actin, γ-actin and also cofilin 2. The unique influence of these miRNAs on the VSMC actin cytoskeleton has recently been highlighted (Xin et al., 2009). We therefore propose that only SMC provide the protein machinery necessary for AMPK to induce cofilin dephosphorylation.

4.3.3 AMPK and changes in actin morphology of VSM

Direct morphological evidence that contractile activation of smooth muscle entails actin filament network branching is still lacking. However, it has been demonstrated in airway smooth muscle that at least for overall actin polymerization and tension generation, N-WASP, the upstream regulator of the central branching factor Arp2/3, is essential (Wenwu Zhang et al., 2005). In endothelial cells, other researchers were able to demonstrate with the help of atomic force microscopy, that actin polymerization and depolymerization as induced by jasplakinolide and latrunculin A, respectively, entail denser, more branched actin networks (jasplakinolide) and coarser, less branched networks (latrunculin A) (Kronlage, Schäfer-Herte, Böning, Oberleithner, & Fels, 2015).

In isometrically stimulated living SMC from LifeAct mice we could observe a loss of mid-central F-actin signal upon AMPK activation which was reversible after AMPK was inhibited. This findings support data which showed that cofilin activity takes predominantly place on pointed ends in the cytosol while actin polymerization happens at barbed ends near the focal adhesions contacts (D D Tang & Anfinogenova, 2008; Dale D. Tang, Zhang, & Gunst, 2005; Wenwu Zhang et al., 2005). Furthermore, Flavahan and coworkers observed that pressurized smooth muscle changes its actin morphology when pressure-induced contraction (i.e. myogenic tone) is developing: As in our isometric setups, they reported changes of F-actin signal in the cell interior reflected as an altering "M-shaped" signal intensity when line scan was performed along tranverse optic sections through the middle of relaxed smooth muscle cells (Flavahan et al., 2005). This "M" was only apparent when low (10-60 mmHg) transmural pressure was applied and smooth muscle was

relaxed. When pressure was augmented to 90 mmHg, the ensuing contractile stimulus led to actin redistribution and the central trough of the "M" was filled with F-actin. Of note, Flavahan and colleagues did not report any substantial changes in vessel diameter when they applied high transmural pressure, making this setting comparable to the isometric wire myograph, i.e. contractile stimulus for VSMC but unaltered cell length. This findings are challenging the current opinion that especially cortical actin is undergoing rearrangements when vascular tone changes (Gunst & Zhang, 2008; D D Tang & Anfinogenova, 2008). While our observations were conducted on VSMC in isolated pressurized or isometrically mounted arteries in situ, most of the studies emphasizing cortical actin dynamics were performed in cultured cells.

As another parameter for actin remodeling we measured filament anisotropy in isometric VSMC and found increased anisotropy in AMPK-activated states. Of note, this increase was reversible when AMPK was inhibited. This indicates that the filaments are more parallel and show less branching. The latter implication was confirmed in cultured SMC (see below). For the determination of anisotropy a Fiji plugin, FibrilTool, was used (Boudaoud et al., 2014). This Plugin has been frequently cited in the recent two years, in particular for cytoskeletal analysis in plant physiology (Sampathkumar et al., 2014) and mammalian cell models (Vergara et al., 2015). To further strengthen the likelihood that the actions of A76 or PT1 on the cytoskeleton were indeed mediated by AMPK we analyzed the actin cytoskeleton of cultured human VSMC. Human cells were chosen because of their larger cell size. Hence, the morphology of the actin filaments was easily assessable other than in isolated mouse SMC the actin filaments of which were less well ordered and thus more difficult to analyze. We found that actin filament thickness was reduced by 7 % when AMPK was activated for 35 min with PT1, corresponding to the plateau of dilation of 48% as depicted in Fig. 3.9A. The opposite (thicker actin filaments) is seen when cofilin is knocked down by RNA interference (Hotulainen, Paunola, Vartiainen, & Lappalainen, 2004). We therefore suggest that thinning of actin filaments is compatible with actin severing by activated cofilin. Our second finding in VSMC was that AMPK reduced actin filament branching. This recapitulates *ex vivo* results involving purified actin filaments (Chan, Beltzner, & Pollard, 2009). In that study, Chan and coworkers were able to show that cofilin decreased actin filament branching by competing with Arp2/3

for actin-binding sites and reducing binding affinity for Arp2/3. Finally, reduced actin branching in the context of AMPK activation has also been postulated by a group which found impaired Arp2/3 function and lamellipodia formation as a result of AMPK dependent phosphorylation and translocation of Arp2/3 from the lamellipodia to the cytosol in p53 knockout VSMC (Yan et al., 2015).

Actin as a regulator of smooth muscle tone has mainly been studied in airway smooth muscle (Mehta & Gunst, 1999; Opazo Saez et al., 2004; Y. Wu & Gunst, 2015; W Zhang, Huang, & Gunst, 2016; Wenwu Zhang et al., 2005), although there is steadily growing body of literature using arterial smooth muscle (Castorena-Gonzalez, Staiculescu, Foote, Polo-Parada, & Martinez-Lemus, 2014; Cipolla, Gokina, & Osol, 2002; Kim, Gallant, Leavis, Gunst, & Morgan, 2008; Moreno-Domínguez et al., 2014). Among these publications are only a few address the actin ultrastructure of arterial smooth muscle in intact vessels (Flavahan et al., 2005). Our study is the first to provide images of changes in the actin cytoskeleton in intact pressurized (isobaric) as well as isometric resistance arteries. Isometric preparations are particularly important since shortening of smooth muscle cells in the process of contraction naturally entails distortions of the cytoskeletal actin structure. Keeping the cells at constant length while still allowing for developing force and tone is a better method to evaluate the ultrastructural effects of actin modulators in intact smooth muscle, especially when considering filament anisotropy. In contrast, imaging of enzymatically isolated cells is often easier to conduct and allows for higher magnification. However, these VSMC are normally of a synthetic phenotype (Beamish, He, Kottke-Marchant, & Marchant, 2010; House, Potier, Bisaillon, Singer, & Trebak, 2008; Yamin & Morgan, 2012) which probably goes along already with an alteration of the actin filaments. Therefore our study which for the first time shows dynamic actin changes in smooth muscle in intact arteries provides new insights in the role of actin in the control of vascular tone.

4.3.4 Potential Role of the actin cytoskeletal changes caused by AMPK

Calcium is an important second messenger not only important for regulating vascular tone. Therefore $[Ca^{2+}]_i$ cannot be lowered indefinitely. Calcium independent relaxation of smooth muscle, also called calcium desensitization, allows

maintainence of "normal" $[Ca^{2+}]_i$ still to fulfill its non-contractile functions. Further, hypoxic tissue-derived signals (such as urocortin) and metabo-protective adipokines (like adiponectin) which are known AMPK activators (Li et al., 2013; W. Zhu, Cheng, Vanhoutte, Lam, & Xu, 2008), have been suggested to affect vascular tone under pathophysiological conditions (Lubomirov et al., 2006; Osuka, Watanabe, Yasuda, & Takayasu, 2012). Therefore, it would be particularly interesting to investigate if these effects are mediated by AMPK and if AMPK activators can be valuable in the therapy of vasospasm (i.e. subarachnoidal hemorrhage). Under these conditions arteries must be kept continously dilated to allow for sufficient perfusion while allowing $[Ca^{2+}]_i$ to be kept at normal basal level so that the cell can react and adapt to non-contractile stimuli (Berridge, Bootman, & Roderick, 2003; Kolias, Sen, & Belli, 2009). This happens best, when the calcium sensitivity of the contractile apparatus is appropriately reduced.

5. Potential therapeutic implications

This thesis characterizes an active role of AMPK in the control of small artery tone. We found that AMPK is involved in the fast adaptation of vascular diameter via $[Ca^{2+}]_i$ dependent pathways while it can also adjust vascular tone via Ca^{2+}-independent pathways by changing the structure of the actin cytoskeleton. Both mechanism cause a significant vasodilation and finally identify AMPK as a potential new target in the therapy of hypertension. Furthermore, all the identified mechanisms here were endothelium-independent. In chronic diseases like the metabolic syndrome or hypertension the endothelium is not appropriately functioning any more. This makes activation of the AMPK in VSMC particularly under these pathological conditions valuable more effective therapeutic option. We found that SERCA activation by phosphorylation of PLN on Thr17 is the main mechanism of fast Ca^{2+}-lowering thus causing vasodilation in VSMC. The parallel activation of BK_{Ca} seems to become important in states where SERCA function is impaired. SERCA as well as BK_{Ca} function has been shown to be disturbed in models of hypertension (especially hyperaldosteronism) and VSMC differentiation from contractile to a more proliferative/synthetic type (Chou et al., 2016; House et al., 2008; Lipskaia et al., 2013; Lipskaia, Limon, Bobe, & Hajjar, 2012). It would be interesting to determine the role of the AMPK on the BK_{Ca} channel and on SERCA activity under such circumstances. The redundant influence of AMPK on the aforementioned targets highlights its role as a key enzyme in $[Ca^{2+}]_i$ regulation and $[Ca^{2+}]_i$ handling in VSMC. Furthermore we have shown in intact arteries that AMPK is able to induce a sustained Ca^{2+}-independent vasodilation which is due to actin depolymerization.

This hitherto unknown AMPK effect on microvascular tone allows for normal Ca^{2+} regulation of cellular processes whilst reducing smooth muscle Ca^{2+} sensitivity. It is therefore tempting to speculate that in states requiring long term local dilation AMPK might be a critical component to maintain maximal vascular conductivity and prevent vasospasms. However, more studies are necessary to substantiate a potential therapeutic value of AMPK stimulators in microvessels.
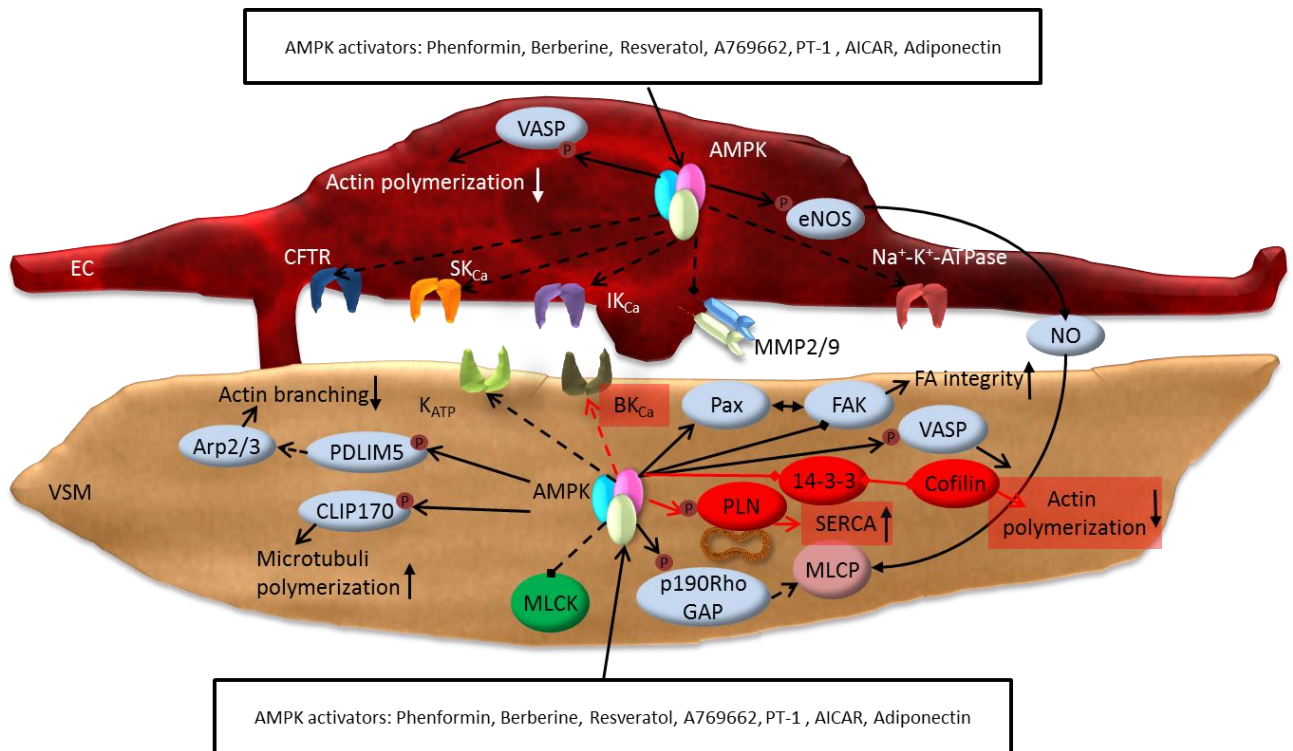
Fig. 5.1: Graphical summary. Revised model of AMPK effects on vascular tone in EC and VSMC. Red lines and red markings are indicating the major findings of this thesis. AMPK exerts its Ca^{2+}-dependent vasodilatory effects via two independent mechanisms allowing redundant control of calcium homeostasis. AMPK activates the BK_{Ca} channel and causes hyperpolarization of VSMC. Furthermore AMPK is activating SERCA via phosphorylation of SERCA regulating protein phospholamban on Thr17. Under the conditions studied here, the prevailing mechanism is an activation of SERCA. AMPK is also causing a slowly developing Ca^{2+}-independent vasodilation which could be attributed to dephosphorylation of actin severing protein Cofilin on Ser3 after liberation of cofilin from 14-3-3. These molecular findings went along with morphological changes in the actin cytoskeleton in VSMC. Thus emphasizes a prominent role of AMPK in the regulation of vascular tone in small arteries.

References

Adachi, T., Weisbrod, R. M., Pimentel, D. R., Ying, J., Sharov, V. S., Schöneich, C., & Cohen, R. a. (2004). S-Glutathiolation by peroxynitrite activates SERCA during arterial relaxation by nitric oxide. *Nature Medicine*, *10*(11), 1200–7. http://doi.org/10.1038/nm1119

Alba, G., El Bekay, R., Alvarez-Maqueda, M., Chacón, P., Vega, A., Monteseirín, J., … Sobrino, F. (2004). Stimulators of AMP-activated protein kinase inhibit the respiratory burst in human neutrophils. *FEBS Letters*, *573*(1-3), 219–25. http://doi.org/10.1016/j.febslet.2004.07.077

Albinsson, S., Nordström, I., & Hellstrand, P. (2004). Stretch of the vascular wall induces smooth muscle differentiation by promoting actin polymerization. *Journal of Biological Chemistry*, *279*(33), 34849–34855. http://doi.org/10.1074/jbc.M403370200

Aldrich, R. W., Brenner, R., Peréz, G. J., Bonev, A. D., Eckman, D. M., Kosek, J. C., … Nelson, M. T. (2000). Vasoregulation by the |[beta]|1 subunit of the calcium-activated potassiumchannel. *Nature*, *407*(6806), 870–876. http://doi.org/10.1038/35038011

Almers, W., & Neher, E. (1985). The Ca signal from fura-2 loaded mast cells depends strongly on the method of dye-loading. *FEBS Letters*, *192*(1), 13–18. http://doi.org/10.1016/0014-5793(85)80033-8

Amberg, G. C., & Navedo, M. F. (2013). Calcium dynamics in vascular smooth muscle. *Microcirculation (New York, N.Y. : 1994)*, *20*(4), 281–9. http://doi.org/10.1111/micc.12046

Aziz, Q., Thomas, A., Khambra, T., & Tinker, A. (2010). Phenformin has a direct inhibitory effect on the ATP-sensitive potassium channel. *European Journal of Pharmacology*, *634*(1-3), 26–32. http://doi.org/10.1016/j.ejphar.2010.02.023

Bae, H. B., Zmijewski, J. W., Deshane, J. S., Tadie, J. M., Chaplin, D. D., Takashima, S., & Abraham, E. (2011). AMP-activated protein kinase enhances the phagocytic ability of macrophages and neutrophils. *Faseb J*, *25*(12), 4358–4368. http://doi.org/10.1096/fj.11-190587

Bain, J., Plater, L., Elliott, M., Shpiro, N., Hastie, C. J., McLauchlan, H., … Cohen, P. (2007). The selectivity of protein kinase inhibitors: a further update. *The Biochemical Journal*, *408*(3), 297–315. http://doi.org/10.1042/BJ20070797

Beamish, J. A., He, P., Kottke-Marchant, K., & Marchant, R. E. (2010). Molecular Regulation of Contractile Smooth Muscle Cell Phenotype: Implications for Vascular Tissue Engineering. *Tissue Engineering Part B: Reviews*, *16*(5), 467–491. http://doi.org/10.1089/ten.teb.2009.0630

Beech, D. J. (2013). Characteristics of Transient Receptor Potential Canonical Calcium-Permeable Channels and Their Relevance to Vascular Physiology and Disease. *Circulation Journal*, *77*(3), 570–579. http://doi.org/10.1253/circj.CJ-13-0154

Berridge, M. J., Bootman, M. D., & Roderick, H. L. (2003). Calcium signalling: dynamics, homeostasis and remodelling. *Nature Reviews. Molecular Cell Biology*, *4*(7), 517–29. http://doi.org/10.1038/nrm1155

Bess, E., Fisslthaler, B., Frömel, T., & Fleming, I. (2011). Nitric oxide-induced activation of the AMP-activated protein kinase α2 subunit attenuates IκB kinase activity and inflammatory responses in endothelial cells. *PloS One*, *6*(6), e20848. http://doi.org/10.1371/journal.pone.0020848

Bettencourt-Dias, M., Giet, R., Sinka, R., Mazumdar, A., Lock, W. G., Balloux, F., … Glover, D. M. (2004). Genome-wide survey of protein kinases required for cell cycle progression. *Nature*, *432*(7020), 980–987. http://doi.org/10.1038/nature03160

Blaustein, M. P., & Lederer, W. J. (1999). Sodium/calcium exchange: its physiological implications. *Physiological Reviews*, *79*(3), 763–854.

Blodow, S., Schneider, H., Storch, U., Wizemann, R., Forst, A.-L., Gudermann, T., & Mederos Y Schnitzler, M. (2014). Novel role of mechanosensitive AT1B receptors in myogenic vasoconstriction. *Pflugers Archiv : European Journal of Physiology*, *466*(7), 1343–53. http://doi.org/10.1007/s00424-013-1372-3

Blume, C., Benz, P. M., Walter, U., Ha, J., Kemp, B. E., & Renne, T. (2007). AMP-activated protein kinase impairs endothelial actin cytoskeleton assembly by phosphorylating vasodilator-stimulated phosphoprotein. *Journal of Biological Chemistry*, *282*(7), 4601–4612. http://doi.org/10.1074/jbc.M608866200

Boels, P. J., Troschka, M., Rüegg, J. C., & Pfitzer, G. (1991). Higher Ca2+ sensitivity of triton-skinned guinea pig mesenteric microarteries as compared with large arteries. *Circulation Research*, *69*(4), 989–996. http://doi.org/10.1161/01.RES.69.4.989

Boettger, T., Beetz, N., Kostin, S., Schneider, J., Krüger, M., Hein, L., & Braun, T. (2009). Acquisition of the contractile phenotype by murine arterial smooth muscle cells depends on the Mir143 / 145 gene cluster. *The Journal of Clinical Investigation*, *119*(9), 2634–2647. http://doi.org/10.1172/JCI38864.2634

Bolz, S.-S., de Wit, C., & Pohl, U. (1999). Endothelium-derived hyperpolarizing factor but not NO reduces smooth muscle Ca2+ during acetylcholine-induced dilation of microvessels. *British Journal of Pharmacology*, 124–134.

Bolz, S.-S., Fisslthaler, B., Pieperhoff, S., de Wit, C., Fleming, I., Busse, R., & Pohl, U. (2000). Antisense oligonucleotides against cytochrome P450 2C8 attenuate EDHF-mediated Ca 2+ changes and dilation in isolated resistance arteries. *FASEB Journal*, *14*(2), 255–260.

Bolz, S.-S., Galle, J., Derwand, R., de Wit, C., & Pohl, U. (2000). Oxidized LDL increases the sensitivity of the contractile apparatus in isolated resistance arteries for Ca(2+) via a rho- and rho kinase-

dependent mechanism. *Circulation*, *102*(19), 2402–10. http://doi.org/10.1161/01.CIR.102.19.2402

Bolz, S.-S., Pieperhoff, S., de Wit, C., & Pohl, U. (2000). Intact endothelial and smooth muscle function in small resistance arteries after 48 h in vessel culture. *American Journal of Physiology. Heart and Circulatory Physiology*, *279*(3), H1434–1439.

Bolz, S.-S., Vogel, L., Sollinger, D., Derwand, R., Boer, C., Pitson, S. M., … Pohl, U. (2003). Sphingosine kinase modulates microvascular tone and myogenic responses through activation of RhoA/Rho kinase. *Circulation*, *108*(3), 342–7. http://doi.org/10.1161/01.CIR.0000080324.12530.0D

Boudaoud, A., Burian, A., Borowska-Wykręt, D., Uyttewaal, M., Wrzalik, R., Kwiatkowska, D., & Hamant, O. (2014). FibrilTool, an ImageJ plug-in to quantify fibrillar structures in raw microscopy images. *Nature Protocols*, *9*(2), 457–463. http://doi.org/10.1038/nprot.2014.024

Bradley, E. a, Eringa, E. C., Stehouwer, C. D. a, Korstjens, I., van Nieuw Amerongen, G. P., Musters, R., … Rattigan, S. (2010). Activation of AMP-activated protein kinase by 5-aminoimidazole-4-carboxamide-1-beta-D-ribofuranoside in the muscle microcirculation increases nitric oxide synthesis and microvascular perfusion. *Arteriosclerosis, Thrombosis, and Vascular Biology*, *30*(6), 1137–42. http://doi.org/10.1161/ATVBAHA.110.204404

Brini, M., & Carafoli, E. (2009). Calcium Pumps in Health and Disease. *Physiological Reviews*, *89*(79), 1341–1378. http://doi.org/10.1152/physrev.00032.2008.

Brozovich, F. V, Nicholson, C. J., Degen, C. V, Gao, Y. Z., Aggarwal, M., & Morgan, K. G. (2016). Mechanisms of Vascular Smooth Muscle Contraction and the Basis for Pharmacologic Treatment of Smooth Muscle Disorders. *Pharmacological Reviews*, *68*(2), 476–532. http://doi.org/10.1124/pr.115.010652

Bryan, P. T., & Marshall, J. M. (1999). Cellular mechanisms by which adenosine induces vasodilatation in rat skeletal muscle: significance for systemic hypoxia. *The Journal of Physiology*, *514*(Pt.1), 163–75.

Cao, X., Luo, T., Luo, X., & Tang, Z. (2014). Resveratrol prevents AngII-induced hypertension via AMPK activation and RhoA / ROCK suppression in mice. *Hypertension Research : Official Journal of the Japanese Society of Hypertension*, *37*(June 2014), 803–810. http://doi.org/10.1038/hr.2014.90.

Castorena-Gonzalez, J. A., Staiculescu, M. C., Foote, C. A., Polo-Parada, L., & Martinez-Lemus, L. A. (2014). The obligatory role of the actin cytoskeleton on inward remodeling induced by dithiothreitol activation of endogenous transglutaminase in isolated arterioles. *American Journal of Physiology. Heart and Circulatory Physiology*, *306*(4), H485–H495.

Chan, C., Beltzner, C. C., & Pollard, T. D. (2009). Cofilin Dissociates Arp2/3 Complex and Branches from Actin Filaments. *Current Biology*, *19*(7), 537–545.

http://doi.org/10.1016/j.cub.2009.02.060

Chandrasekera, P. C., Kargacin, M. E., Deans, J. P., & Lytton, J. (2009). Determination of apparent calcium affinity for endogenously expressed human sarco (endo) plasmic reticulum calcium-ATPase isoform SERCA3, (43), 1105–1114. http://doi.org/10.1152/ajpcell.00650.2008.

Chen, Z. P., Mitchelhill, K. I., Michell, B. J., Stapleton, D., Rodriguez-Crespo, I., Witters, L. a, … Kemp, B. E. (1999). AMP-activated protein kinase phosphorylation of endothelial NO synthase. *FEBS Letters*, *443*(3), 285–9.

Cheranov, S. Y., & Jaggar, J. H. (2002). Sarcoplasmic reticulum calcium load regulates rat arterial smooth muscle calcium sparks and transient K(Ca) currents. *The Journal of Physiology*, *544*, 71–84. http://doi.org/10.1113/jphysiol.2002.025197

Chou, C., Chen, Y., Hung, C., Chang, Y., Tzeng, Y., Wu, X., … Group, S. (2016). Function : From Clinical to Bench Research, *100*(November 2015), 4339–4347. http://doi.org/10.1210/jc.2015-2752

Chutkow, W. A., Pu, J., Wheeler, M. T., Wada, T., Makielski, J. C., Burant, C. F., … Terzic, A. (2002). Episodic coronary artery vasospasm and hypertension develop in the absence of Sur2 KATP channels. *Journal of Clinical Investigation*, *110*(2), 203–208. http://doi.org/10.1172/JCI15672

Cipolla, M. J., Gokina, N. I., & Osol, G. (2002). Pressure-induced actin polymerization in vascular smooth muscle as a mechanism underlying myogenic behavior. *The FASEB Journal : Official Publication of the Federation of American Societies for Experimental Biology*, *16*(1), 72–76. http://doi.org/10.1096/cj.01-0104hyp

Colyer, J., & Wang, J. H. (1991). Dependence of cardiac sarcoplasmic reticulum calcium pump activity on the phosphorylation status of phospholamban. *The Journal of Biological Chemistry*, *266*(26), 17486–93.

Cox, R. H., & Rusch, N. J. (2002). New expression profiles of voltage-gated ion channels in arteries exposed to high blood pressure. *Microcirculation (New York, N.Y. : 1994)*, *9*(4), 243–57. http://doi.org/10.1038/sj.mn.7800140

Crowley, S. D., Gurley, S. B., Oliverio, M. I., Pazmino, A. K., Griffiths, R., Flannery, P. J., … Coffman, T. M. (2005). Distinct roles for the kidney and systemic tissues in blood pressure regulation by the renin-angiotensin system. *The Journal of Clinical Investigation*, *115*(4), 1092–9. http://doi.org/10.1172/JCI23378

Dai, Y.-P., Bongalon, S., Mutafova-Yambolieva, V. N., & Yamboliev, I. a. (2008). Distinct effects of contraction agonists on the phosphorylation state of cofilin in pulmonary artery smooth muscle. *Advances in Pharmacological Sciences*, *2008*, 362741. http://doi.org/10.1155/2008/362741

de Wit, C., Schäfer, C., von Bismarck, P., Bolz, S.-S., & Pohl, U. (1997). Elevation of plasma viscosity induces sustained NO-mediated dilation in the hamster cremaster microcirculation in vivo.

Pflügers Archiv : European Journal of Physiology, *434*(4), 354–61.

Dietrich, A., Mederos Y Schnitzler, M., Gollasch, M., Gross, V., Storch, U., Dubrovska, G., … Birnbaumer, L. (2005). Increased Vascular Smooth Muscle Contractility in TRPC6 − / − Mice. *Molecular and Cellular Biology*, *25*(16), 6980–6989. http://doi.org/10.1128/MCB.25.16.6980

Dong, Y., Zhang, M., Liang, B., Xie, Z., Zhao, Z., Asfa, S., … Zou, M.-H. (2010). Reduction of AMP-activated protein kinase alpha2 increases endoplasmic reticulum stress and atherosclerosis in vivo. *Circulation*, *121*(6), 792–803. http://doi.org/10.1161/CIRCULATIONAHA.109.900928

Dreiza, C. M., Brophy, C. M., Komalavilas, P., Furnish, E. J., Joshi, L., Pallero, M. a, … Panitch, A. (2005). Transducible heat shock protein 20 (HSP20) phosphopeptide alters cytoskeletal dynamics. *The FASEB Journal : Official Publication of the Federation of American Societies for Experimental Biology*, *19*(2), 261–263. http://doi.org/10.1096/fj.04-2911fje

Earley, S., & Brayden, J. E. (2015). Transient receptor potential channels in the vasculature. *Physiological Reviews*, *95*(2), 645–90. http://doi.org/10.1152/physrev.00026.2014

Eggermont, J. A., Wuytack, F., Verbist, J., & Casteels, R. (1990). Expression of endoplasmic-reticulum Ca2+-pump isoforms and of phospholamban in pig smooth-muscle tissues. *Biochem J*, *271*(3), 647–653.

El-Toukhy, A., Given, A. M., Ogut, O., & Brozovich, F. V. (2006). PHI-1 interacts with the catalytic subunit of myosin light chain phosphatase to produce a Ca^{2+} independent increase in MLC_{20} phosphorylation and force in avian smooth muscle. *FEBS Letters*, *580*(24), 5779–5784. http://doi.org/10.1016/j.febslet.2006.09.035

Enkhjargal, B., Godo, S., Sawada, A., Suvd, N., Saito, H., Noda, K., … Shimokawa, H. (2014). Endothelial AMP-Activated Protein Kinase Regulates Blood Pressure and Coronary Flow Responses Through Hyperpolarization Mechanism in Mice. *Arteriosclerosis, Thrombosis, and Vascular Biology*, 1505–1513. http://doi.org/10.1161/ATVBAHA.114.303735

Eto, M., Karginov, A., & Brautigan, D. L. (1999). A Novel Phosphoprotein Inhibitor of Protein Type-1 Phosphatase Holoenzymes [†]. *Biochemistry*, *38*(51), 16952–16957. http://doi.org/10.1021/bi992030o

Eto, M., Ohmori, T., Suzuki, M., Furuya, K., & Morita, F. (1995). A novel protein phosphatase-1 inhibitory protein potentiated by protein kinase C. Isolation from porcine aorta media and characterization. *Journal of Biochemistry*, *118*(6), 1104–7.

Félétou, M., Huang, Y., & Vanhoutte, P. M. (2011). Endothelium-mediated control of vascular tone: COX-1 and COX-2 products. *British Journal of Pharmacology*, *164*(3), 894–912. http://doi.org/10.1111/j.1476-5381.2011.01276.x

Félétou, M., & Vanhoutte, P. M. (2009). EDHF: An update. *Clinical Science (London, England : 1979)*,

117(4), 139–55. http://doi.org/10.1042/CS20090096

Fisslthaler, B., & Fleming, I. (2009). Activation and signaling by the AMP-activated protein kinase in endothelial cells. *Circulation Research*, *105*(2), 114–27. http://doi.org/10.1161/CIRCRESAHA.109.201590

Flavahan, N. a, Bailey, S. R., Flavahan, W. a, Mitra, S., & Flavahan, S. (2005). Imaging remodeling of the actin cytoskeleton in vascular smooth muscle cells after mechanosensitive arteriolar constriction. *American Journal of Physiology. Heart and Circulatory Physiology*, *288*(2), H660–H669. http://doi.org/10.1152/ajpheart.00608.2004

Ford, R. J., Rush, J. W. E., Alvarez, Y., Blume, C., Benz, P., Walter, U., … Shyy, J. (2011). Endothelium-dependent vasorelaxation to the AMPK activator AICAR is enhanced in aorta from hypertensive rats and is NO and EDCF dependent. *American Journal of Physiology. Heart and Circulatory Physiology*, *300*(1), H64–75. http://doi.org/10.1152/ajpheart.00597.2010

Ford, R. J., Teschke, S. R., Reid, E. B., Durham, K. K., Kroetsch, J. T., & Rush, J. W. E. (2012). AMP-activated protein kinase activator AICAR acutely lowers blood pressure and relaxes isolated resistance arteries of hypertensive rats. *Journal of Hypertension*, *30*(4), 725–33. http://doi.org/10.1097/HJH.0b013e32835050ca

Freeman, A. K., & Morrison, D. K. (2011). 14-3-3 Proteins: diverse functions in cell proliferation and cancer progression. *Seminars in Cell & Developmental Biology*, *22*(7), 681–7. http://doi.org/10.1016/j.semcdb.2011.08.009

Fryer, L. G. D., Hajduch, E., Rencurel, F., Salt, I. P., Hundal, H. S., Haxdie, D. G., & Carling, D. (2000). Activation of Glucose Transport by AMP-Activated Protein Kinase via Stimulation of Nitric Oxide Synthase. *Diabetes*, *49*(December), 1978–1985.

Gadalla, A. E., Pearson, T., Currie, A. J., Dale, N., Hawley, S. a., Sheehan, M., … Frenguelli, B. G. (2004). AICA riboside both activates AMP-activated protein kinase and competes with adenosine for the nucleoside transporter in the CA1 region of the rat hippocampus. *Journal of Neurochemistry*, *88*(5), 1272–1282. http://doi.org/10.1046/j.1471-4159.2003.02253.x

Gallant, C., Appel, S., Graceffa, P., Leavis, P., Lin, J. J.-C., Gunning, P. W., … Morgan, K. G. (2011). Tropomyosin variants describe distinct functional subcellular domains in differentiated vascular smooth muscle cells. *American Journal of Physiology. Cell Physiology*, *300*, C1356–C1365. http://doi.org/10.1152/ajpcell.00450.2010

Galvez, A., Gimenez-Gallego, G., Reuben, J. P., Roy-Contancin, L., Feigenbaum, P., Kaczorowski, G. J., & Garcia, M. L. (1990). Purification and characterization of a unique, potent, peptidyl probe for the high conductance calcium-activated potassium channel from venom of the scorpion Buthus tamulus. *Journal of Biological Chemistry*, *265*(19), 11083–11090.

Gerthoffer, W. T. (2005). Actin cytoskeletal dynamics in smooth muscle contraction. *Canadian Journal of Physiology and Pharmacology*, *83*(10), 851–856. http://doi.org/10.1139/y05-088

Giet, R., Sinka, R., Mazumdar, A., Lock, W. G., Balloux, F., Zafiropoulos, P. J., … Winter, S. (n.d.). Genome-wide survey of protein kinases required for cell cycle progression, (cdc). http://doi.org/10.1038/nature03160

Goirand, F., Solar, M., Athea, Y., Viollet, B., Mateo, P., Fortin, D., … Garnier, A. (2007). Activation of AMP kinase α1 subunit induces aortic vasorelaxation in mice. *The Journal of Physiology*, *581*(3), 1163–1171. http://doi.org/10.1113/jphysiol.2007.132589

Gruber, H. E., Hoffer, M. E., McAllister, D. R., Laikind, P. K., Lane, T. a., Schmid-Schoenbein, G. W., & Engler, R. L. (1989). Increased adenosine concentration in blood from ischemic myocardium by AICA riboside. Effects on flow, granulocytes, and injury. *Circulation*, *80*(5), 1400–1411. http://doi.org/10.1161/01.CIR.80.5.1400

Gruzman, A., Babai, G., & Sasson, S. (2009). Adenosine Monophosphate-Activated Protein Kinase (AMPK) as a New Target for Antidiabetic Drugs: A Review on Metabolic, Pharmacological and Chemical Considerations. *The Review of Diabetic Studies : RDS*, *6*(1), 13–36. http://doi.org/10.1900/RDS.2009.6.13

Gunst, S. J., & Zhang, W. (2008). Actin cytoskeletal dynamics in smooth muscle: a new paradigm for the regulation of smooth muscle contraction. *American Journal of Physiology. Cell Physiology*, *295*(3), C576–C587. http://doi.org/10.1152/ajpcell.00253.2008

Hallows, K. R., Kobinger, G. P., Wilson, J. M., Witters, L. A., Foskett, J. K., Aleksandrov, L., … Moller, D. (2003). Physiological modulation of CFTR activity by AMP-activated protein kinase in polarized T84 cells. *American Journal of Physiology. Cell Physiology*, *284*(5), C1297–308. http://doi.org/10.1152/ajpcell.00227.2002

Hardie, D. G. (2013). AMPK: a target for drugs and natural products with effects on both diabetes and cancer. *Diabetes*, *62*(7), 2164–72. http://doi.org/10.2337/db13-0368

Hardie, D. G. (2014). AMP-Activated Protein Kinase: Maintaining Energy Homeostasis at the Cellular and Whole-Body Levels. *Annual Review of Nutrition*, *34*(1), 31–55. http://doi.org/10.1146/annurev-nutr-071812-161148

Hardie, D. G., & Ashford, M. L. J. (2014). AMPK: regulating energy balance at the cellular and whole body levels. *Physiology (Bethesda, Md.)*, *29*(2), 99–107. http://doi.org/10.1152/physiol.00050.2013

Hardie, D. G., Schaffer, B. E., & Brunet, A. (2016). AMPK: An Energy-Sensing Pathway with Multiple Inputs and Outputs. *Trends in Cell Biology*, *26*(3), 190–201. http://doi.org/10.1016/j.tcb.2015.10.013

Hartshorne, D. J., Ito, M., & Erdödi, F. (1998). Myosin light chain phosphatase: subunit composition, interactions and regulation. *Journal of Muscle Research and Cell Motility*, *19*(4), 325–41.

Hocking, K. M., Baudenbacher, F. J., Putumbaka, G., Venkatraman, S., Cheung-Flynn, J., Brophy, C. M., & Komalavilas, P. (2013). Role of Cyclic Nucleotide-Dependent Actin Cytoskeletal Dynamics: [Ca2+]i and Force Suppression in Forskolin-Pretreated Porcine Coronary Arteries. *PLoS ONE*, *8*(4). http://doi.org/10.1371/journal.pone.0060986

Horman, S., Morel, N., Vertommen, D., Hussain, N., Neumann, D., Beauloye, C., … Rider, M. H. (2008). AMP-activated protein kinase phosphorylates and desensitizes smooth muscle myosin light chain kinase. *Journal of Biological Chemistry*, *283*(27), 18505–18512. http://doi.org/10.1074/jbc.M802053200

Hotaling, N. A., Bharti, K., Kriel, H., & Simon, C. G. (2015). Dataset for the validation and use of DiameterJ an open source nanofiber diameter measurement tool. *Data in Brief*, *5*, 13–22. http://doi.org/10.1016/j.dib.2015.07.012

Hotulainen, P., Paunola, E., Vartiainen, M., & Lappalainen, P. (2004). Actin-depolymerizing Factor and Cofilin-1 Play Overlapping Roles in Promoting Rapid F-Actin Depolymerization in Mammalian Nonmuscle Cells. *Molecular Biology of the Cell*, *16*(2), 649–664. http://doi.org/10.1091/mbc.E04-07-0555

House, S. J., Potier, M., Bisaillon, J., Singer, H. a, & Trebak, M. (2008). The non-excitable smooth muscle: calcium signaling and phenotypic switching during vascular disease. *Pflügers Archiv : European Journal of Physiology*, *456*(5), 769–85. http://doi.org/10.1007/s00424-008-0491-8

Huang, P. L., Huang, Z., Mashimo, H., Bloch, K. D., Moskowitz, M. A., Bevan, J. A., & Fishman, M. C. (1995). Hypertension in mice lacking the gene for endothelial nitric oxide synthase. *Nature*, *377*(6546), 239–242. http://doi.org/10.1038/377239a0

Iwamoto, T., Kita, S., Zhang, J., Blaustein, M. P., Arai, Y., Yoshida, S., … Katsuragi, T. (2004). Salt-sensitive hypertension is triggered by Ca2+ entry via Na+/Ca2+ exchanger type-1 in vascular smooth muscle. *Nature Medicine*, *10*(11), 1193–9. http://doi.org/10.1038/nm1118

Kanchanawong, P., Shtengel, G., Pasapera, A. M., Ramko, E. B., Davidson, M. W., Hess, H. F., & Waterman, C. M. (2010). Nanoscale architecture of integrin-based cell adhesions. *Nature*, *468*(7323), 580–4. http://doi.org/10.1038/nature09621

Kim, H. R., Gallant, C., Leavis, P. C., Gunst, S. J., & Morgan, K. G. (2008). Cytoskeletal remodeling in differentiated vascular smooth muscle is actin isoform dependent and stimulus dependent. *Am J Physiol Cell Physiol*, *295*(3), C768–78. http://doi.org/10.1152/ajpcell.00174.2008

Kitazawa, T., & Kitazawa, K. (2012). Size-dependent heterogeneity of contractile Ca2+ sensitization in rat arterial smooth muscle. *Journal of Physiology*, *590*(21), 5401–5423.

Kolias, A. G., Sen, J., & Belli, A. (2009). Pathogenesis of cerebral vasospasm following aneurysmal subarachnoid hemorrhage: Putative mechanisms and novel approaches. *Journal of Neuroscience Research*, *87*(1), 1–11. http://doi.org/10.1002/jnr.21823

Kondratowicz, A. S., Hunt, C. L., Davey, R. a, Cherry, S., & Maury, W. J. (2013). AMP-activated protein kinase is required for the macropinocytic internalization of ebolavirus. *Journal of Virology*, *87*(2), 746–55. http://doi.org/10.1128/JVI.01634-12

Koss, K. L., Grupp, I. L., & Kranias, E. G. (1997). The relative phospholamban and SERCA2 ratio: a critical determinant of myocardial contractility. *Basic Research in Cardiology*, *92 Suppl 1*(6), 17–24.

Kranias, E. G., & Hajjar, R. J. (2012). Modulation of cardiac contractility by the phopholamban/SERCA2a regulatome. *Circulation Research*, *110*(12), 1646–1660. http://doi.org/10.1161/CIRCRESAHA.111.259754

Kronlage, C., Schäfer-Herte, M., Böning, D., Oberleithner, H., & Fels, J. (2015). Feeling for Filaments: Quantification of the Cortical Actin Web in Live Vascular Endothelium. *Biophysical Journal*, *109*(4), 687–698. http://doi.org/10.1016/j.bpj.2015.06.066

Lalli, J., Harrer, J. M., Luo, W., Kranias, E. G., & Paul, R. J. (1997). Targeted Ablation of the Phospholamban Gene Is Associated With a Marked Decrease in Sensitivity in Aortic Smooth Muscle. *Circulation Research*, *80*(4), 506–513. http://doi.org/10.1161/01.RES.80.4.506

Lamont, C., Vainorius, E., & Wier, W. G. (2003). Purinergic and Adrenergic Ca $^{2+}$ Transients during Neurogenic Contractions of Rat Mesenteric Small Arteries. *The Journal of Physiology*, *549*(3), 801–808. http://doi.org/10.1113/jphysiol.2003.043380

Lee, J. H., Koh, H., Kim, M., Kim, Y., Lee, S. Y., Karess, R. E., … Chung, J. (2007). Energy-dependent regulation of cell structure by AMP-activated protein kinase. *Nature*, *447*(7147), 1017–1020. http://doi.org/10.1038/nature05828

Lee, Y. K., Park, S. Y., Kim, Y. M., Lee, W. S., & Park, O. J. (2009). AMP kinase/cyclooxygenase-2 pathway regulates proliferation and apoptosis of cancer cells treated with quercetin. *Experimental & Molecular Medicine*, *41*(3), 201–7. http://doi.org/10.3858/emm.2009.41.3.023

Lehman, W., & Morgan, K. G. (2012). Structure and dynamics of the actin-based smooth muscle contractile and cytoskeletal apparatus. *Journal of Muscle Research and Cell Motility*, *33*(6), 461–469. http://doi.org/10.1007/s10974-012-9283-z

Li, J., Qi, D., Cheng, H., Hu, X., Miller, E. J., Wu, X., … Young, L. H. (2013). Urocortin 2 autocrine/paracrine and pharmacologic effects to activate AMP-activated protein kinase in the heart. *Proceedings of the National Academy of Sciences of the United States of America*, *110*(40), 16133–8. http://doi.org/10.1073/pnas.1312775110

Liang, B., Wang, S., Wang, Q., Zhang, W., Viollet, B., Zhu, Y., & Zou, M.-H. (2013). Aberrant Endoplasmic Reticulum Stress in Vascular Smooth Muscle Increases Vascular Contractility and Blood Pressure in Mice Deficient of AMP-Activated Protein Kinase-α2 In Vivo. *Arteriosclerosis, Thrombosis, and Vascular Biology*, *33*(3), 595–604. http://doi.org/10.1161/ATVBAHA.112.300606

Lipskaia, L., Bobe, R., Chen, J., Turnbull, I. C., Lopez, J. J., Merlet, E., … Hadri, L. (2013). Synergistic Role of Protein Phosphatase Inhibitor 1 and SERCA2a in the Acquisition of the Contractile Phenotype of Arterial Smooth Muscle Cells. *Circulation*. http://doi.org/10.1161/CIRCULATIONAHA.113.002565

Lipskaia, L., Limon, I., Bobe, R., & Hajjar, R. (2012). Calcium Cycling in Synthetic and Contractile Phasic or Tonic Vascular Smooth Muscle Cells.

Lubomirov, L. T., Reimann, K., Metzler, D., Hasse, V., Stehle, R., Ito, M., … Schubert, R. (2006). Urocortin-induced decrease in Ca2+ sensitivity of contraction in mouse tail arteries is attributable to cAMP-dependent dephosphorylation of MYPT1 and activation of myosin light chain phosphatase. *Circulation Research*, *98*(9), 1159–67. http://doi.org/10.1161/01.RES.0000219904.43852.3e

Marin, T. L., Gongol, B., Martin, M., King, S. J., Smith, L., Johnson, D. A., … Shyy, J. Y.-J. (2015). Identification of AMP-activated protein kinase targets by a consensus sequence search of the proteome. *BMC Systems Biology*, *9*, 13. http://doi.org/10.1186/s12918-015-0156-0

Matchkov, V. V., Boedtkjer, D. M., & Aalkjaer, C. (2015). The role of Ca2+ activated Cl- channels in blood pressure control. *Current Opinion in Pharmacology*, *21*, 127–137. http://doi.org/10.1016/j.coph.2015.02.003

Mehta, D., & Gunst, S. J. (1999). Actin polymerization stimulated by contractile activation regulates force development in canine tracheal smooth muscle. *Journal of Physiology*, *519*(3), 829–840. http://doi.org/10.1111/j.1469-7793.1999.0829n.x

Meininger, G. A., Zawieja, D. C., Falcone, J. C., Hill, M. A., & Davey, J. P. (1991). Calcium measurement in isolated arterioles during myogenic and agonist stimulation. *Am J Physiol*, *261*(3 Pt 2), H950–9.

Michael, S. K., Surks, H. K., Wang, Y., Zhu, Y., Blanton, R., Jamnongjit, M., … Mendelsohn, M. E. (2008). High blood pressure arising from a defect in vascular function. *Proceedings of the National Academy of Sciences*, *105*(18), 6702–6707. http://doi.org/10.1073/pnas.0802128105

Miranda, L., Carpentier, S., Platek, A., Hussain, N., Gueuning, M. A., Vertommen, D., … Horman, S. (2010). AMP-activated protein kinase induces actin cytoskeleton reorganization in epithelial cells. *Biochemical and Biophysical Research Communications*, *396*(3), 656–661.

http://doi.org/10.1016/j.bbrc.2010.04.151

Mistry, D. K., & Garland, C. J. (1998). Characteristics of Single, Large-Conductance Calcium-Dependent Potassium Channels (BK Ca) from Smooth Muscle Cells Isolated from the Rabbit Mesenteric Artery. *Journal of Membrane Biology*, *164*(2), 125–138. http://doi.org/10.1007/s002329900399

Moon, S., Han, D., Kim, Y., Jin, J., Ho, W.-K., & Kim, Y. (2014). Interactome analysis of AMP-activated protein kinase (AMPK)-α1 and -β1 in INS-1 pancreatic beta-cells by affinity purification-mass spectrometry. *Scientific Reports*, *4*, 4376. http://doi.org/10.1038/srep04376

Moosmang, S., Schulla, V., Welling, A., Feil, R., Feil, S., Wegener, J. W., … Klugbauer, N. (2003). Dominant role of smooth muscle L-type calcium channel Cav1.2 for blood pressure regulation. *The EMBO Journal*, *22*(22), 6027–34. http://doi.org/10.1093/emboj/cdg583

Moreno-Domínguez, A., El-Yazbi, A. F., Zhu, H.-L., Colinas, O., Zhong, X. Z., Walsh, E. J., … Cole, W. C. (2014). Cytoskeletal Reorganization Evoked by Rho-associated kinase- and Protein Kinase C-catalyzed Phosphorylation of Cofilin and Heat Shock Protein 27, Respectively, Contributes to Myogenic Constriction of Rat Cerebral Arteries. *Journal of Biological Chemistry*, *289*(30), 20939–20952. http://doi.org/10.1074/jbc.M114.553743

Murányi, A., Derkach, D., Erdődi, F., Kiss, A., Ito, M., & Hartshorne, D. J. (2005). Phosphorylation of Thr695 and Thr850 on the myosin phosphatase target subunit: Inhibitory effects and occurrence in A7r5 cells. *FEBS Letters*, *579*(29), 6611–6615. http://doi.org/10.1016/j.febslet.2005.10.055

Nakano, A., Kato, H., Watanabe, T., Min, K.-D., Yamazaki, S., Asano, Y., … Takashima, S. (2010). AMPK controls the speed of microtubule polymerization and directional cell migration through CLIP-170 phosphorylation. *Nature Cell Biology*, *12*(6), 583–590. http://doi.org/10.1038/ncb2060

Navedo, M. F., & Amberg, G. C. (2013). Local regulation of L-type Ca^{2+} channel sparklets in arterial smooth muscle. *Microcirculation (New York, N.Y. : 1994)*, *20*(4), 290–8. http://doi.org/10.1111/micc.12021

Nieves-Cintron, M., Amberg, G. C., Nichols, C. B., Molkentin, J. D., & Santana, L. F. (2007). Activation of NFATc3 Down-regulates the beta1 Subunit of Large Conductance, Calcium-activated K+ Channels in Arterial Smooth Muscle and Contributes to Hypertension. *Journal of Biological Chemistry*, *282*(5), 3231–3240. http://doi.org/10.1074/jbc.M608822200

Nour-Eldine, W., Ghantous, C. M., Zibara, K., Dib, L., Issaa, H., Itani, H. A., … Zeidan, A. (2016). Adiponectin Attenuates Angiotensin II-Induced Vascular Smooth Muscle Cell Remodeling through Nitric Oxide and the RhoA/ROCK Pathway. *Frontiers in Pharmacology*, *7*(April), 1–15. http://doi.org/10.3389/fphar.2016.00086

Nourian, Z., Li, M., Leo, M. D., Jaggar, J. H., Braun, A. P., Hill, M. A., … Li, M. (2014). Large

Conductance Ca2+-Activated K+ Channel (BKCa) α-Subunit Splice Variants in Resistance Arteries from Rat Cerebral and Skeletal Muscle Vasculature. *PLoS ONE*, *9*(6), e98863. http://doi.org/10.1371/journal.pone.0098863

Omae, T., Nagaoka, T., Tanano, I., & Yoshida, A. (2013). Adiponectin-induced dilation of isolated porcine retinal arterioles via production of nitric oxide from endothelial cells. *Investigative Ophthalmology & Visual Science*, *54*(7), 4586–94. http://doi.org/10.1167/iovs.13-11756

Onselaer, M.-B., Oury, C., Hunter, R. W., Eeckhoudt, S., Barile, N., Lecut, C., … Horman, S. (2014). The Ca(2+) /calmodulin-dependent kinase kinase β-AMP-activated protein kinase-α1 pathway regulates phosphorylation of cytoskeletal targets in thrombin-stimulated human platelets. *Journal of Thrombosis and Haemostasis : JTH*, *12*(6), 973–86. http://doi.org/10.1111/jth.12568

Opazo Saez, A., Zhang, W., Wu, Y., Turner, C. E., Tang, D. D., Gunst, S. J., … Gunst, S. J. (2004). Tension development during contractile stimulation of smooth muscle requires recruitment of paxillin and vinculin to the membrane. *Am J Physiol Cell Physiol*, *286*(2), C433–C447. http://doi.org/10.1152/ajpcell.00030.2003

Osuka, K., Watanabe, Y., Yasuda, M., & Takayasu, M. (2012). Adiponectin activates endothelial nitric oxide synthase through AMPK signaling after subarachnoid hemorrhage. *Neuroscience Letters*, *514*(1), 2–5. http://doi.org/10.1016/j.neulet.2011.12.041

Palanivel, R., Ganguly, R., Turdi, S., Xu, A., & Sweeney, G. (2014). Adiponectin stimulates Rho-mediated actin cytoskeleton remodeling and glucose uptake via APPL1 in primary cardiomyocytes. *Metabolism: Clinical and Experimental*, *63*(10), 1363–1373. http://doi.org/10.1016/j.metabol.2014.07.005

Pang, T., Zhang, Z.-S., Gu, M., Qiu, B.-Y., Yu, L.-F., Cao, P.-R., … Li, J. (2008). Small molecule antagonizes autoinhibition and activates AMP-activated protein kinase in cells. *The Journal of Biological Chemistry*, *283*(23), 16051–60. http://doi.org/10.1074/jbc.M710114200

Pinter, K., Grignani, R. T., Watkins, H., & Redwood, C. (2013). Localisation of AMPK γ subunits in cardiac and skeletal muscles. *Journal of Muscle Research and Cell Motility*, *34*(5-6), 369–78. http://doi.org/10.1007/s10974-013-9359-4

Potocnik, S. J., & Hill, M. a. (2001). Pharmacological evidence for capacitative Ca(2+) entry in cannulated and pressurized skeletal muscle arterioles. *British Journal of Pharmacology*, *134*(2), 247–56. http://doi.org/10.1038/sj.bjp.0704270

Poythress, R. H., Gallant, C., Vetterkind, S., & Morgan, K. G. (2013). Vasoconstrictor-induced endocytic recycling regulates focal adhesion protein localization and function in vascular smooth muscle. *American Journal of Physiology. Cell Physiology*, *305*(2), C215–27. http://doi.org/10.1152/ajpcell.00103.2013

Puetz, S., Lubomirov, L. T., & Pfitzer, G. (2009). Regulation of smooth muscle contraction by small GTPases. *Physiology (Bethesda, Md.)*, *24*, 342–56. http://doi.org/10.1152/physiol.00023.2009

Qiao, Y.-N., He, W.-Q., Chen, C.-P., Zhang, C.-H., Zhao, W., Wang, P., … Zhu, M.-S. (2014). Myosin Phosphatase Target Subunit 1 (MYPT1) Regulates the Contraction and Relaxation of Vascular Smooth Muscle and Maintains Blood Pressure. *Journal of Biological Chemistry*, *289*(32), 22512–22523. http://doi.org/10.1074/jbc.M113.525444

Raeymakers, L., & Jones, L. R. (1986). Evidence for the presence of phospholamban in the endoplasmic reticulum of smooth muscle. *Biochimica et Biophysica Acta*, *882*, 258–265.

Raghow, R., Seyer, J., & Kang, A. (2006). Connective Tissues of the Subendothelium. In J. Creager, M.A., Dzau, V.J., Loscalzo (Ed.), *Vascular Medicine. A Companion to Braunwald's Heart Disease* (7th ed., pp. 31–60).

Randriamboavonjy, V., Isaak, J., Frömel, T., Viollet, B., Fisslthaler, B., Preissner, K. T., & Fleming, I. (2010). AMPK α2 subunit is involved in platelet signaling, clot retraction, and thrombus stability. *Blood*, *116*(12), 2134–40. http://doi.org/10.1182/blood-2010-04-279612

Rembold, C. M., Tejani, A. D., Ripley, M. L., & Han, S. (2007). Paxillin phosphorylation, actin polymerization, noise temperature, and the sustained phase of swine carotid artery contraction. *American Journal of Physiology. Cell Physiology*, *293*(3), C993–C1002. http://doi.org/10.1152/ajpcell.00090.2007

Ren, J., Albinsson, S., & Hellstrand, P. (2010). Distinct effects of voltage- and store-dependent calcium influx on stretch-induced differentiation and growth in vascular smooth muscle. *Journal of Biological Chemistry*, *285*(41), 31829–31839. http://doi.org/10.1074/jbc.M109.097576

Riedl, J., Flynn, K. C., Raducanu, A., Gärtner, F., Beck, G., Bösl, M., … Wedlich-Söldner, R. (2010). Lifeact mice for studying F-actin dynamics. *Nature Methods*, *7*(3), 168–9. http://doi.org/10.1038/nmeth0310-168

Rivera, L., Morón, R., Zarzuelo, A., & Galisteo, M. (2009). Long-term resveratrol administration reduces metabolic disturbances and lowers blood pressure in obese Zucker rats. *Biochemical Pharmacology*, *77*(6), 1053–1063. http://doi.org/10.1016/j.bcp.2008.11.027

Ross, E., Ata, R., Thavarajah, T., Medvedev, S., Bowden, P., Marshall, J. G., & Antonescu, C. N. (2015). AMP-Activated Protein Kinase Regulates the Cell Surface Proteome and Integrin Membrane Traffic. *PloS One*, *10*(5), e0128013. http://doi.org/10.1371/journal.pone.0128013

Ross, F. A., Rafferty, J. N., Dallas, M. L., Ogunbayo, O., Ikematsu, N., McClafferty, H., … Evans, a M. (2011). Selective expression in carotid body type I cells of a single splice variant of the large conductance calcium- and voltage-activated potassium channel confers regulation by AMP-activated protein kinase. *The Journal of Biological Chemistry*, *286*(14), 11929–36.

http://doi.org/10.1074/jbc.M110.189779

Rubio, M. P., Geraghty, K. M., Wong, B. H. C., Wood, N. T., Campbell, D. G., Morrice, N., … Mackintosh, C. (2004). 14-3-3-Affinity Purification of Over 200 Human Phosphoproteins Reveals New Links To Regulation of Cellular Metabolism, Proliferation and Trafficking. *Biochem J*, *379*(Pt 2), 395–408. http://doi.org/10.1042/BJ20031797

Sag, D., Carling, D., Stout, R. D., & Suttles, J. (2008). Adenosine 5′-Monophosphate-Activated Protein Kinase Promotes Macrophage Polarization to an Anti-Inflammatory Functional Phenotype. *The Journal of Immunology*, *181*(12), 8633–8641. http://doi.org/10.4049/jimmunol.181.12.8633

Saito, S.-Y., Hori, M., Ozaki, H., & Karaki, H. (1996). Cytochalasin Inhibits Smooth Muscle Contraction By Directly Inhibiting Contractile Apparatus. *Journal of Smooth Muscle Research*, *32*(2), 51–60.

Sampathkumar, A., Krupinski, P., Wightman, R., Milani, P., Berquand, A., Boudaoud, A., … Meyerowitz, E. M. (2014). Subcellular and supracellular mechanical stress prescribes cytoskeleton behavior in Arabidopsis cotyledon pavement cells. *eLife*, *3*, e01967. http://doi.org/10.7554/eLife.01967

Sanchez, M., & McManus, O. B. (1996). Paxilline Inhibition of the Alpha-subunit of the High-conductance Calcium-activated Potassium Channel. *Neuropharmacology*, *35*(7), 963–968.

Sanders, K. M. (2001). Mechanisms of calcium handling in smooth muscles. *The Journal of Applied Physiology*, *91*(3), 1438–1449.

Sarelius, I., & Pohl, U. (2010). Control of muscle blood flow during exercise: local factors and integrative mechanisms. *Acta Physiologica (Oxford, England)*, *199*(4), 349–65. http://doi.org/10.1111/j.1748-1716.2010.02129.x

Sausbier, M., Arntz, C., Bucurenciu, I., Zhao, H., Zhou, X.-B., Sausbier, U., … Ruth, P. (2005). Elevated blood pressure linked to primary hyperaldosteronism and impaired vasodilation in BK channel-deficient mice. *Circulation*, *112*(1), 60–8. http://doi.org/10.1161/01.CIR.0000156448.74296.FE

Schaffer, B. E., Levin, R. S., Hertz, N. T., Maures, T. J., Schoof, M. L., Hollstein, P. E., … Brunet, A. (2015). Identification of AMPK Phosphorylation Sites Reveals a Network of Proteins Involved in Cell Invasion and Facilitates Large-Scale Substrate Prediction. *Cell Metabolism*, *22*(5), 907–921. http://doi.org/10.1016/j.cmet.2015.09.009

Schiffrin, E. L. (2012). Vascular remodeling in hypertension: Mechanisms and treatment. *Hypertension*, *59*(2 SUPPL. 1), 367–374. http://doi.org/10.1161/HYPERTENSIONAHA.111.187021

Schneider, H., Schubert, K. M., Blodow, S., Kreutz, C.-P., Erdogmus, S., Wiedenmann, M., … Pohl, U. (2015). AMPK Dilates Resistance Arteries via Activation of SERCA and BK Ca Channels in Smooth Muscle. *Hypertension*, *66*(1), 108–116. http://doi.org/10.1161/HYPERTENSIONAHA.115.05514

Scott, J. W., van Denderen, B. J. W., Jorgensen, S. B., Honeyman, J. E., Steinberg, G. R., Oakhill, J. S., … Kemp, B. E. (2008). Thienopyridone drugs are selective activators of AMP-activated protein kinase beta1-containing complexes. *Chemistry & Biology*, *15*(11), 1220–30. http://doi.org/10.1016/j.chembiol.2008.10.005

Serné, E. H., de Jongh, R. T., Eringa, E. C., IJzerman, R. G., & Stehouwer, C. D. a. (2007). Microvascular dysfunction: a potential pathophysiological role in the metabolic syndrome. *Hypertension*, *50*(1), 204–11. http://doi.org/10.1161/HYPERTENSIONAHA.107.089680

Sharov, V. S., Dremina, E. S., Galeva, N. a, Williams, T. D., & Schöneich, C. (2006). Quantitative mapping of oxidation-sensitive cysteine residues in SERCA in vivo and in vitro by HPLC-electrospray-tandem MS: selective protein oxidation during biological aging. *The Biochemical Journal*, *394*(Pt 3), 605–15. http://doi.org/10.1042/BJ20051214

Short, J., Dere, R., Houston, K., Cai, S.-L., Kim, J., Bergeron, J., … Walker, C. (2010). AMPK-Mediated Phosphorylation of Murine p27 at T197 Promotes Binding of 14-3-3 Proteins and Increases p27 Stability. *Mol Ecular Carcinogenesis*, *45*(5), 429–39. http://doi.org/10.1038/nmeth.2250.Digestion

Sluchanko, N. N., & Gusev, N. B. (2010). 14-3-3 Proteins and Regulation of Cytoskeleton. *Biochemistry (Mosc)*, *75*(13), 1528–1546. http://doi.org/10.1134/S0006297910130031

Somlyo, A. P., & Somlyo, A. V. (2009). Ca 2ε Sensitivity of Smooth Muscle and Nonmuscle Myosin II : Modulated by G Proteins , Kinases , and Myosin Phosphatase. *Physiological Reviews*, 1325–1358. http://doi.org/10.1152/physrev.00023.2003

Staiculescu, M. C., Galinanes, E., Zhao, G., Ulloa, U., Jin, M., Beig, M., … Martinez-Lemus, L. A. (2013). Prolonged vasoconstriction of resistance arteries involves vascular smooth muscle actin polymerization leading to inward remodelling. *Cardiovascular Research*, *98*(3), 428–436.

Steinberg, G. R., & Kemp, B. E. (2009). AMPK in Health and Disease. *Physiological Reviews*, *89*, 1025–1078. http://doi.org/10.1152/physrev.00011.2008.

Stone, J. D., Narine, A., Shaver, P. R., Fox, J. C., Vuncannon, J. R., & Tulis, D. a. (2013). AMP-activated protein kinase inhibits vascular smooth muscle cell proliferation and migration and vascular remodeling following injury. *American Journal of Physiology. Heart and Circulatory Physiology*, *304*(3), H369–81. http://doi.org/10.1152/ajpheart.00446.2012

Sun, G.-Q., Li, Y.-B., Du, B., & Meng, Y. (2015). Resveratrol via activation of AMPK lowers blood pressure in DOCA-salt hypertensive mice. *Clinical and Experimental Hypertension (New York, N.Y. : 1993)*, *37*(8), 616–21. http://doi.org/10.3109/10641963.2015.1036060

Szewczyk, M. M., Davis, K. a, Samson, S. E., Simpson, F., Rangachari, P. K., & Grover, A. K. (2007). Ca2+-pumps and Na2+-Ca2+-exchangers in coronary artery endothelium versus smooth muscle.

Journal of Cellular and Molecular Medicine, *11*(1), 129–38. http://doi.org/10.1111/j.1582-4934.2007.00010.x

Tada, M., Kirchberger, M. A., & Katz, A. M. (1975). Phosphorylation of a 22,000-dalton component of the cardiac sarcoplasmic reticulum by adenosine 3':5'-monophosphate-dependent protein kinase. *Journal of Biological Chemistry*, *250*(7), 2640–2647.

Tang, D. D., & Anfinogenova, Y. (2008). Physiologic properties and regulation of the actin cytoskeleton in vascular smooth muscle. *J Cardiovasc Pharmacol Ther*, *13*(2), 130–140. http://doi.org/10.1177/1074248407313737

Tang, D. D., & Tan, J. (2003). Role of Crk-associated substrate in the regulation of vascular smooth muscle contraction. *Hypertension*, *42*(4 II), 858–863. http://doi.org/10.1161/01.HYP.0000085333.76141.33

Tang, D. D., & Tan, J. J. (2003). Downregulation of profilin with antisense oligodeoxynucleotides inhibits force development during stimulation of smooth muscle. *Am J Physiol Heart Circ Physiol*, *285*(4), H1528–36. http://doi.org/10.1152/ajpheart.00188.2003

Tang, D. D., Zhang, W., & Gunst, S. J. (2005). The Adapter Protein CrkII Regulates Neuronal Wiskott-Aldrich Syndrome Protein, Actin Polymerization, and Tension Development during Contractile Stimulation of Smooth Muscle. *Journal of Biological Chemistry*, *280*(24), 23380–23389. http://doi.org/10.1074/JBC.M413390200

Tang, M., Wang, G., Lu, P., Karas, R. H., Aronovitz, M., Heximer, S. P., … Mendelsohn, M. E. (2003). Regulator of G-protein signaling-2 mediates vascular smooth muscle relaxation and blood pressure. *Nature Medicine*, *9*(12), 1506–1512. http://doi.org/10.1038/nm958

Tejani, A. D., Walsh, M. P., & Rembold, C. M. (2011). Tissue length modulates "stimulated actin polymerization," force augmentation, and the rate of swine carotid arterial contraction. *AJP: Cell Physiology*, *301*(6), C1470–C1478. http://doi.org/10.1152/ajpcell.00149.2011

Trebak, M. (2012). STIM/Orai signalling complexes in vascular smooth muscle. *The Journal of Physiology*, *590*(17), 4201–4208. http://doi.org/10.1113/jphysiol.2012.233353

Van Den Akker, J., Schoorl, M. J. C., Bakker, E. N. T. P., & Vanbavel, E. (2010). Small artery remodeling: Current concepts and questions. *Journal of Vascular Research*, *47*(3), 183–202. http://doi.org/10.1159/000255962

Vandesompele, J., De Preter, K., Pattyn, F., Poppe, B., Van Roy, N., De Paepe, A., & Speleman, F. (2002). Accurate normalization of real-time quantitative RT-PCR data by geometric averaging of multiple internal control genes. *Genome Biology*, *3*(7), research0034.1–0034.11.

Vazquez-Martin, A., Oliveras-Ferraros, C., & Menendez, J. A. (2009). The active form of the metabolic sensor: AMP-activated protein kinase (AMPK) directly binds the mitotic apparatus and travels

from centrosomes to the spindle midzone during mitosis and cytokinesis. *Cell Cycle*, *8*(15), 2385–2398. http://doi.org/10.4161/cc.8.15.9082

Vergara, D., Ferraro, M. M., Cascione, M., del Mercato, L. L., Leporatti, S., Ferretta, A., … Gaballo, A. (2015). Cytoskeletal Alterations and Biomechanical Properties of parkin-Mutant Human Primary Fibroblasts. *Cell Biochemistry and Biophysics*, *71*(3), 1395–1404. http://doi.org/10.1007/s12013-014-0362-1

Walsh, M. P., & Cole, W. C. (2013). The role of actin filament dynamics in the myogenic response of cerebral resistance arteries. *J Cereb Blood Flow Metab*, *33*(1), 1–12. http://doi.org/10.1038/jcbfm.2012.144

Wang, S., Liang, B., Viollet, B., & Zou, M. (2011a). Accentuates Agonist-Induced Vascular Smooth Muscle Contraction and High Blood Pressure in Mice. *Hypertension*. http://doi.org/10.1161/HYPERTENSIONAHA.110.168906

Wang, S., Liang, B., Viollet, B., & Zou, M.-H. (2011b). Inhibition of the AMP-activated protein kinase-α2 accentuates agonist-induced vascular smooth muscle contraction and high blood pressure in mice. *Hypertension*, *57*(5), 1010–7. http://doi.org/10.1161/HYPERTENSIONAHA.110.168906

Wang, Y., Chen, L., Li, M., Cha, H., Iwamoto, T., & Zhang, J. (2015). Conditional knockout of smooth muscle sodium calcium exchanger type-1 lowers blood pressure and attenuates Angiotensin II-salt hypertension. *Physiological Reports*, *3*(1), e12273. http://doi.org/10.14814/phy2.12273

Wang, Y., Huang, Y., Lam, K. S. L., Li, Y., Wong, W. T., Ye, H., … Li, C. (2009). Berberine prevents hyperglycemia-induced endothelial injury and enhances vasodilatation via adenosine monophosphate-activated protein kinase and endothelial nitric oxide synthase. *Cardiovascular Research*, *82*(3), 484–92. http://doi.org/10.1093/cvr/cvp078

Weerasekara, V. K., Panek, D. J., Broadbent, D. G., Mortenson, J. B., Mathis, A. D., Logan, G. N., … Andersen, J. L. (2014). Metabolic-stress-induced rearrangement of the 14-3-3ζ interactome promotes autophagy via a ULK1- and AMPK-regulated 14-3-3ζ interaction with phosphorylated Atg9. *Molecular and Cellular Biology*, *34*(24), 4379–88. http://doi.org/10.1128/MCB.00740-14

Weisová, P., Alvarez, S. P., Kilbride, S. M., Anilkumar, U., Baumann, B., Jordán, J., … Prehn, J. H. M. (2013). Latrepirdine is a potent activator of AMP-activated protein kinase and reduces neuronal excitability. *Translational Psychiatry*, *3*(September), e317. http://doi.org/10.1038/tp.2013.92

Wellman, G. C., Santana, L. F., Bonev, A. D., Nelson, M. T., & Nelson, M. T. (2001). Role of phospholamban in the modulation of arterial Ca 2 ε sparks and Ca 2 ε -activated K ε channels by cAMP, 1029–1037.

Weston, a H., Egner, I., Dong, Y., Porter, E. L., Heagerty, a M., & Edwards, G. (2013). Stimulated release of a hyperpolarizing factor (ADHF) from mesenteric artery perivascular adipose tissue:

involvement of myocyte BKCa channels and adiponectin. *British Journal of Pharmacology*, *169*(7), 1500–9. http://doi.org/10.1111/bph.12157

Woollhead, A. M., Scott, J. W., Hardie, D. G., & Baines, D. L. (2005). Phenformin and 5-aminoimidazole-4-carboxamide-1-β-D-ribofuranoside (AICAR) activation of AMP-activated protein kinase inhibits transepithelial Na $^+$ transport across H441 lung cells. *The Journal of Physiology*, *566*(3), 781–792. http://doi.org/10.1113/jphysiol.2005.088674

Wray, S., & Burdyga, T. (2010). Sarcoplasmic Reticulum Function in Smooth Muscle. *Physiological Reviews*, *90*(1), 113–178. http://doi.org/10.1152/physrev.00018.2008.

Wu, K., Bungard, D., Lytton, J., Stabley, J. N., Ii, J. M. D., Dominguez, C. E., … Lyt-, J. (2001). Regulation of SERCA Ca 2 + pump expression by cytoplasmic [Ca 2 +] in vascular smooth muscle cells. *American Journal of Physiology. Cell Physiology*, *280*, C843–C851.

Wu, Y., & Gunst, S. J. (2015). Vasodilator Stimulated Phosphoprotein (VASP) Regulates Actin Polymerization and Contraction in Airway Smooth Muscle by a Vinculin-dependent Mechanism. *Journal of Biological Chemistry*, *290*(18), jbc.M115.645788. http://doi.org/10.1074/jbc.M115.645788

Wyatt, C. N., Mustard, K. J., Pearson, S. A., Dallas, M. L., Atkinson, L., Kumar, P., … Evans, A. M. (2007). AMP-activated Protein Kinase Mediates Carotid Body Excitation by Hypoxia *. *Journal of Biological Chemistry*, *282*(11), 8092–8098. http://doi.org/10.1074/jbc.M608742200

Xie, M., & Roy, R. (2015). AMP-Activated Kinase Regulates Lipid Droplet Localization and Stability of Adipose Triglyceride Lipase in C. elegans Dauer Larvae. *PloS One*, *10*(6), e0130480. http://doi.org/10.1371/journal.pone.0130480

Xin, M., Small, E. M., Sutherland, L. B., Qi, X., McAnally, J., Plato, C. F., … Olson, E. N. (2009). MicroRNAs miR-143 and miR-145 modulate cytoskeletal dynamics and responsiveness of smooth muscle cells to injury. *Genes and Development*, *23*(18), 2166–2178. http://doi.org/10.1101/gad.1842409

Yamin, R., & Morgan, K. G. (2012). Deciphering actin cytoskeletal function in the contractile vascular smooth muscle cell. *The Journal of Physiology*, *590*(Pt 17), 4145–54. http://doi.org/10.1113/jphysiol.2012.232306

Yan, Y., Tsukamoto, O., Nakano, a, Kato, H., Kioka, H., Ito, N., … Takashima, S. (2015). Augmented AMPK activity inhibits cell migration by phosphorylating the novel substrate Pdlim5. *Nat Commun*, *6*, 6137. http://doi.org/ncomms7137 [pii]\r10.1038/ncomms7137

Zaborska, K. E., Wareing, M., Edwards, G., & Austin, C. (2016). Loss of anti-contractile effect of perivascular adipose tissue in offspring of obese rats. *International Journal of Obesity*, (April), 1–10. http://doi.org/10.1038/ijo.2016.62

Zhang, J., Herrera, A. M., Paré, P. D., & Seow, C. Y. (2010). Dense-body aggregates as plastic structures supporting tension in smooth muscle cells. *American Journal of Physiology. Lung Cellular and Molecular Physiology*, *299*(5), L631–8. http://doi.org/10.1152/ajplung.00087.2010

Zhang, W., Huang, Y., & Gunst, S. (2016). P21-Activated Kinase (Pak) Regulates Airway Smooth Muscle Contraction by Regulating Paxillin Complexes that mediate Actin Polymerization. *Journal of Physiology*, *0*, 1–22. http://doi.org/10.1017/CBO9781107415324.004

Zhang, W., Wu, Y., Du, L., Tang, D. D., & Gunst, S. J. (2005). Activation of the Arp2/3 complex by N-WASp is required for actin polymerization and contraction in smooth muscle. *American Journal of Physiology. Cell Physiology*, *288*(5), C1145–C1160. http://doi.org/10.1152/ajpcell.00387.2004

Zhao, L.-M., Wang, Y., Yang, Y., Guo, R., Wang, N.-P., & Deng, X.-L. (2014). Metformin Restores Intermediate-Conductance Calcium-Activated K+ channel- and Small-Conductance Calcium-Activated K+ channel-Mediated Vasodilatation Impaired by Advanced Glycation End Products in Rat Mesenteric Artery. *Molecular Pharmacology*, *86*(5), 580–591. http://doi.org/10.1124/mol.114.092874

Zheng, B., & Cantley, L. C. (2007). Regulation of epithelial tight junction assembly and disassembly by AMP-activated protein kinase. *Proceedings of the National Academy of Sciences of the United States of America*, *104*(3), 819–22. http://doi.org/10.1073/pnas.0610157104

Zhu, W., Cheng, K. K. Y., Vanhoutte, P. M., Lam, K. S. L., & Xu, A. (2008). Vascular effects of adiponectin : molecular mechanisms and potential therapeutic intervention STRUCTURAL PROPERTIES AND DIVERSE. *Clinical Science*, *374*, 361–374. http://doi.org/10.1042/CS20070347

Zhu, Y., Bian, Z., Lu, P., Karas, R. H., Bao, L., Cox, D., … Mendelsohn, M. E. (2002). Abnormal vascular function and hypertension in mice deficient in estrogen receptor beta. *Science*, *295*(5554), 505–508. http://doi.org/10.1126/science.1065250

Acknowledgements

Publications and Conference Papers resulting from this thesis

Schneider H*, **Schubert KM***, Blodow S, Kreutz C-P, Erdogmus S, Wiedenmann M, Qiu J,Fey T, Ruth P, Lubomirov LT, Pfitzer G, Mederos y Schnitzler M, Hardie DG, Gudermann T, Pohl U: *AMPK dilates resistance arteries via activation of SERCA and BK_{Ca} channels in smooth muscle;* Hypertension. 2015 Jul;66(1):108-16; (*shared first authorship)
Impact factor 7,6

Schubert KM*, Qiu J,*, Blodow S, Wiedenmann M, Lubomirov LT, Pfitzer G, Pohl U, Schneider H: *The AMP-related kinase (AMPK) induces Ca2+-independent dilation of resistance arteries by interfering with actin filament formation*
in revision at Circ Res.

date	Congress/destination	abstract title	presentation
04/2010	Joint Meeting of the Scandinavian and German Physiological Societies/Kopenhagen	Activation of the AMP-activated protein kinase (AMPK) induces vasodilation in mouse mesenteric arteries ***Acta Physiologica 2010**; Volume 198, Supplement 677 :P-TUE-3*	poster
09/2010	9th World Congress for Microcirculation/Paris (France)	AMPK induces vasodilation of microvessels by reducing smotth muscle calcium sensitivity	oral
03/2011	90th Annual Meeting Deutsche Physiologsche Gesellschaft/Regensburg (Germany)	AMP-activated protein kinase (AMPK) induces vasodilation of hamster microvessels by activating the BKCa-channel ***Acta Physiologica 2011**; Volume 201, Supplement 682:O59*	oral
05/2011	10th International Symposium on Resistance Arteries (ISRA)/Rebild (Denmark)	Vasodilation of hamster resistance arteries caused by the AMP-activated protein kinase (AMPK) are BK channel dependent	poster
09/2011	Joint Scientific Meeting of The Turkish Society of	Dual vasodilator mechanism of the AMP-activated protein kinase (AMPK) in arterial	oral

		microvessels *Acta Physiologica 2011*; Volume 203, Supplement 686:OC03	
10/2011	Joint Meeting of the European Society for Microcirculation (ESM) and the German Society of Microcirculation and Vascular Biology (GfMVB)/Munich (Germany)	Role of AMP-activated kinase (AMPK) in control of resistance vessel tone: assessment by AMPK activators A769662 and metformin *J Vasc Res* 2011;48 (Suppl.1):271	poster
09/2012	Joint Scientific Meeting of The Spanish Society of Physiological Sciences and FEPS in Santiago de Compostela (Spain)	Vasodilation of microvessels by the AMP-activated protein kinase (AMPK) involves reduction of smooth muscle calcium sensitivity and activation of BKCa channels *Acta Physiologica 2012*; Volume 206, Supplement 693 :O480	oral
10/2013	11th International Symposium on Mechanisms of Vasodilatation (MOVD)/ Zurich (Switzerland)	5' adenosine monophosphate activated protein kinase (AMPK) induces vasodilation of microvessels by reducing smooth muscle calcium sensitivity *MOVD 2013*; oral presentations, endothelial dependent dilations, no. 7, S. 16 and AMP-activated protein kinase (AMPK) dilates microvessels via activation of the BKCa channel *MOVD 2013*; posters, vascular responsiveness, no. 4/9, S. 57	oral (presented by Holger Schneider) poster
03/2014	93rd annual meeting of the German Physiological Society (DPG)/ Mainz (Germany)	5' adenosine monophosphate-activated protein kinase (AMPK) induces vasodilation by dually acting on smooth muscle membrane potential and calcium pumps	poster (presented by Holger Schneider)
08/2014	Joint Meeting of the Federation of European Physiological Societies (FEPS) and the Hungarian Physiological	Multimodal action of 5'adenosine monophosphate-activated protein kinase (AMPK) in reducing vascular tone of resistance arteries: Effects on calcium stores and membrane potential.	poster (presented by Holger Schneider)

	Society/ Budapest (Hungary)		
09/2014	11th International Symposium on Resistance Arteries (ISRA)/ Banff (Canada)	5'adenosine monophosphate-activated protein kinase (AMPK) induces vasodilation in resistance arteries *via* BK_{Ca}-mediated hyperpolarization and sarco/endoplasmic reticulum Ca^{2+}-ATPase (SERCA)-driven calcium sequestration.	poster (presented by Holger Schneider)
09/2014	Federation of American Societies for Experimental Biology Science Research Conference (FASEB SRC)(AMPK: Biological action and therapeutic perspectives)/ Barga, (Italy)	Dual control of AMPK-induced vasodilation in resistance vessels by SERCA and BK_{Ca} channels.	poster (presented by Steffi Blodow)
06/2015	Joint 28th European Society for Microcirculation (ESM) and the 8th European Vascular Biology Organization (EVBO) Meeting/ Pisa (Italy)	AMPK dilates resistance arteries via activation of SERCA and BKCa channels in smooth muscle	poster (presented by Jiehua Qiu)
09/2015	Endothelium-Dependent Hyperpolarizations in Health and Disease (EDH)/ Nyborg (Denmark)	AMPK relaxes vascular smooth muscle of resistance arteries by dual action on BKCa channels and SERCA	oral (presented by Holger Schneider)
07/2016	Joint Meeting of the American Physiological Society and The Physiological Society / Dublin (Ireland)	The AMP-activated Protein kinase (AMPK) reduces calcium sensitivity of microvascular smooth muscle by interfering with thin filament dynamics	Poster (presented by Ulrich Pohl)

Curriculum Vitae

Professional Experience

09/2015 – today	**Scientific Assistant, Walter Brendel Centre, LMU Munich, Cardiovascular Physiology and Pathophysiology (Prof. Pohl)** Methods: functional analysis of isolated small arteries (pharmcological stimulation, biomechanics [stress-strain curves]), electrophysiology (membrane potencial), tissue culture and transfection, immunoprecipitation, calcium imaging, confocal microscopy, Western Blot, cell isolation, cell culture Co-supervison of two doctoral candidates Teaching in physiology for pre-medical students: -circulation (summer semester 2016)
05/2014 – 04/2015	**Practical Year** ▪ Surgery: Tygerberg Hospital, University of Stellenbosch in Cape Town/South Africa (Prof. Warren) ▪ Internal Medicine: Klinikum Rechts der Isar der TU Munich (Prof. Laugwitz) ▪ Neurology: Queens Square Hospital, University College London/Great Britain (Prof. Reilly) and Concord Repatriation Hospital, University of Sydney/Australia (Prof. Corbett)
	Medical Electives
08/2013	▪ Neurology: Mahatma Gandhi Mission Hospital in Mumbai, India (Prof. Banerjee)
08/2012	▪ Pediatrics: Rift Valley Provincial General Hospital in Nakuru, Kenya (Dr. Nyangena)
08/2011	▪ Gynecology and Obstetrics: RD&E Hospital Exeter (Peninsula College of Medicine), Great Britain (Prof. Hannemann)
08/2008	▪ Internal Medicine, Emergency: St.Marien Hospital, Lünen (Prof. Perings)

Education

04/2009 – today	**Doctoral Thesis within the promotion project FöFoLe („Förderung für Forschung und Lehre")** Walter Brendel Centre, LMU Munich, Cardiovascular Physiology and Pathophysiology (Prof. Pohl) Title: "*Function of endothelial podosomes on the integrity of microvessels*"
03/2011 – today	**Ph.D-thesis, Medical Life Science and Technology, TU Munich** Walter Brendel Centre, LMU Munich, Cardiovascular Physiology and Pathophysiology (Prof. Pohl)

	Thema: *"The role of the AMPK in the microcirculation"*
12/2013	**USMLE Step 1-test**
10/2005 – 05/2015	**Medical Studies, TU Munich** (grade: 2,16)
	Second part of the medical examination (grade: 2)
	First part of the medical examination (grade: 2,5)
05/2015	**university-entrance diploma, Sportgymnasium Schwerin** (grade: 1,4)
09/2007	
05/2005	

Publications

2016	Kirsch J, Schneider H, Pagel JI, Rehberg M, Singer M, Hellfritsch J, Chillo O**, Schubert KM**, Qiu J, Pogoda K, Kameritsch P, Uhl B, Pircher J, Deindl E, Müller S, Kirchner T, Pohl U, Conrad M, Beck H: *Loss of mitochondrial thioredoxin reductase in endothelial cells leads to endothelial dysfunction and a pro-thrombotic and pro-inflammatory phenotype.* Arteriosclerosis, Thrombosis and Vascular Biology; Accepted for publication; **Impact factor 6,0**
	Fey T, **Schubert KM**, Schneider H, Fein E, Kleinert E, Pohl U, Dendorfer A: *Impaired endothelial shear stress induces podosome assembly via VEGF up-regulation*; FASEB J. 2016 Aug;30(8):2755-66; **Impact factor 5,0**
2015	Schneider H*, **Schubert KM***, Blodow S, Kreutz C-P, Erdogmus S, Wiedenmann M, Qiu J, Fey T, Ruth P, Lubomirov LT, Pfitzer G, Mederos y Schnitzler M, Hardie DG, Gudermann T, Pohl U: *AMPK dilates resistance arteries via activation of SERCA and BK_{Ca} channels in smooth muscle*; Hypertension. 2015 Jul;66(1):108-16; (*geteilte Erstautorenschaft) **Impact factor 7,6**
2014	Direnberger S, Mues M, Micale V, Wotjak CT, Dietzel S, **Schubert M**, Scharr A, Hassan S, Wahl-Schott C, Biel M, Krishnamoorthy G, Griesbeck O*. Biocompatibility of a genetically encoded calcium indicator in a transgenic mouse model. Nat Commun.* 2012; 28(3)1031; **Impact factor 10,01**

Oral Presentations

09/2012	Joint Scientific Meeting of The Spanish Society of Physiological Sciences and FEPS, Santiago de Compostela, Spain
09/2011	Joint Scientific Meeting of The Turkish Society of Physiological Sciences and FEPS, Istanbul, Turkey
03/2011	90th German Physiology Meeting, Regensburg; Germany
03/2010	9th World Congress for Microcirculation, Paris, France

Scholarships/ Awards

06/2016	Georg Heberer Award from the American Chiles Foundation (Portland, Oregon, USA) for the Paper: „*AMPK dilates resistance arteries via activation of SERCA and BK$_{Ca}$ channels in smooth muscle*"
06/2014	Participant at the Nobel Laureat Meeting for Physiology und Medicine in Lindau/Germany as candidate of the Bavarian Academy of Sciences and Humanities
05/2011	"Basic & Clinical Pharmacology & Toxicology" (BCPT) Award for the best poster presentation with the title: "*Vasodilation of hamster resistance arteries caused by the AMP-activated protein kinase (AMPK) are BK channel dependent*" beim 10th International Symposium on Resistance Arteries (ISRA), Rebild, Denmark
09/2010	Young-Investigator-Award of The Japanese Society for Microcirculation for the submitted paper entitled: *"AMPK induces vasodilation of microvessels by reducing smooth mucle calcium sensitivity"* at the 9th World Congress for Microcirculation" in Paris, France
03/2007-05/2015	Scholarship at the „bischöflichen Studienförderung des Cusanuswerkes"

Further Qualifications

Language skills	▪ **English**: business fluent ▪ **Latin**: Latinum
computer literacy	▪ **Microsoft-Office**: Excel, Outlook, PowerPoint, Word ▪ **Reference Management**: Mendeley ▪ **Scientific Graphing and Statistical Analysis**: Sigma Plot ▪ **Image analysis, Makros**: Fiji/ImageJ, Imaris, Huygens (Deconvolution)